MODULATING MACROPHAGE RESPONSE TO BIOMATERIALS

By

TORAL ZAVERI

A DISSERTATION PRESENTED TO THE GRADUATE SCHOOL
OF THE UNIVERSITY OF FLORIDA IN PARTIAL FULFILLMENT
OF THE REQUIREMENTS FOR THE DEGREE OF
DOCTOR OF PHILOSOPHY

UNIVERSITY OF FLORIDA

2011

To Mom, Dad and Khanjan

ACKNOWLEDGMENTS

I would like to express my heartiest gratitude to Dr. Benjamin Keselowsky for his support and guidance without which none of this work would have been possible. His encouragements and suggestions made the research more interesting and challenging. His patience and faith made me successfully complete this endeavor even after facing countless hurdles and roadblocks. I would like to acknowledge my supervisory committee: Dr. Michael Clare-Salzler, Dr. Steve Ghivizzani, Dr. Brandi Ormerod and Dr. Yiider Tseng for serving on my supervisory committee, for their valuable time and support /teachings, guidance and support.

I am thankful to all my past and present colleagues in Dr. Keselowsky's group: Dr. Abhinav Acharya, Jerome Karpiak, Natalia Dolgova, Jamal Lewis, Matt Carsten and Matt Sines. I would especially like to acknowledge Natalia as she has been a mentor throughout my PhD, guiding me through the intricacies of lab experiments. I really appreciate her help with the mouse surgeries which was the most daunting part of my PhD research, owing to my immense fear of mice. I would also like to give special thanks to Jamal as he has assisted me with several of my experiments and particularly mouse surgeries. I acknowledge the help of the Pathology mouse colony staff: Fred and Ronnie. It is from them that I have learnt the basics of mouse colony breeding and was successfully able to maintain my Mac-1 KO mouse colony. I take this opportunity to thank Dave Miller from the CGRC ACS facility for his help in maintaining the Mac-1 KO colony and working with my schedule in having a ready supply of mice available. I would also like to thank the ACS vet technicians who help me set up and practice mice surgeries.

Histology experiments were a major part of my research and I would like to thank Marda Jorgensen from the CTAC facility for her support and guidance in teaching me the intricacies of paraffin embedding, sectioning and staining. I would like to offer special thanks to Dr Wronski for guiding me and allowing me to work in his lab for the PMMA embedding procedure. I thank everyone in his lab especially Alicia and Alyssa for guiding me at each step of the PMMA embedding process as well as helping out with the staining process. I had very limited time to finish my experiments and they have been more than cooperative in helping me meet my time line.

Before I begin to acknowledge all my friends here in Gainesville, I would like to give my biggest thanks to Kamal, without whom I would have never had the courage to come to US in the 1st place or ever consider switching to the PhD program. I would also like to thank my friends from my undergraduate years Bhagyashree, Kanchan, Reshma, Jatin, Karishma and Kartik who supported me through emails and phone calls during the initial stay in Gainesville when I had made no friends here.

During my stay here in Gainesville I made some close friends, which have been my biggest support away from home. They have supported me both personally as well as professionally in sharing the frustrations of PhD life. The few people who have been there for me throughout the PhD have been Neetu, Sushant and Dushyant. They have been patient enough to understand my research, suggest solutions and share the frustrations on a daily basis. They became my family away from home, stood by me through the toughest times of my life and never left my side even for a single day. I will always remember the countless beach trips that we took and the Gator nights we went to so religiously. Neetu with her hard working and dedicated nature was the biggest

source of inspiration to persevere through all difficulties. Her warm heart, contagious laughter and vivacious nature filled my days with joy. It is from Sushant that I have learnt the biggest lessons of my life, lessons of patience, understanding and selflessness and it is in him I have found my closest friend. He makes talking to him so easy and with him I have had the most memorable days of my life exploring Gainesville like never before. Another person that made a big impact on me in these years at UF has been Sungho, his versatile and multicultural nature helped me understand and cope with the cultural differences that I faced in the US. I have learnt a lot from him about biomedical engineering as well as the world owing to his insatiable thirst for knowledge and interest in history, geography, art and anthropology. I would also like to thank all my other roommates – Amee Mehta, Preeti Sood and Mamta Chahar who became my friends and made the stay at Gainesville an enjoyable experience. For making Gainesville fun and exciting, large number of my friends played a role and I would like to thank, Abhishek, Purushottam, Aniruddh, Vibhava, Richa, Karam, Arul, Parnitha, Anu, Jaesoek and Ashwini. I would like to thank my cousin Monali who lives in Miami and hence is the nearest family member. Whenever I missed family, Miami was never too far and her warm hospitality made me feel I am back in India.

This acknowledgment would not be complete without thanking my parents, my brother Jesal, my husband Khanjan and his family. My parents have always been very supportive and encouraging for my education and no price or sacrifice has ever been big enough for them when it came to ensuring that I got the best of education as well as what life had to offer. They visited me in Gainesville every single year and spent a month with me, which turned out to be the best time of the year for me. Khanjan has

been my biggest support in the last 2 years, especially towards the end when the end though in sight seemed very far. He encouraged me to strive harder and never lose focus. Whenever I was frustrated with work he made me laugh and I got to work with infused vigor. To everyone who made the last 6 years of my life comfortable, enjoyable and worth all the pursuit that goes into this degree – I couldn't have done it without you.

TABLE OF CONTENTS

page

LIST OF FIGURES

LIST OF ABBREVIATIONS

AAD	Aminoactinomycin D
ANOVA	Analysis of variance
AFM	Atomic force microscopy
BMM	Bone marrow derived Macrophages
BSA	Bovine serum albumin
CD	Cluster of differentiation
CR3	Complement receptor-3
°C	Degrees Celsius
DMEM	Dulbecco’s modified eagle medium
ECM	Extracellular matrix proteins
ELISA	Enzyme-linked immunosorbent assay
EU	Endotoxin units
FAK	Focal adhesion kinase
FBGC	Foreign Body Giant Cells
FBR	Foreign Body Reaction
FBS	Fetal bovine serum
Fg	Fibrinogen
FN	Fibronectin
ICAM	Intercellular Adhesion Molecule
ICP	Inductively Coupled Plasma
IFN	Interferon
IL	Interleukin
LCCM	L-929 cell conditioned medium
LPS	Lipopolysaccharide

MAPK	Mitogen-activated protein kinase
MCSF	Macrophage Colony Stimulating Factor
MIP	Macrophage inflammatory protein
NR	Nanorods
NF- κβ	Nuclear factor-kappa beta
PBS	Phosphate Buffered Saline
PDGF	Platelet derived growth factor
PET	Polyethylene Terephthalate
PGE	Prostaglandin-E
RANKL	Receptor activator for NF- κβ ligand
RANTES	Regulated upon Activation, Normal T-cell Expressed, and Secreted
ROS	Reactive Oxygen Species
SEM	Scanning electron microscopy
Ser	Serum
TGF	Transforming growth factor
TLR	Toll-like receptors
TNF-α	Tumor necrosis factor alpha
TRAP	Tartrate-Resistant Acid Phosphatase
UHMWPE	Ultra-high molecular weight polyethylene
VN	Vitronectin
ZnO	Zinc oxide

Abstract of Dissertation Presented to the Graduate School
of the University of Florida in Partial Fulfillment of the
Requirements for the Degree of Doctor of Philosophy

MODULATING MACROPHAGE RESPONSE TO BIOMATERIALS

By

Toral Zaveri

December 2011

Chair: Benjamin Keselowsky
Major: Biomedical Engineering

Macrophages recruited to the site of biomaterial implantation are the primary mediators of the chronic foreign body response to implanted materials. Since foreign body response limits performance and functional life of numerous implanted biomaterials/medical devices, various approaches have been investigated to modulate macrophage interactions with biomaterial surfaces to mitigate this response. In this work we have explored two independent approaches to modulate the macrophage inflammatory response to biomaterials. The first approach targets surface integrins, cell surface receptors that mediate cell adhesion to biomaterials through adhesive proteins spontaneously adsorbed on biomaterial surfaces. The second approach involves surface modification of biomaterials using nanotopographic features since nanotopography has been reported to modulate cell adhesion and viability in a cell type-dependent manner. More specifically, Zinc Oxide (ZnO) nanorod surface was investigated for its role in modulating macrophage adhesion and survival in vitro and foreign body response in vivo.

For the first approach, we have investigated the role of integrin Mac-1 and RGD-binding integrins in the in-vivo osteolysis response and macrophage inflammatory

processes of phagocytosis as well as inflammatory cytokine secretion in response to particulate biomaterials. We have also investigated the in vivo foreign body response (FBR) to subcutaneously implanted biomaterials by evaluating the thickness of fibrous capsule formed around the implants after 2 weeks of implantation. The role of Mac-1 integrin was isolated using a Mac-1 KO mouse and comparing it to a WT control. The role of RGD binding integrins in FBR was investigated by coating the implanted biomaterial with ELVAX™ polymer loaded with Echistatin which contains the RGD sequence. For the in-vivo osteolysis study and to study the in-vitro macrophage response to particulate biomaterials, we used the RGD peptide encapsulated in ELVAX™ and dissolved in macrophage media respectively. By studying the phagocytosis, inflammatory and FBR of macrophages from integrin knockout mice, as well as using various integrin blocking techniques we aim to identify the role of various integrins in macrophage inflammatory response. These integrins can serve as therapeutic targets for mitigating this inflammatory response and improve functional life of implanted biomaterials.

Zinc oxide (ZnO) has been investigated in a number of biomedical applications and surfaces presenting well-controlled nanorod structures of ZnO have recently been developed. In order to investigate the influence of nanotopography on macrophage adhesive response, we evaluated macrophage adhesion and viability on ZnO nanorods, compared to a relatively flat sputtered ZnO controls and using glass substrates for reference. We found that although macrophages are capable of initially adhering to and spreading on ZnO nanorod substrates, the number of adherent macrophages on ZnO nanorods was reduced compared to ZnO flat substrate and glass. While these data

suggest nanotopography may modulate macrophage adhesion, reduced cell viability on both sputtered and nanorod ZnO substrate indicates appreciable toxicity associated with ZnO. In order to determine long-term physiological responses, ZnO nanorod-coated and sputtered ZnO-coated polyethylene terephthalate (PET) discs were implanted subcutaneously in mice for 14 days. Upon implantation, both ZnO-coated discs resulted in a discontinuous cellular fibrous capsule indicative of unresolved inflammation, in contrast to uncoated PET discs, which resulted in typical foreign body capsule formation. Hence although ZnO substrates presenting nanorod topography have previously been shown to modulate cellular adhesion in a topography-dependent fashion for specific cell types, this work demonstrates that for primary murine macrophages, cell adhesion and viability correlate to both nanotopography and toxicity of dissolved Zn, parameters which are likely interdependent. Considering the toxicity of ZnO nanorod surface towards macrophages, their role as an antibacterial surface was explored.

Antibacterial coating approaches are being investigated to modify implants to reduce bacterial adhesion and viability in order to reduce implant-associated infection. To assess the efficacy of ZnO nanorod surfaces as an anti-bacterial coating, we evaluated bacterial adhesion and viability, compared to sputtered ZnO and glass substrates. Common implant-associated pathogens, Pseudomonas aeruginosa and Staphylococcus epidermidis were investigated. ZnO nanorod surface and sputtered ZnO demonstrated a significant bactericidal effect, killing respectively 2.5x and 1.7x times the number of bacteria dead on glass. A similar bactericidal effect of ZnO substrates on S. epidermidis was also evident, with sputtered ZnO and ZnO nanorod

substrates killing respectively 22x and 32x times bacteria dead on glass. These data support the further investigation of ZnO nanorod coatings for bacterial adhesion resistance and bactericidal properties.

CHAPTER 1
INTRODUCTION

Biological Response to Biomaterials

The National Institutes of Health defines biomaterials as ‘Substance or combination of substances - natural or synthetic in origin that have been designed to interact with biological systems for any period of time to treat, augment or replaces any tissue, organ, or function of the body [1]. Biomaterials are used in medical devices, tissue engineering constructs as well as biotechnological applications. The biomaterials product industry is rapidly expanding; it had a market size of $25.5 billion in 2008 and has been projected to grow 15% annually until 2013 [2]. Some common application of biomaterials are artificial joints, bone plates for fracture fixation, dental implants, artificial heart valves, intraocular lenses as well as skin grafts [3]. A variety of materials are being used as biomaterials including metals, polymer, ceramics, composites as well as modified natural materials - autografts, allografts and xenografts [3]. An essential property for biomaterials is biocompatibility, which is the ability to exist in contact with tissues of the human body without causing an unacceptable degree of harm to the body [4]. Although, most implantable materials are non-immunogenic and non-toxic, implants made of such materials have been shown to trigger various degrees of host immune response which limits their performance and lifetime in vivo. The duration and intensity of the immune response varies depending on the size, shape, chemical and physical properties of the biomaterial as well as the site of the implant [5]. The host immune response plays a role in various clinical problems associated with implants such as aseptic loosening of artificial joints, [6,7] degradation and surface cracking of pacemaker leads, [8] fibrous encapsulation around breast implants [9,10] and drug

delivery systems [11]. As these complications eventually lead to implant failure it requires surgical removal and replacement, increasing both the risk to patients as well as health care costs [6]. These host responses that ensue as soon as a biomaterial is implanted in the body and described in the order that they occur are injury, blood–material interactions, provisional matrix formation, acute inflammation, chronic inflammation, granulation tissue development, foreign body reaction, and fibrous capsule development [5,12]. This series of host responses influence the eventual success or failure of an implanted device and hence, a number of studies have been conducted trying to elucidate the various steps of the host immune response and identify therapeutic targets to mitigate this response.

Injury, Blood–material Interactions and Provisional Matrix Formation

The process of implantation, regardless of the location of the implant, causes an injury due to the surgical procedure of implantation as well as disruption of tissue integrity [13]. This injury results in the implant coming in contact with blood, the fibrinogen in the blood is then cleaved into fibrin and a blood clot is formed that promotes platelet adhesion and aggregation [14]. Activated platelets release interleukin 8 (IL8), RANTES (Regulated upon Activation, Normal T-cell Expressed, and Secreted) and macrophage inflammatory protein 1 alpha (MIP1α) which attract and activate phagocytes, [15] leading to the initiation of a non-specific inflammatory response. The injury to vascularized connective tissue activates a number of wound healing systems such as extrinsic and intrinsic coagulation systems, the complement system, the fibrinolytic system, the kinin-generating system and platelets [5]. Thrombus formation leads to the development of a blood-based transient provisional matrix [5]. The provisional matrix formed provides a structural framework composed of fibrin cross

linked with factor XIIIa [16] and several biochemical and cellular components which participate in the processes of wound healing and foreign body reaction [5]. This matrix contains adhesive molecules such as fibronectin and thrombospondin bound to fibrin as well as platelet granule components released during platelet aggregation [16]. Platelet granule components include thrombospondin released from α granules and cytokines include TGF-α, TGF-β, Platelet derived growth factor (PDGF), platelet factor 4 and platelet derived endothelial cell growth factor [16]. Thus, the provisional matrix comprises of naturally derived components from the body itself, is biodegradable and functions as a sustained release system for bioactive agents that control the subsequent phases of wound healing [5]. The cells that infiltrate the implant site as a result of injury and release bioactive agents include neutrophils, mast cells, monocytes, macrophages, fibroblasts and endothelial cells listed in the temporal order as they arrive at the site of injury [5].

Protein Adsorption on Biomaterial Surface

Immediately following exposure to physiologic fluids, implanted materials spontaneously adsorb a layer of host proteins which form the mediating layer between the recruited leukocytes and the implant surfaces [5,17,18]. Thus, even before the cells come in contact with the implant, the biomaterial surface is coated with various proteins and the interaction of these proteins with adhesion receptors on inflammatory cells leads to the recognition of the foreign body. The adsorbed proteins are not foreign to the body however they still help in recognition of foreign objects because the confirmation and density of proteins on the biomaterial surface is different than its native state and concentration in the body. Proteins such as fibrinogen, fibronectin, vitronectin, albumin, immunoglobulins and complement factor C3 have been shown to adsorb onto

biomaterial surfaces [19-21]. The type and surface density of adsorbed proteins depend on surface properties of the biomaterial as well the solution concentration of proteins [18]. Interestingly, the Vroman effect dictates that the type and amount of protein adsorbed on the biomaterial surface is dynamic, as adsorbed proteins may desorb due to other proteins having higher affinity for the surface [22]. Upon adsorption, proteins can undergo conformational changes to reduce surface energy and thus expose different ligand binding sites and create bioactive sites for the interaction of cells with biomaterials [5,17,21,23]. For example, when fibrinogen comes in contact with hydrophobic biomaterial surfaces it adopts an energetically more favorable conformation, thereby exposing the otherwise occult epitopes P1 (γ 190-202) and P2 (γ377-395), [24] which are binding sites for β_2 integrins present on macrophage surface [25,26]. When surface receptors such as integrins bind to different active sites of adsorbed proteins they modulate cellular responses such as adhesion, morphology, growth, differentiation, and activation [27]. Based on different surface chemistries and thus differential protein adsorption, studies have demonstrated differences in cell behaviors including adhesion, [21,28,29] differentiation, [30,31] activation, [24,32-34] and apoptosis [35-37] on biomaterial surfaces. Thus adsorbed proteins lead to recognition of foreign substances in the body, macrophage adhesion to biomaterial surface and promote macrophage activation [5].

Acute Inflammation

The first cells to arrive at the implant site are neutrophils and mast cells- the main players of the acute inflammatory response [5,38]. The activated neutrophils secrete a number of chemokines and cytokines such as IL-8 and MIP-1α in the early phase of the inflammatory response that further contribute to the development of the inflammatory

response. During the acute inflammation phase, mast cell degranulation and histamine release causes phagocyte recruitment and the fibrinogen adsorbed on implant surface facilitates phagocyte adhesion [5,17,38,39]. During the degranulation process, mast cells also release interleukin-4 (IL-4) and interleukin-13 (IL-13) which have been shown to play a role in macrophage fusion to form foreign body giant cell (FBGC) [40,41] and thus determine the extent and degree of the subsequent development of the foreign body reaction. This acute inflammation around biomaterials usually resolves in less than one week, depending on the extent of injury at the implant site, [5,39] following which chronic inflammation phase begins.

Chronic Inflammation

The chronic inflammation phase is characterized by the presence of mononuclear cells, i.e. monocytes, macrophages, plasma cells and lymphocytes at the implant site [42]. Unlike the acute inflammation phase which last only couple of days, this phase can extend from few days to even years depending on the type and persistence of inflammatory stimulus [5]. In case of biocompatible materials, chronic inflammatory response resolves in less than two weeks. If it lasts longer, it could indicate that there is some infection associated with the implant [39]. Among the cells that arrive at the implant site during chronic inflammation, macrophages are most important as they secrete a large variety of biologically active products that participate in the subsequent phases of wound healing [5]. The biologically active products secreted by macrophages include neutral proteases, chemotactic factors, arachidonic acid metabolites, reactive oxygen metabolites, complement components, coagulation factors, growth-promoting factors, and cytokines [5].

Granulation Tissue and Foreign Body Reaction

After chronic inflammation, the next phase in the sequence of events following biomaterial implantation is formation of granulation tissue which marks the beginning of the wound healing phase. The granulation tissue is composed of macrophages, fibroblasts and vascular endothelial cells. The fibroblasts proliferate and synthesize collagen and proteoglycans which form the fibrous capsule around implants. The endothelial cells proliferate, maturate and organize themselves into capillaries thus initiating neovascularization. The macrophages may fuse together to form FBGC, which form a part of the foreign body capsule along with macrophages and collagen from fibroblasts [5]. FBGCs release reactive oxygen intermediates (ROIs), degradative enzymes, and acid into the space between the cell membrane and biomaterial surface which has been shown to mediate degradation of biomaterial surfaces [5,8].

Approaches to Modulate Foreign Body Response

Since protein adsorption on the surface is the first step in the cascade of events that occur upon biomaterial implantation, several studies have investigated non-fouling surface which significantly reduce protein adsorption to modulate foreign body response [43,44]. A number of studies have also demonstrated that different surface chemistries result in differential protein adsorption on the surface, both in terms of type and protein confirmation, exposing different active sites for cell binding and ultimately influencing cellular response [21,45]. For example, hydrophilic and anionic surfaces have been shown to promote anti-inflammatory cytokine secretion by monocytes and macrophages upon adhering to the surface [46]. This can be attributed to differential protein adsorption on these surfaces as compared to hydrophobic and cationic surfaces, which results in the availability of different set of binding sites for integrins. Macrophage

activation is controlled by binding and clustering of integrins on the cell surface that triggers the signaling reactions that are propagated into the cell (outside-in signaling) leading to a functional response [47]. The next interaction investigated for modulating macrophage response is the binding of macrophages to the adsorbed protein layer that is mediated through surface receptors such as integrins. Numerous studies have examined the role of macrophage integrins in the various steps of the foreign body response. For example the binding of neutrophil and macrophage integrin, Mac-1 (CD11b/CD18), to fibrinogen adsorbed on biomaterial surface is shown to mediate adhesion of phagocytes to biomaterial implants [17,48]. Different types of macrophages are beneficial to the wound healing response as they participate in tissue repair and angiogenesis. Studies have been conducted to explore activation of macrophages towards the alternatively activated macrophages which have an anti- inflammatory phenotype as compared to classically activated macrophages [49,50].

Approaches that have been investigated to modulate inflammatory response to biomaterials involve (1) surface modification of biomaterials – physical and chemical [51,52], (2) surface treatment of biomaterial surface in order to release bioactive molecules that have been shown to modulate the foreign body response [53], (3) targeting receptors or signaling pathways in macrophages that participate in the inflammatory response to biomaterials [54].

Macrophage Response to Biomaterials

Macrophages are sentinels of the body, they participate in clearance of tissue debris and apoptotic cells and wound healing [55]. They respond to foreign invasion in the body ranging from pathogens to biomaterial implants [5,55]. As reviewed in the earlier sections, macrophages form majority of the cell type recruited to site of

biomaterial implantation and they play a significant role in the various phases of foreign body response [5]. Macrophages recruited to site of implant secrete cytokines, chemokines, and growth factors that signal the recruitment and activation of other cells such as lymphocytes, fibroblasts, endothelial cells, and smooth muscle cells that participate in the various stages of the foreign body response [5]. Macrophages may undergo frustrated phagocytosis when trying to phagocytose bulk biomaterials; they fuse to form FBGCs and encapsulate the implanted material [5]. The foreign body response and fibrous encapsulation severely limits the functional performance of the implanted biomaterial in vivo such as pacemaker leads, [8] drug delivery [11] and recording electrodes [56]. Since macrophages play such a central role in the response to implanted materials various studies have explored modulating macrophage response using different approaches such as surface chemistry and surface roughness to modulate macrophage adhesion to biomaterials [57-61]. Some of these techniques reduce macrophage adhesion to biomaterial surface by making anti-fouling surfaces which resist protein adsorption thus abrogating macrophage-surface interaction [60]. Nanotopographic surfaces which have features in the nanometer size range have also been explored to modulate macrophage adhesion and function [62,63]. Since features of nanotopographic surfaces are in the biological size range, they have been explored for various cell surface interactions [64-67]. Another link between the macrophages and biomaterial surface are receptors called integrins present on macrophage surface that bind to the adsorbed protein. Binding of integrins to their ligands leads to integrin clustering and downstream signaling that may result in alteration in cell growth, differentiation, migration, attachment and spreading [68]. Macrophages interact with

adhesion proteins via integrins, which is evident from the decrease in cell attachment observed in the presence of anti-integrin antibodies [69].

Integrins

Integrins are a large family of cell adhesion receptors that play an important role in cell-ECM and cell-cell interaction [70,71]. They are heterodimeric transmembrane receptors composed of an α and a β chain (glycoprotein subunits) that are non-covalently associated, where each subunit contributes and is required for ligand binding [70,71]. There are 8 β and 16 α chains which combine together to form 24 known integrin receptors, [70] for example α_M combines with β_2 to form integrin $\alpha_M\beta_2$ (Mac-1). Integrins have a long extracellular domain that forms the site for ligand binding and recognizes specific amino acid sequences [70]. They have a short intracellular domain that directs intracellular signaling by providing binding sites for signaling molecules such as protein kinases, calcium binding proteins, focal adhesion kinases (FAK), tyrosine and MAP kinases [72]. Ligand binding of integrins causes clustering of integrins to form focal contacts which contain structural proteins such as vinculin, talin [73] and α-actinin as well as signaling molecules such as FAK, Src and paxillin. These structural proteins link the cytoskeleton to the ECM and thus modulate cell adhesion and signaling [72]. Thus integrins through this outside-in signalling, enables a cell to sense its location, local environment, adhesive state and surrounding matrix [71]. Integrins are normally present in an inactive state and when bound to a ligand, conformational changes take place. These changes lead to affinity modulation for the ligand resulting in stronger binding [71]. This is termed as inside-out signaling and it enables cells to modulate adhesive behavior without changing the number of receptors on its surface [74]. Integrins have binding sites for ligand interaction for example, majority of integrins that

have the β_2 subunit contain an inserted (I) domain in the α subunit composed of about 200 amino acids that acts as the major ligand-binding site [75]. Integrins control various cell functions such as cell survival, proliferation, migration and differentiation [76]. Thus they serve as therapeutic targets for directing or disrupting intracellular cell signaling. Cells interact with adhesive proteins adsorbed on biomaterial surface through these adhesion receptors-integrins [5,14,77].

Role of Integrins in Host Immune Response to Biomaterials

Integrins are shown to play a role in the various stages of the host immune response.

Blood material interaction: Platelet integrin $\alpha_{IIb}\beta_3$ mediates initial adhesion of platelets to biomaterial surface adsorbed fibrinogen [78].

Acute inflammation: Integrins on neutrophils surface control the migration of neutrophils through ECM during their extravasation to the implant site [79]. Neutrophils have several integrins such as $\alpha_M\beta_2$, $\alpha_V\beta_3$, and β_1 integrins (α_4,α_5 and α_6) that contribute to the adhesion and motility of neutrophils towards the site of implant [79]. Upon binding of neutrophils integrins to ECM proteins, a signaling cascade is initiated within the cell that leads to change in shape, proliferation and survival [79].

Chronic inflammation: Upon chemokine signaling from the wound site by the neutrophils and mast cells, monocytes in circulation adhere to the endothelium and extravasate through the blood vessels to the site of injury. The β_1 and β_2 integrin families have been shown to play a role in this process of adhesion and extravasation of monocytes [80]. Upon reaching the implant site, β_2 integrin family and particularly $\alpha_M\beta_2$ integrin has been shown to mediate adhesion to biomaterial surface [81].

Granulation tissue and foreign body reaction: β_1 and β_2 integrin have been shown to play a role in fusion of macrophages to form foreign body giant cells.[82]

Macrophage Integrins

Macrophages express integrins of the β_1, β_2, β_3 and β_5 family. Macrophages and monocytes have multiple integrins, some of which include $\alpha_M\beta_2$,$\alpha_X\beta_2$,$\alpha_V\beta_2$ and $\alpha_M\beta_2$ [83].

Integrins present on macrophages direct various cell functions as explained here:

1. Macrophage adhesion to extracellular matrix(ECM) proteins: This interaction is important from the point of view of phagocytosis as interaction with different ECM proteins stimulates phagocytosis via Fcγ and complement receptors [83].

2. Macrophage adhesion to other cells: Macrophages are a component of the innate immune system which provides signaling for the adaptive immune system. This signaling requires cell-cell interaction between macrophages, T-cells and B-cells [83]. Additionally macrophages are scavengers of the body and are responsible for the clearance of apoptotic cells. This requires the macrophage interaction and recognition of apoptotic cells. Recognition of apoptotic cells is mainly mediated by α_V integrin and ingestion of these cells elicits an anti-inflammatory response [83].

3. Macrophage migration and spreading: Integrins act as scaffolds between the cell cytoskeleton and the external environment thus directing cell migration and spreading. Cell migration is critical for the process of extravasations of cells to sites of inflammation, spreading and activation [83].

4. Phagocytosis: The pathways involved in integrin mediated spreading and migration are distinct from those involved in integrin-mediated phagocytosis. Hence it is possible to disrupt phagocytosis without disrupting migration. Various integrins implicated in macrophage phagocytosis are $\alpha_M\beta_2$, $\alpha_V\beta_3$, $\alpha_V\beta_5$ and $\alpha_5\beta_1$ [83].

Since integrins present on macrophages direct various inflammatory processes, they serve as ideal therapeutic targets for modulating the macrophage inflammatory response.

Mac-1 integrin

Mac-1 is an important leukocyte receptor that plays a role in recruitment and activation of immune cells so as to mount an inflammatory response [84]. It is

expressed on monocytes, neutrophils and certain lymphocytes and it quantitatively up-regulated and transformed to an active state by inflammatory mediators [84]. Mac-1 integrin is known by several names such as complement receptor 3 (CR3), $\alpha_M\beta_2$ and CD11b/CD18. It binds to a myriad of ligands such as ECM proteins (fibrinogen, [85] fibronectin, [86] collagen, [87] vitronectin [88]), counter receptors such as ICAM-1,2,3, [89] products of coagulation and complement such as iC3b, [90], factor X, [91] complement factor H [92] as well as other non-protein substances such as heparin [93]. The integrin Mac-1 mediates cell adhesion to a number of proteins that adsorb out of physiologic fluids onto synthetic materials including complement factor fragment C3bi, albumin, vitronectin, and fibrinogen [5,70,71]. Mac-1 plays a role in phagocytosis of C3bi complement-coated targets such as pathogens, apoptotic cells, fat and oil droplets, [94,95] as well as in adhesion dependent respiratory burst and degranulation [94,96]. When Mac-1 binds to its ligands it alters leukocyte adhesion and activation [97]. For example, during recruitment to an inflammation site, Mac-1 along with other integrins such as LFA-1 and VLA-4 modulate leukocyte rolling, adhesion and extravasation through the endothelium and migration through tissues by interaction with ECM proteins [97]. Binding of Mac-1 to its ligands triggers numerous signaling cascades such as the NF-κB pathway and secretion of cytokines (IL-1β and TNF-α) and chemokines which help amplify the inflammatory response [97]. Notably, Mac-1 also mediates adhesion to denatured proteins [42,98]. This is important because proteins that adsorb onto extremely hydrophobic surfaces of some biomaterials such as UHMWPE, undergo extensive denaturation/unfolding [5,14,77]. Mac-1 has been shown to be the major macrophage receptor directing phagocytosis of titanium-alloy wear

particles [99]. For these reasons, Mac-1 is a primary candidate for mediating macrophage molecular recognition and response to particulate as well as bulk biomaterials [33,98]. Thus therapies that target the Mac-1 receptor are expected to block macrophage activation and mitigate the inflammatory response to implanted biomaterials.

RGD binding integrins

The peptide sequence arginine-glycine-aspartic acid (RGD) was first discovered in the protein fibronectin as the recognition site for fibronectin receptor ($\alpha_5\beta_1$) [100]. However now it is known that it is the binding site within several proteins such as vitronectin, fibronectin, fibrinogen, vonWillebrand factor, thrombospondin, laminin and collagen [101]. Of the known twenty integrins, definitely eight and possibly up to twelve of them recognize the RGD sequence in their ligands [101]. The α chain of the known RGD binding integrins α_5, α_8, α_V and α_{IIb} form an integrin sub-family as they show more sequence similarities as compared to other α subunits [102]. Short peptides containing RGD sequence have been shown to have an adhesion promoting as well as adhesion blocking effect. When immobilized on a surface it promotes cell adhesion [103,104] whereas in solution it prevents cell adhesion in a concentration dependant manner [105]. As RGD peptides can bind to a number of integrin receptors and can be used to mimic several proteins, use of RGD peptides enables targeting a wide range of ligand-receptor interactions.

Integrin Targeted Therapies

Anti-adhesion therapies using antibodies, peptides, and peptidomimetic inhibitors against adhesion receptors have shown to be effective in various animal disease models [106-108] as well as in clinical trials [109,110].

Mac-1 Targeted Therapies

The α chain of Mac-1, CD11b contains a 200-amino acid “inserted domain” or “I domain,” which is important in ligand binding [75]. Antibodies to this domain are shown to block binding to ICAM-1, iC3b and fibrinogen [75]. Mutations within the I-domain of Mac-1 have been shown to prevent binding of ICAM-1 and iC3b [111,112].

Antibody blocking

Antibodies to Mac-1 have been shown to interrupt the adhesive and migratory capability of leukocytes and reduce tissue injury in models of inflammation [113,114]. M1/70 is a rat-derived IgG2b mAb directed to the α subunit of mouse Mac-1 (CD11b) [115] with broad species cross-reactivity. It is shown to block adhesion, homotypic aggregation, and complement dependent binding and phagocytosis of complement opsonized erythrocytes [116-118]. Blocking adhesion and hence phagocytosis of wear particles can be an approach to modulate macrophage inflammatory response and reduce peri-implant osteolysis.

Neutrophil inhibitory factor (NIF)

NIF is a 41-kDa glycoprotein isolated from canine hookworm, Ancylostoma caninum [119]. It binds to the I-domain of Mac-1 integrin with high affinity and blocks the Mac-1 binding to several ligands such as C3bi, ICAM-1, and fibrinogen [119]. It is shown to block neutrophils adhesion to protein-coated surfaces and inhibit neutrophil functions [120]. In several animal models of disease it has been shown to be effective in attenuating the deleterious effects resulting from excessive activation of polymorphonuclear cell in inflammatory disease [121].

Targeted Therapies for RGD Binding Integrin

Peptides containing the RGD sequence have been shown to inhibit cell adhesion. For example, RGD peptide is shown to inhibit adhesion of Human K562 erythroleukemia cells on fibronectin-coated dishes in a concentration-dependent manner [105]. $\alpha_V\beta_3$ has been reported to be the primary integrin that mediates adhesion to RGD peptides for numerous cell types [122,123]. Hence RGD mimetics that target integrins other than Mac-1 on the macrophage surface may compete with protein coated biomaterial surface and arrest the macrophage inflammatory response at the very first step of adhesion.

Disintegrins are a group of low molecular weight, cysteine-rich polypeptides isolated from snake venom and contain an Arg-Gly-Asp (RGD) loop maintained by specific disulfide bridges [124]. They are shown to bind and interfere with various integrin mediated process such as inhibition of platelet aggregation via the blockade of $\alpha_{IIb}ß_3$ integrin [124].

Echistatin, a 49-residue protein purified from the venom of the saw-scaled viper Echis carinatus. Echistatin contains the Arg-Gly-Asp (RGD) sequence which is much more potent than the tetrapeptide Arg-Gly-Asp-Phe [125] sequence and binds to integrins such as $\alpha_Vß_3$ through this RGD binding site. Its binding to integrin $\alpha_Vß_3$ is irreversible and has a high affinity. [126] Since $\alpha_Vß_3$ is a receptor predominantly expressed on osteoclasts, echistatin is shown to inhibit osteoclastic bone resorption in vitro and in vivo by binding to $\alpha_Vß_3$, which is known to modulate osteoclast function [127]. It is also shown to inhibit fibrinogen-dependent platelet aggregation and cell adhesion [125]. Thus echistatin through its RGD binding site can serve as an effective integrin targeted therapy.

Polymers for Sustained Release of Integrin-targeted Therapies

The therapies discussed above need to be delivered to the site of implant in a controlled time release fashion in order for it to appropriately intervene and disrupt the different stages of the foreign body response. Depending on the specific application, a number of polymers have been explored in biomaterials application for achieving desired release characteristics as well ensuring that the therapeutic molecule is released in the biologically active state [128]. For example, for tissue engineering as well as temporary drug delivery application, degradable polymers such as Poly(lactide-co-glycolide) are desired as they are biocompatible and degrade into safe by products in the body obviating the need for polymer removal [129].

Controlled release systems for drug delivery are useful in applications requiring a continuous, long term sustained release of the drug at certain specified concentrations [130,131]. These controlled release systems include polymer matrices that encapsulate the drug, can be implanted at site of action thus preventing systemic effect and can be designed to achieve the desired release profile [130].

ELVAX™, ethylene vinyl acetate copolymer is non-inflammatory, non-biodegradable and has been greatly explored for drug delivery to the brain since its early reports by Langer and Folkman in the 1970s [131]. It has been investigated for delivery of various compounds in a slow-release, sustained fashion to the brain [132,133] as well as for orthodontic applications [134]. ELVAX™ can be molded into desired shapes for placement into specific tissue regions, can be designed to release the drug over extended periods of time [135] and macromolecules have been shown to retain their biological activity after release from ELVAX™ [136].

Clinical Significance

Arthritis and Total Joint Replacement

The term arthritis is used to describe a milieu of conditions resulting from inflamed or damaged joints and is a leading cause of disability amongst Americans [137]. It is a chronic condition accompanied with pain and immobility leading to severe economic loss both in terms of decrease in work productivity as well as health care costs amounting to $128 billion annually in 2003 [138]. Some of the common medical conditions that lead to arthritic joints are osteoarthritis, rheumatoid arthritis, juvenile arthritis, gout, fibromyalgia and Lupus erythematosus [137]. In 2006, 46 million Americans (1 in 5 adults) suffered from arthritis or chronic joint symptoms making arthritis second only to heart disease as the leading cause of work disability [137]. For arthritic patients, joint replacement is considered only when physical therapy and pain management have failed [139].

Hip joint replacement is a successful therapy for patients suffering from debilitating arthritis (osteoarthritis and rheumatoid arthritis), congenital hip dysplasia (CHD) and joint fracture to return mobility and relieve pain by replacing the damaged hip joint. Total hip replacement system replaces the head of the femur as well as the acetabular cup with a pair of material surfaces articulating with each other [140]. Over the years, different combinations of surfaces have been investigated as apposing joint surfaces such as metal-on-polyethylene, ceramic-on-polyethylene, metal-on-metal and ceramic-on-ceramic [141]. From these, the most popular combination has been the combination of an ultra-high-molecular weight polyethylene (UHMWPE) acetabular component and a metal femoral component [141].

Failure of Total Hip Replacement: Aseptic loosening

Hip replacement surgery is one of the most successful surgeries of the 20th century [142]. In 2004 over 230,000 hip replacement surgeries were performed in the U.S alone each costing an average of $35,000 [143]. However the replaced joint has a functional life of about 10-15 years with a failure rate of 10% at 10 years post -surgery [144]. As younger and younger people are electing for this surgery, having a longer functional life of the joint is necessary. Additionally, a report published by the American joint replacement registry predicts savings of $65.2 million annually through a mere reduction of 2% in U.S rates for revision surgeries that are performed to replace the malfunctioning implant [145]. Aseptic loosening is a major reason for the failure of the artificial joint accounting for greater than 70% of the revision surgeries [146]. This loosening occurs due to osteolysis around the joint known as periprosthetic osteolysis. As a result of osteolysis (bone degradation), the tight fit between the artificial joint and bone is lost, resulting in micromotion causing joint instability, pain and ultimately need for revision surgery [6]. Revision surgeries are more complicated and less reliable than primary joint replacement surgeries due to the osteolysis around the implant and hence require special bone grafting techniques [6]. In 2004, about 46,000 revision surgeries were performed in the US each costing an average of $45,000 [143].

The majority of hip joints that are replaced in the US have a metallic or ceramic femoral stem and a metal ball articulating with a UHMWPE acetabular cup liner [147-149]. UHMWPE is widely used in orthopedic implants because of its higher impact strength and abrasion properties compared to other polymeric materials [150]. In spite of UHMWPE having better wear resistance and mechanical characteristics compared to other materials, due to the constant motion/cyclic mechanical load at the joint results in

the UHMWPE liner wearing out and generation of micron sized wear debris particles [148]. The wear debris consists of particles derived from the various components of the implant including UHMWPE, bone cement in the form of PMMA, or metal, with predominant proportion of UHMWPE particles [147,149]. The size range of the generated wear particles is 0.5-5 μm with bulk of the particles being in the submicron range [151]. The wear particles settle in the space between the joint and the bone where macrophages phagocytose these microparticles and become activated [152]. Activated macrophages release prostaglandins and cytokines such as TNF-α, IL-1β, IL-6 and PGE-2 which lead to activation of bone resorbing pathways via formation of osteoclasts leading to periprosthetic osteolysis [152]. Extensive research is focused towards development of bearing surfaces with better frictional and wear properties in order to reduce wear debris generation. However friction and wear cannot be completely eliminated. In order to mitigate the problem of peri-prosthetic osteolysis various pharmacological approaches targeting cytokines such as TNF-α [153-155] as well as use of biophosphanates [156,157] have been investigated. Since activated macrophages and the cytokines they secrete ultimately lead to the problem of aseptic loosening, they are potential targets for therapeutic intervention.

Role of Macrophages in Wear Debris Induced Periprosthetic Osteolysis

Microparticles settle in the space between the implant shaft and the bone. Macrophages phagocytose these microparticles and become activated giving rise to an inflammatory response [152]. An analysis of tissue explanted from patients undergoing joint revision surgeries indicates that the pseudosynovial membrane formed around the artificial joint is rich in macrophages and foreign body giant cells (FBGC) associated with UHMWPE particles [147,158-161]. Since the UHMWPE particles are not

biodegradable, they are not cleared from the body when macrophages phagocytose them. When the amount of wear particles generated exceed the clearance capacity of macrophages, the particles persist in the body, form granulomatous tissue and lead to chronic inflammation [162]. The activated macrophages release prostaglandins, cytokines, metalloproteinases and lysosomal enzymes such as TNF-α, IL-1β, IL-6, and PGE-2 which lead to activation of bone resorbing pathways [7,152,163,164]. IL-1, IL-6 and TNF-α have been reported to stimulate differentiation and maturation of osteoclast precursors thus participating in osteoclasts-mediated bone resorption [163,165,166]. Thus there is osteoclast formation, osteolysis of bone around the implant and ultimately implant loosening [167]. A schematic of the process of aseptic loosening is depicted in the Figure 1-1.

Macrophages have integrin receptors on their surface through which they interact with the layer of proteins adsorbed on the wear particle surface resulting in macrophage activation. When cultured in serum-free media with particles free of adsorbed proteins, macrophages exhibit only basal levels of activation, as measured by secretion of IL-1β, IL-6 and TNF-α [42]. Due to their hydrophobic nature, polyethylene wear particles have been shown to activate complement pathway leading to opsonization with iC3b which is a ligand for Mac-1 receptor on macrophages [168]. UHMWPE surfaces have also been shown to adsorb other proteins such as albumin, fibronectin and IgG [169]. Thus disrupting this integrin-protein interaction will down-regulate contact, adhesion and resulting phagocytosis of wear particles by macrophages and open up avenues for mitigating macrophage inflammatory response.

Role of Osteoclasts and Integrins on Osteoclasts

Osteoclasts are the primary cells responsible for bone resorption that leads to peri-prosthetic osteolysis resulting in aseptic loosening of joint implants [170]. Cytokines such as IL-1, IL-6 and TNF-α released by activated macrophages have been reported to stimulate differentiation and maturation of osteoclast precursors to mature osteoclasts which participate in the actual process of bone resorption [163,165,166]. The inflammatory cytokines also cause up-regulation of RANKL on stromal cells [167]. The RANKL on osteoblasts binds to RANK on osteoclast precursors causing them to mature. Osteoclasts actively migrate on the surface of bones and undergo alternating cycles of migration and resorption [171]. Osteoclasts migrate to the site of resorption, bind to bone surface creating a sealing zone between the osteoclasts and bone [172]. The sealing zone provides the perfect microenvironment isolated from the surrounding for the products secreted from the osteoclasts such as acids and proteolytic enzymes that degrade the mineralized bone matrix [173].

The integrins present on osteoclasts surface are $\alpha_V\beta_3$ [174,175], $\alpha_2\beta_1$ [174,175], $\alpha_V\beta_5$ [175] and $\alpha_V\beta_1$ [174,175]. Integrins mediate the migration and attachment of the osteoclasts to the bone surface which involves integrin interaction with extracellular matrix (ECM). For example integrin $\alpha_V\beta_3$ has been shown to play a role in osteoclast migration and formation of the sealing zone [176]. Integrin $\alpha_2\beta_1$ mediates osteoclasts adhesion to native collagen type I [177]. Thus, integrins are key players in the osteoclast resorption process [122].

Surface Modification Approaches to Modulate FBR

Implantation of biomaterials into the body results in initial tissue injury as well as long-term inflammatory responses [5]. Macrophages are recruited to the site of

biomaterial implantation and are the primary mediator of the foreign body response [5,14]. Macrophages and foreign body giant cells (FBGC), formed by fusion of macrophages, secrete reactive oxygen species, enzymes and acidic products which degrade the biomaterial [39]. Furthermore, macrophages secrete inflammatory cytokines which recruit more macrophages and other cell types to the implant site such as fibroblasts, which secrete a collagenous matrix to form a fibrous capsule [39]. All together, this foreign body response is responsible for the isolation and degradation of the implant [178,179]. This limits the function of numerous implanted devices such as cardiac pacemaker leads, electrodes and orthopedic implants [149,180]. Due to the primary role that macrophages play in the body's response to implanted materials, various approaches have been investigated to modulate macrophage interactions with biomaterial surfaces in order to mitigate inflammatory responses [52,181]. Notably, the extent of the inflammatory response mounted by the body has been shown to be influenced by the implant material and its surface properties [5,39]. Because of their unique surface properties, there is great interest in exploring nanostructured materials for potential biomaterial applications.

Nanostructured Materials

Nanostructured materials, whose structural elements have dimensions in the range of 1–100 nm, exhibit unique properties compared to bulk materials due to small dimensions and large surface area relative to volume [182]. These nanostructured materials are being investigated for use in an increasing number of applications such as microelectronics, sensor technology, semiconductors and cosmetics as well as medical applications such as biosensors, tissue engineering and drug delivery vehicles [183].Since biological systems operate in the nanometer size range, nanostructured

materials present possibilities for unique biological interactions. For example, increased osteoblast adhesion and mineralization has been demonstrated on nanostructured surfaces of both titanium dioxide and zinc oxide (ZnO), as compared to micron-sized surface topographies [65]. Interestingly, different cell types have been demonstrated to elicit differential responses to a given nanostructured material. For example, carbon nanotubes have been shown to promote adhesion of osteoblasts [66] whereas they inhibit adhesion of other cells such as fibroblasts, [184] chondrocytes, [184] smooth muscle cells [184] as well as macrophages [63]. In particular, altered cell adhesion and viability of fibroblasts, umbilical vein endothelial cells and capillary endothelial cells has been reported on ZnO nanorods as compared to ZnO flat substrates [185].

Zinc Oxide (ZnO) Nanorod Surface

Zinc oxide has unique optical, semiconducting, piezoelectric and magnetic properties hence, it is used for different applications in fields such as semiconductors, biosensors and piezoelectrics [186]. Furthermore, ZnO is used in a number of both exploratory and well-established biomedical applications. For example, ZnO nanorods grown on high electron mobility transistors devices have been shown to be highly sensitive for glucose detection, [187] while ZnO has long been used as a component in various biomedical applications such as dental filling materials (e.g., temporary fillings) [188] and sunscreens [189]. Additionally, ZnO has been investigated as a component in topical wound healing ointments [190-192] and is used in commercially available products for the treatment of venous ulcers [193] and acne [194]. Nanoparticles of ZnO are also known for their anti-bacterial activity against both gram-negative and gram-positive bacteria [65,195,196].

Due to various biological applications of ZnO, especially as nanoparticles, a number of research groups have investigated the cytotoxicity of ZnO. Cell type-specific results have been reported. Zinc oxide is reported as non-toxic to cultured human dermal fibroblasts [197] and T-cells [196] whereas it exhibited toxicity to neuroblastoma cells [198] and vascular endothelial cells [199].

Implant Infection

Medical implants are being extensively used in every organ of the human body, with success in replacing or repairing physiologic functions. However, a major impediment is implant-associated infections caused by bacterial adhesion to biomaterials, which necessitate implant removal, extended care and prolonged antibiotic treatment [200-202]. This additional care significantly contributes to health care costs. For example, of the 2.6 million orthopedic devices implanted annually in the US, approximately 112,000 (4.3%) become infected [203]. The primary cause of revision surgeries- aseptic loosening has been discussed in detail above however implant-associated infections happen to rank second in the list for reasons for revision surgery especially for knee arthroplasties [204]. The most common cause of infection is the generally non-pathogenic and ubiquitous bacteria S. epidermidis which is normally found on human skin and under normal circumstances is well tolerated by the immune system [205,206]. However, when adherent to implanted surfaces, bacteria develop a protective biofilm resistant to immune and antibiotic attack and can develop multiple resistance to antibiotics [207,208]. Many implant-associated infections therefore require surgical removal of the implant. Estimated costs of implant-associated infections exceeds $3 billion annually in the US [203]. Although Staphylococcus species account for majority (45 to 55%) of orthopedic implants associated infections [209],

Pseudomonas aeruginosa is also seen to be the cause of infections in 4 to 6% of infected orthopedic devices [210].

In order to address this problem, implant coating strategies have been developed with the goal to eliminate initial bacterial adhesion and/or kill adherent bacteria. Various strategies have been investigated. For example, surface coatings which support low levels of protein adsorption, termed non-fouling, including surfaces modified with polyethylene glycol, polyethylene oxide brushes and hydrophilic polyurethanes, demonstrate resistance to bacterial adhesion [211,212]. However, the effectiveness of these coatings toward resisting biofilm formation is limited and results vary depending on bacterial species [213]. A more recent approach is the use of “active” coatings which provide continuous release of bactericidal agents [214-217].

Thesis Outline

This thesis addresses the common issues associated with implanted biomaterials and suggests two separate approached to modulate this response. The first approach is based on macrophage integrins that have been shown to modulate various steps of the macrophage inflammatory response. The second approach is a surface modification approach studying the effect of nanostructured biomaterial surface on macrophage adhesion and viability.

Macrophage response to two classes of biomaterials – particulate and bulk has been investigated and the role of integrins in response to these has been quantified. Chapter 1 provides background of the field and the significance of this project. Chapter 2 details the role of integrins in macrophage response to particulate biomaterials that mimic the wear particles generated from wear of joint implants. Mac-1 and RGD-binding integrins have been investigated for their role in in-vivo osteolysis resulting from the

particulate biomaterial. The steps and mechanisms involved in this osteolysis process are further elucidated by studying macrophage response to these microparticles in vitro. Chapter 3 explores the role of the Mac-1 and TGD-binding integrins in the in-vivo response to subcutaneously implanted bulk biomaterials and explores them as therapeutic targets for modulating the foreign body response. It further explores a drug delivery coating for biomaterials for the delivery of anti-integrin peptides. Chapter 4 present results demonstrating the role of ZnO nanorod surface on adhesion and viability of macrophages and the in-vivo effect of coating biomaterials with the nanostructured coating. Based on the results of Chapter 4, ZnO nanorod surface was investigated as an anti-bacterial surface for common implant-associated infections in Chapter 5. Finally, Chapter 6 gives overall conclusions and recommendations for future work.

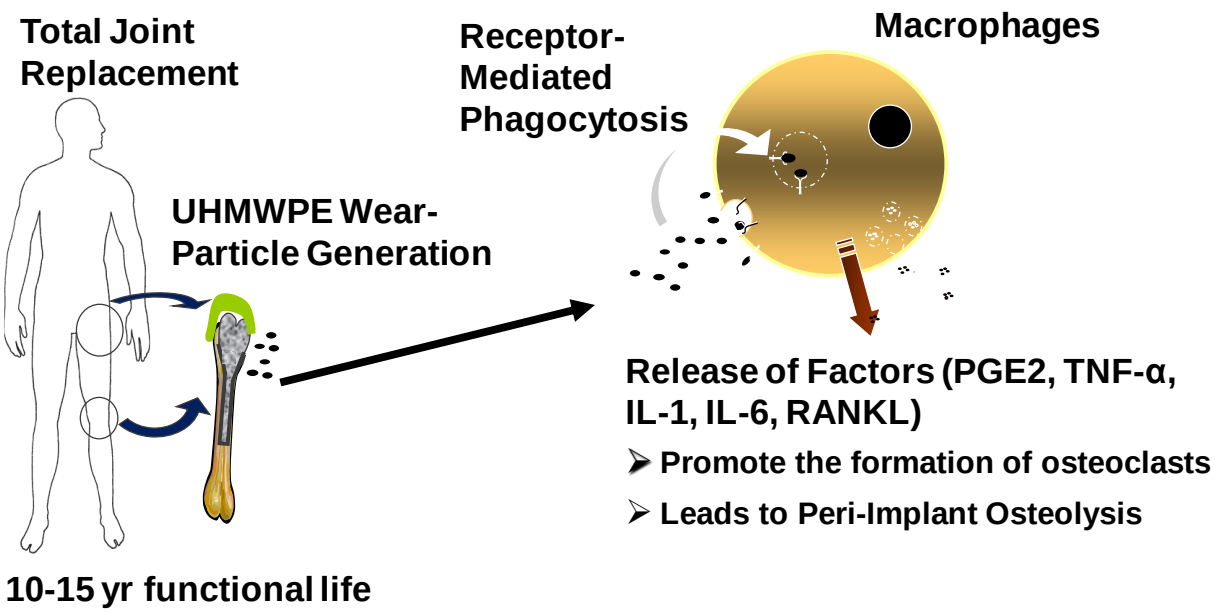

Figure 1-1. Schematic of the process of aseptic loosening resulting from activation of macrophages upon phagocytosis of wear particles.

CHAPTER 2
ROLE OF INTEGRINS IN MACROPHAGE RESPONSE TO PARTICULATE BIOMATERIALS

Background

Aseptic loosening due to peri-implant osteolysis is one of the major reasons for failure of joint implants [218]. This osteolysis results from biological response to wear debris particles generated during mechanical loading of the artificial joints [158]. Joint implants have components made of metals, polymers and ceramics hence, micron size particles of these materials resulting from wear are found in the space between the implant and bone where they mediate the bone resorptive process [147,149,151,158,219]. An analysis of tissue explanted from patients undergoing joint revision surgeries indicates that the pseudosynovial membrane formed around the artificial joint is rich in macrophages and foreign body giant cells (FBGC) associated with wear particles [147,159-161,220]. Macrophages are the scavengers of the body and they attempt to clear the particles by the process of phagocytosis [152]. When the amount of wear particles generated exceed the clearance capacity of macrophages, the particles persist in the body, form granulomatous tissue and lead to chronic inflammation [162]. The activated macrophages release prostaglandins, cytokines, metalloproteinases and lysosomal enzymes such as TNF-α, IL-1β, IL-6, and PGE-2 which lead to activation of bone resorbing pathways [7,152,163,164]. Due to osteolysis the tight fit between the bone and implanted joint established during joint surgery is lost; there is joint instability, pain and need of revision surgery [7]. Revision surgeries are more complicated and less reliable than primary joint replacement surgeries due to the osteolysis around the implant which requires special bone grafting techniques [6]. As

younger and younger people are electing for joint implant surgery, having a longer functional life of the artificial joint is necessary.

Wear debris particles generated in the body are coated with adhesive proteins, which spontaneously adsorb onto the biomaterial surface from the physiologic fluids [5,18]. Macrophages interact with wear particles through the interface of the adsorbed proteins and cell surface receptors called integrins [5,14,77]. Integrins present on macrophages direct various cell functions such as adhesion to extracellular matrix (ECM) proteins, adhesion and signaling to other cell types, cell migration and spreading as well as phagocytosis [83]. As integrins such as Mac-1 present on macrophages direct various inflammatory processes, they serve as ideal therapeutic targets for modulating the macrophage inflammatory response [94-96,221]. Fibrinogen is one of the primary components of plasma deposited on biomaterial surface mediating the acute inflammatory response through phagocyte recruitment to implanted material [17]. Mac-1, a leukocyte integrin present on macrophages and neutrophils functions as a fibrinogen receptor and this receptor-mediated interaction between Mac-1 and fibrinogen has been shown to direct macrophage adhesion and activation [222]. Additionally albumin has been shown to be adsorbed from human serum onto wear particles of various materials (titanium alloy, poly (methyl methacrylate) and critically, polyethylene) and enhance particle-induced macrophage activation [42]. The leukocyte integrin Mac-1($\alpha_M\beta_2$, CD11b/CD18) mediates macrophage adhesion to adsorbed proteins and is shown to direct phagocytosis of titanium-alloy wear particles [99].

Among the mileu of proteins that adsorb onto the biomaterial surface, majority of them such as fibrinogen, fibronectin and vitronectin, contain a tripeptide, Arg-Gly-Asp

(RGD), that serves as the recognition sequence for integrins [101]. Hence, RGD peptide upon binding to integrins on the macrophage surface may compete with protein coated wear particles and arrest the macrophage inflammatory response at the very first step of adhesion. Peptides containing the RGD sequence have been shown to inhibit cell adhesion. For example, RGD peptide is shown to inhibit adhesion of human K562 erythroleukemia cells on fibronectin-coated dishes in a concentration dependent manner [105].

In this chapter, we have investigated the role of integrin Mac-1 and RGD binding integrins in macrophage response to particulate biomaterials such as those generated as wear particles from total joint replacements. To study the role of integrins in particle induced osteolysis in-vivo, polyethylene (PE) MPs were implanted on mouse calvaria and the resulting osteolysis was quantified. For delivering the RGD peptide for receptor blocking to the site of MP implant, discs prepared from ELVAX™ polymer loaded with the RGD peptide were placed over the implanted MPs on the calvarial surface. ELVAX™ is a non-inflammatory and non-biodegradable polymer that has been investigated for slow and sustained release of compounds into the brain [132] as well as tooth space [134].

For the particulate biomaterial system we have used commercially available spherical polystyrene (PS) microparticles (MPs) of 1 μm diameter as well as spherical and oblong PE MPs of size 0.5-5 μm. Macrophage inflammatory response depends on size and shape of phagocytosed particle. Sizes 0.5-5 μm are shown to be most reactive for macrophages [223,224] hence, we have selected MPs in this size range. To study the role of integrin Mac-1 in macrophage response to particulate biomaterials, we

quantify phagocytosis of PS MPs and PE MPs and the subsequent inflammatory cytokine secretion by macrophages harvested from Mac-1 knockout (KO) mice and compare it to wild type (WT) controls. Similar studies were performed to study the role of RGD-binding integrins using RGD peptide for blocking the integrin receptors on macrophages. The RGD peptide binds to the integrins on macrophage surface, blocking the site of binding and thus competing with the protein coated MPs preventing their binding. Additionally, when integrins are bound by a soluble ligand, the soluble ligand cannot generate sufficient force required for integrin signaling which is dependant on a physical resistance force [225]. Integrin signaling upon binding to soluble ligands is incomplete as the full range of signaling proteins found in substrate-immobilized integrin-ligand interaction are not recruited due to the lack of mechanical resistance [226]. This results in cells receiving a negative or unproductive signal regarding its environment and alters cell functioning [227].

Various studies have reported a lack of inflammatory cytokine secretion in the absence of detectable endotoxin levels on the MPs used for macrophage phagocytosis [7,228-230]. Endotoxin refers to the lipopolysaccharide (LPS) complex associated with the outer membrane of Gram-negative pathogens such as Escherichia coli [231]. In order to further investigate the effect of endotoxin in this work, we quantify macrophage particle uptake and subsequent cytokine secretion upon exposure to particles with known amount of endotoxin and compare it to particles with undetectable endotoxin levels (< 0.02EU/ml). We also investigate different receptor-ligand interactions involved in MP uptake and inflammatory cytokine secretion by coating MPs with different opsonizing proteins such as bovine serum albumin (BSA), fibrinogen (Fg), fibronectin

(FN), vitronectin (VN) and serum (Ser) and comparing responses across different proteins.

By studying the phagocytosis, inflammatory cytokine secretion and in vivo osteolytic response of macrophages from receptor knockout mice as well as using integrin blocking studies, we aim to identify and block receptors responsible for macrophage adhesion, phagocytosis and activation in response to biomaterials. Another aspect of macrophage-material interaction is binding of macrophage integrins to proteins adsorbed onto biomaterials which trigger down-stream signaling in the macrophage leading to its activation. Studying this ligand- receptor interaction further increases our understanding of macrophage-biomaterial interactions. Once the role of receptors that mediates foreign body response is delineated, they can serve as a therapeutic target for integrin targeted therapies.

Experimental Procedure

ELVAX™ Disc Preparation for Controlled Release of RGD

In order to deliver RGD peptide to the site of MP implantation, ELVAX™ discs loaded with RGD peptide were prepared by solvent extraction method. Briefly, a 10% (w/v) solution of the ELVAX™ polymer was prepared by dissolving it in methylene chloride. Polymer/drug discs were prepared by mixing the ELVAX™ polymer solution and RGD dissolved in phosphate buffered saline (PBS) (10mg in 50 µL) in a ratio of 6.5:3.5 (v/v) in sealed glass vessels. This solution was agitated vigorously for 15 min followed by sonication in a water bath at 25°C for 15 min. Each disc was made using 35 µL of the resulting dispersion by placing a drop on a treated coverslip, followed by quick-freezing on dry ice and then dried under vacuum to remove any solvent by evaporation. The coverslip was treated with Rain-X to allow easy peeling of the film

from the coverslip surface. The resulting films were 7 mm in diameter and 0.2 mm in thickness. Control discs prepared from ELVAX™™ polymer were prepared similarly.

Determination of Loading and Release Kinetics of RGD from ELVAX™™ Discs

To study the loading efficiency of the RGD peptide into the ELVAX™™ polymer, the discs were dissolved in methylene chloride followed by addition of PBS in order to extract the peptide in the aqueous phase. This emulsion was agitated vigorously for 15 min followed by sonication in a water bath at 25°C for 15 min. The emulsion was then centrifuged at 10000 g for 10 min to enable separation of the oil and water phase of the emulsion. RGD dissolved in PBS was collected and spectrophotometric analysis was used to determine the concentration of peptide encapsulated in the disc.

To study the release kinetics of the encapsulated RGD peptide from the prepared discs, the discs were placed on a shaker in PBS (pH=7.4) at 37°C. The supernatant was collected and replenished with fresh PBS every 3 days. Using spectrophotometric analysis, the concentration of RGD peptide in the supernatant was determined and the release was plotted as a percentage of loaded RGD released over 3 weeks.

Mouse Calvarial Osteolysis Model

To study the role of different integrins in wear particle-induced osteolysis, we used an established mouse calvarial osteolysis model [165,232,233]. UHMWPE microparticles were implanted directly on the surface of the calvarial bone and the extent of osteolysis was quantified using histomorphometry. Briefly, mice were anesthetized with 70–80 mg/kg ketamine and 5-7 mg/kg xylazine. The head of the mouse was shaved and the calvaria were exposed with a one centimeter incision in the frontal plane between the two ears. 6 mg of UHMWPE MPs in 30 µL of FBS was spread on the calvarial surface and the incision was closed using wound clips. Mice designated

as “sham” underwent surgery without particles spread on the calvarium. Mice designated as “vehicle” underwent surgery with 30 µL of FBS without particles spread on the calvarium. Mice were placed in different groups based on the hypothesis to be tested.

Hypothesis 1: Mac-1 integrin plays a role in wear particle induced osteolysis

Group 1: Mac-1 KO mice with 0.1% Serum coated MPs

Group 2: WT mice with 0.1% Serum coated MPs

Control 1: Vehicle - WT mice with 0.1% Serum

Control 2: Sham surgery on WT mice

Hypothesis 2: RGD binding integrins play a role in wear particle induced osteolysis

Group 1: WT mice with 0.1% Serum coated MPs with RGD peptide loaded ELVAX™™ polymer film

Group 2: WT mice with 0.1% Serum coated MPs with blank ELVAX™ polymer film

Control 1: Vehicle - WT mice with 0.1% Serum

Control 2: Sham surgery on WT mice

All the surgeries were performed at the same time. Common groups across different hypothesis tests were not repeated but were used for analysis and comparison.

Seven days post-surgery, mice were euthanized by CO_2 asphyxiation and the calvaria removed for histological processing. The calvaria were fixed in 10% formalin and decalcified using 10% Ethylenediaminetetraacetic acid (EDTA) at 4°C for 7 days. The calvaria were embedded in paraffin and five micron sections were taken in the frontal plane around the area where the MPs were spread and osteolysis was expected. The sections were stained with hemotoxylin and eosin for nuclei (dark blue) and

collagen (pink) and imaged using phase-contrast microscopy (Axiovert 200M Carl Zeiss inverted fluorescent microscope). Area of bone resorption was measured by tracing the area of bone around the midline suture.

Macrophage Generation

Bone marrow-derived macrophages were generated from 7-10 week-old C57BL6/J mice using a 10 day culture protocol [234,235]. Animals were handled in accordance with protocol approved by the Institutional Animal Care and Use Committee (IACUC) at University of Florida. Briefly, mice were euthanized by CO_2 asphyxiation followed by cervical dislocation and tibias and femurs were harvested for isolating marrow cells. Marrow cells were obtained by flushing the shaft of the bones with a 25 G needle using wash media comprising of RPMI™ media (Hyclone Laboratories Inc, Logan, Utah) containing 1% fetal bovine serum (FBS) (Hyclone Laboratories Inc, Logan, Utah) and 1% penicillin-streptomycin-neomycin antibiotic mixture (Hyclone Laboratories Inc, Logan, Utah). The macrophage were cultured in a growth media comprising of Dulbecco's Modified Eagle's Medium (DMEM)/F12(1:1) (Cellgro, Herndon,VA) medium containing 1% penicillin-streptomycin, 1% L-glutamine (Lonza, Walkersville, MD), 1% non-essential amino acids (Lonza, Walkersville, MD), 1% sodium pyruvate (Lonza, Walkersville, MD), 10% fetal bovine serum (FBS) and 10% L-929 cell conditioned media (LCCM). The LCCM serves as an established source of macrophage colony stimulating factor, which pushes the differentiation of marrow cells towards the macrophage phenotype [236]. To produce LCCM, L-929 cells were grown to a confluent monolayer in 150 cm^2 tissue culture flasks. 50 mL media was added to each flask for 7 days after which all the media in the flask was replaced with fresh media for 7 additional days. The media collected at day 7 and 14 was pooled, sterile-filtered and stored at -20°C. From

the isolated marrow cells, the red blood cells were lysed using ACK (Ammonium-Chloride-Potassium) lysis buffer. (Lonza, Walkersville, MD) The precursor cells were isolated using centrifugation, resuspended in macrophage growth medium and then seeded in a tissue culture treated T-flask (day 0) to remove fibroblasts and mature macrophages as they would adhere to the flask. After 48 hours (day 2), the floating cells were collected, resuspended in fresh media and seeded on low attachment plates for 4 additional days. The cells in the low attachment plates were supplemented with 1 ng/mL IL-3 (Peprotech, Rocky Hill, NJ) for expansion of the macrophage precursor cells. Half of the media in the low attachment wells was exchanged on day 4 with fresh growth media. At the end of 6 days, cells were lifted from the low attachment wells by gentle pipetting, re-suspended and seeded on tissue culture-treated polystyrene plates for 2 more days to allow macrophage adhesion and maturation. On day 8, all the media in the wells was replaced with fresh media and at day 10 of culture, the cells were ready for experiment. The purity of the macrophage culture was verified by staining for CD11b (α chain of Mac-1) and F4/80 murine macrophage markers and analyzed using flow cytometry. Macrophages isolated from at least 4 separate mice were used for each type of experiment.

Polystyrene(PS) Microparticle Preparation

For the particulate biomaterial system, we used commercially available fluorescent polystyrene particles Fluoresbrite® YG Microspheres (Polysciences Inc, Warrington, Pennsylvania). Macrophage inflammatory response depends on particle size and shape. Sizes 0.5-5 μm are shown to be most reactive, [223,224] hence we have used commercially available spherical microparticles (MPs) of 1 μm diameter. According to previously published studies, detectable level of endotoxin on MPs has been shown to

be a prerequisite for inflammatory cytokine secretion [228-230]. Hence we have compared phagocytosis and subsequent cytokine secretion of MPs coated with known level of endotoxin to MPs with undetectable endotoxin levels. In order for the particles to have a known amount of endotoxin, the particles were coated with LPS by incubating in 0.7-1.2 µg/mL (depending on the protein to be adsorbed later) LPS solution for 3 hours to obtain a final endotoxin concentration of 100 EU/mL. The LPS coated MPs were then protein coated by incubating with various ECM proteins such as human plasma-derived fibronectin (FN) (BD Bioscience), human plasma-derived vitronectin (VN) (BD Bioscience) and bovine plasma fibrinogen (FG) (Mp Biomedicals) as well as with FBS and Bovine serum albumin (BSA) (Fisher Bioreagents). Species- specific protein sequence homologies, as compared to murine, are as follows: FN – 92%, COL – 89%, VN – 76%, FG – 81% and BSA – 70%; determined by HomoloGene, an online resource made available through the National Center for Biotechnology Information. The concentration of protein solution used for coating is 200 µg/mL and the particles were incubated overnight in the protein solution. The particles are vortexed into the protein solution and allowed to incubate with the protein overnight at 4°C. After overnight incubation, the particles are separated from protein solution by filtration (pore size 0.22 µm) and resuspended in PBS. Analysis of endotoxin on MPs was performed in duplicate with the Chromo-limulus amoebocyte lysate (Chromo-LAL™) assay (Associates of Cape Cod Incorporated, Falmouth, MA).

Endotoxin Testing

A high sensitivity Limulus Amebocyte Lysate (LAL) test was performed to measure the endotoxin level on the MPs coated with or without LPS. 50 uL of the Chromo-LAL™ substrate (Limulus Amebocyte Lysate colyophilized with chromogenic substrate) is

mixed with 50 µl of endotoxin free water containing protein coated MPs in a 96 well plate. The 96 well plate is then read in a microplate reader that has been set to read absorbance at 405 nm every 2 min for 2 hours. A threshold value of 0.2 for absorbance was selected and the time point that the sample crossed the threshold value was used for calculating the endotoxin concentration with the help of a standard curve plotted with the control standard endotoxin (CSE) provided by the manufacturer. The detection limit of the assay at 2 h is 0.04 EU/mL.

Quantification of Macrophage Phagocytosis of PS MPs

1×10^5 macrophages were plated in 96 well tissue culture plates. A predetermined number of fluorescent polystyrene MPs are added to each well in order to feed a fixed number (10, 20 and 40) of particles per cell and incubated at 37°C, 5% CO_2 to allow phagocytosis. Phagocytosis was evaluated at the end of 2, 3.5, 5 and 7.5 hours after two PBS washes to remove MPs not phagocytosed by cells and read in a fluorescent plate reader. The number of MPs phagocytosed was determined from a standard curve obtained by plotting relative fluorescence intensity versus MP number. The results are reported as MPs/cell and normalized for cell numbers by staining cell nuclei with DAPI and measuring fluorescence intensity per well. For the RGD blocking experiments, macrophages were incubated with 1 mM and 10 mM RGD in macrophage media for 1 hour prior to feeding the MPs for quantifying MP uptake at 2 and 24 hours respectively. MP uptake at 2 hours and 24 hours after feeding 20 MPs per cell was quantified as described above.

Quantification of Macrophage Cytokine Production upon Phagocytosis of PS MPs

For quantification of macrophage cytokine production, 1×10^6 macrophages were plated in 12 well tissue culture plates. MPs were added to each well in order to get a cell

to MP ratio of 1:25. The well plates are incubated at 37°C, 5% CO_2 for 24 hours to allow phagocytosis and secretion of cytokines. A negative control of cells incubated with no MPs and positive control of cells incubated with 1µg/mL LPS was also set up to study baseline cytokine secretion and activation by a strong inflammatory signal (LPS). After 24 hours the supernatant is collected and frozen at -20°C for cytokine analysis using sandwich ELISA. The supernatant was assayed for cytokines TNF-α and IL-6 using sandwich ELISA kits (R & D Systems) according to manufacturer's directions.

For the RGD blocking experiments, 1 x 10^5 macrophages were incubated with 2.5 µM RGD in macrophage media for 1 h prior to feeding 20 MPs per cell. After 24 h, the supernatant was collected and frozen at -20°C for cytokine analysis using sandwich ELISA.

Polyethylene (PE) Microparticle Preparation

Polyethylene microparticles form the majority of the wear particles isolated from the periprosthetic tissue harvested from patients undergoing revision surgery [147,149]. The retrieved polyethylene particles are rounded or elongated and in the size range of 0.1-5 µm with a high proportion of submicron size particles [219,237,238]. For mimicking the wear debris particles generated in the body, we have used commercially available UHMWPE particles (Shamrock Technologies, Newark, NJ) in the size range of 0.5-5 µm. Macrophage inflammatory response to wear particles depends on the size and shape of the particles with a size range of 0.5-5 shown to be most reactive [223,224].

PE MP preparation for phagocytosis experiments

In order to visualize and quantify the number of PE MPs phagocytosed by the macrophages the proteins used to coat the particles are fluorescently labeled using

Alexa Fluor® succinimidyl ester fluorescent dyes. Succinimidyl esters provide an efficient and convenient way to selectively link the Alexa Fluor® dyes to primary amines (R-NH2) located on proteins. For protein conjugation the Alexa Fluor dye was mixed with protein (5 mg/mL) according to the desired labeling efficiency and allowed to react by stirring for one hour at room temperature. After one hour, the unreacted dye was separated from the protein solution by centrifugation through spin filters with a pore size of 3 kDa. The particles are vortexed into the protein solution and allowed to incubate with the protein overnight at 4°C. After overnight incubation, the particles are separated from labeled protein solution by filtration (pore size 0.22 μm) and resuspended by sonication into unlabelled protein solution.

PE MP preparation for cytokine experiments

According to previously published studies, detectable level of endotoxin on MPs has been shown to be a prerequisite for inflammatory cytokine secretion [228-230]. Hence we have quantified cytokine secretion upon phagocytosis of MPs coated with known level of endotoxin to MPs with undetectable endotoxin levels. In order to remove any adherent endotoxin on the UHMWPE MPs, they were washed in 70% ethanol for 72 hours by continuous shaking and ethanol change every 24 hours. To coat the clean MPs with a known amount of endotoxin, the particles were incubated with 100% ethanol containing 3-5 μg/mL (depending on the protein to be adsorbed later) LPS for 1 hour. The clean MPs to be used as endotoxin free controls were also incubated in 100% ethanol without LPS. After 1 hour, the MPs are separated from ethanol by spin filtration (pore size 0.22 μm) and resuspended in solutions of various ECM proteins such as human plasma-derived fibronectin (FN) (BD Bioscience) and bovine plasma fibrinogen (FG) (Mp Biomedicals) as well as with FBS and Bovine serum albumin (BSA) (Fisher

Bioreagents). The concentration of FN,Fg and BSA used for coating was 250 µg/mL and serum was 5% in PBS. MPs with or without LPS coating were incubated with protein solutions for 2 hours after which the endotoxin levels on the MPs was measured.

The size distribution of the particles with different adsorbed proteins was determined using LS1320 Coulter counter (PERC, University of Florida) to ensure different proteins do not change the size distribution of MPs due to aggregation. The size and surface properties of MPs were also visualized using Scanning Electron Microscopy (SEM). (MAIC facility, University of Florida).

Inverted Cell Culture Technique for Phagocytosis of UHMWPE MPs

The density of UHMWPE is 0.94g/cm^3 which is lesser than water (1g/cm^3) hence when suspended in media, the MPs float to the surface and don't make contact with macrophages adherent on well bottom. A number of studies have used various techniques to confine the MPs to the bottom of well plates. For example, Harada et al. have embedded polyethylene particles in agarose solution coated on the bottom of the wells and cultured macrophages on the agarose layer to ensure cell MPs contact [239]. Shanbag et al. suspended the particles in serum and coated well bottoms followed by macrophage seeding [240,241]. The disadvantage of such techniques is the limited interaction of the macrophages with the confined particles. Rao et al. have used well plates sealed with silicone sheets and inverted to bring macrophages in contact with particles [242]. I created an inverted culture system comprising of a glass coverslip inverted over Viton O rings which keep the coverslip at some height from the bottom of the well as shown in the Figure 2-4. The UHMWPE MPs float up to the surface of the media which is adjusted to be at the level of the coverslip allowing free interaction

between the cells and MPs. Such a free interaction mimics the kind of interaction between macrophages and wear particles in the joint space around the implant.

Quantification of Macrophage Phagocytosis of PE MPs

1 x 10^5 macrophages were plated in 96 well tissue culture plates. A predetermined number of fluorescently labeled protein coated PE MPs are added to each well in order to feed a fixed number (20 and 40) of particles per cell. The wells are filled to the brim, sealed with a sealing tape, inverted and incubated at 37°C, 5% CO_2 to allow phagocytosis. Phagocytosis was evaluated at the end of 2, 3.5, 5 and 7.5 hours after two PBS washes to remove MPs not phagocytosed by cells and read in a fluorescent plate reader. The number of MPs phagocytosed was determined from a standard curve obtained by plotting relative fluorescence intensity versus MP number. The results are reported as MPs/cell and normalized for cell numbers by staining cell nuclei with DAPI and measuring fluorescence intensity per well.

Quantification of Macrophage Cytokine Production

For quantification of macrophage cytokine production, 1 x 10^6 macrophages were grown on 22 x 22 mm glass coverslips.(Fisherbrand, Fisher Scientific) To allow macrophage contact with MPs for phagocytosis, the inverted culture system as described in the previous section was utilized. Protein coated MPs with or without adsorbed LPS were added to each well in order to get a cell : MPs ratio of 1:10. The well plates are incubated at 37°C, 5% CO2 for 24 hours to allow phagocytosis and secretion of cytokines. A negative control of cells incubated with no MPs and positive control of cells incubated with 1µg/mL LPS was also set up to study baseline cytokine secretion and activation by a strong inflammatory signal (LPS). After 24 hours the supernatant is collected and frozen at -20°C for cytokine analysis using sandwich

ELISA. The supernatant was assayed for cytokines TNF-α and lL-6 using sandwich ELISA kits (R & D systems) according to manufacturer's directions.

Statistical Analysis

Statistical analyses were performed using general linear nested model ANOVA, using Systat (Version 12, Systat Software, Inc., San Jose, CA). Pair-wise comparisons were made between the different groups separately for each protein using Tukey's Honestly-Significant-Difference Test with p-values of less than or equal to 0.05 considered to be significant.

Results

Loading and Release Kinetics of RGD from ELVAX™™ Discs

In order to determine the loading efficiency of RGD into the ELVAX™™ discs and determine the exact amount of RGD loaded per disc, the discs were dissolved in methylene chloride and the RGD was extracted into water phase of the emulsion. The loading efficiency of RGD into the ELVAX™™ disc was 92%, with 2.3 mg RGD encapsulated per disc. The release of RGD from the disc was characterized over 3 weeks to estimate the peptide that may be released into the implant site. There is burst of RGD from the discs in the 1st 4 days, releasing about 50% of the encapsulated peptide (Figure 2-1). This is followed by a gradual increase to 65 % of the encapsulated peptide in the next 4 days followed by a plateau phase (Figure 2-1). During the plateau phase there is negligible release of 0.5% of the encapsulated peptide per week for the next 2 weeks of testing (Figure 2-1).

Role of RGD-binding Integrins in MP-induced Osteolysis

In order to determine the role of RGD-binding integrins in particle induced osteolysis, the resulting osteolysis upon implantation of PE MPs along with ELVAX™™

polymer discs releasing RGD peptide was quantified. The area of osteolysis was compared to the calvaria which had PE MPs along with blank ELVAX™™ polymer discs implanted upon it. Control groups of sham, vehicle only and vehicle + blank ELVAX™™ were included to study osteolysis resulting from surgery alone, 0.1% Serum used to resuspend the MPs and the blank ELVAX™™ disc respectively. The area of osteolysis between the control groups vehicle only and vehicle + blank ELVAX™™ was not significantly different hence, they were combined under the vehicle control group.

The area of osteolysis in the mice releasing RGD peptide was 50% lower as compared to the mice with the blank ELVAX™™ discs (Figure 2-2 A), indicating a major role played by RGD binding integrins in the osteolytic process. Hematoxyline and Eosin stained sections of the mouse calvaria from the different groups (Figure 2-2 B,C,D,E) depicting the area of osteolysis(Figure 2-2 D & E, yellow arrows) enable visualization of the difference in area of osteolysis. The area of osteolysis for the MPs and RGD releasing ELVAX™™ samples as well as MPs and blank ELVAX™™ samples was significantly higher than vehicle and sham control groups (Figure 2-2 A). The area of osteolysis between the two control groups sham and vehicle only was not significantly different (Figure 2-2 A), indicating that the 0.1% FBS used as a vehicle to resuspend the MPs does not significantly contribute to the osteolytic process.

Role of Mac-1 Integrins in MP-induced Osteolysis

Using an established model to quantify osteolysis, the role of Mac-1 integrin in wear particle induced osteolysis was quantified. PE MPs mimicking the wear particles generated from total joint replacements in vivo was implanted on mouse calvarium and the resulting osteolysis in 1 week was quantified using histomorphometry. Control

groups of sham and vehicle only were common between the RGD binding integrin and Mac-1 integrin studies.

The area of osteolysis in the Mac-1 KO mouse was 60% lower as compared to WT controls (Figure 2-3 A). Hematoxyline and eosin stained sections of the mouse calvaria from the different groups (Figure 2-3 B,C,D,E) depicting the area of osteolysis (yellow arrows) enable visualization of the difference in area of osteolysis between Mac-1 KO and WT mice. When compared to the vehicle control group, the area of osteolysis in Mac-1 KO mice was not significantly higher (Figure 2-3 A) indicating that the absence of the integrin significantly reverses the osteolytic effect resulting from the MPs.

Purity of Macrophage Culture and Mac-1 KO Macrophages

The percentage of WT macrophages co-expressing CD11b and F4/80 was ~90%, indicating a relatively pure WT macrophage population (Figure 2-4 A). The percentage of macrophages from Mac-1 KO mice expressing CD11b was ~1%, thus confirming absence of the receptor on the macrophage surface (Figure 2-4B).

Role of Mac-1 and RGD-binding Integrins in Macrophage MP Uptake of PS MPs

To explore the role of different ligand-receptor interaction as well as endotoxins in macrophage particle uptake, MPs were coated by adsorption with different opsonizing proteins and LPS respectively. There was no significant difference in the macrophage MP uptake between PS MPs pre-coated with and without LPS (Figure 2-5 A). Macrophages phagocytosed differential number of particles depending on the protein coated on the PS MPs with the highest uptake of MPs for fibrinogen coated MPs and lowest uptake of BSA coated MPs for most ratios and time points tested (Figure 2-6, 2-7 & 2-8).

In order to determine the role of integrin Mac-1 in macrophage MP uptake, we quantified the MP uptake at different cell to MP ratios and different time points for Mac-1 KO macrophages and compared it to macrophages from WT mice. The absence of Mac-1 integrin on macrophage surface down regulates phagocytic uptake of fibrinogen, serum, vitronectin and fibronectin opsonized PS MPs with MP uptake down to 60-85% as compared to WT controls (Figure 2-6, 2-7, 2-8). Uptake of MPs coated with BSA was higher for WT macrophages as compared to Mac-1 KO at lower cell:MP ratio of 1:10 (Figure 2-6). However for higher ratios of 1:20 and 1:40 this relationship is reversed (Figure 2-7 & 2-8).

To determine the role of RGD-binding integrins in macrophage MP uptake, we quantified the MP uptake at cell : MP ratio of 1:20 in a 1 mM (for 2 hours) and 10 mM (for 24 hours) RGD peptide solution in the macrophage culture media**.** At the end of 2 and 24 hours, the number of MPs taken up by the cells was quantified and compared to unblocked samples. At 2 hours, the MP uptake of RGD blocked samples decrease to 30-50% for FN, Fg, Ser and VN coated MPs and 77% for BSA as compared to unblocked samples (Figure 2-9 A). This difference in MP uptake became further amplified at 24 hours when the MP uptake was reduced to 10-30% as compared to unblocked samples for all the protein coated MPs (Figure 2-9 B).

Role of Mac-1 and RGD-binding Integrins in Macrophage Inflammatory Cytokine Secretion in Response to PS MPs

To determine the role of endotoxins adsorbed on MPs in macrophage activation and inflammatory cytokine secretion, macrophages were fed MPs coated with LPS and without LPS. There was a significant difference in the macrophage secretion of TNF-α and IL-6 between MPs pre-coated with LPS and without LPS as MPs without LPS had

undetectable levels (< 30pg/mL) of cytokine secretion (Figure 2-5 B). The role of different ligand-receptor interaction in macrophage inflammatory cytokine secretion was explored by feeding macrophages with MPs coated with different opsonizing proteins and quantifying the resulting cytokine secretion. For Mac-1 KO macrophages, BSA coated MPs had the highest IL-6 and TNF-α secretion as compared to other protein coatings (Figure 2-10 A & B). Additionally, for Mac-1 KO macrophages, FN coated MPs had the higher TNF-α secretion as compared to Fg and Serum coated MPs. For WT macrophages, Ser and FN coated MPs had significantly higher IL-6 secretion as compared to Fg and BSA and significantly higher TNF-α secretion as compared to Fg only (Figure 2-10 A & B).

In order to determine the role of integrin Mac-1 in macrophage inflammatory cytokine secretion, we quantified the secretion of TNF-α and IL-6 upon MP uptake by Mac-1 KO macrophages and compared it to macrophages from WT mice. The absence of Mac-1 integrin on macrophage surface down regulates IL-6 secretion upon uptake of Fg, FN, Serum and VN opsonized PS MPs with a reduction of 30-50% as compared to WT control (Figure 2-10 A). A similar reduction is observed in TNF- α secretion upon uptake of Serum, FN and VN opsonized PS MPs with a reduction of 20-40% as compared to WT control (Figure 2-10 B). There is significant decrease in the TNF-α and IL-6 secretion by Mac-1 KO macrophages for the positive controls incubated with soluble LPS, the secretion was reduced to 20-40% as compared to WT controls. Interestingly, TNF-α and IL-6 secretion for the Mac-1 KO macrophages was 3.4x and 1.3x higher than the WT controls for the BSA coated MPs. All the MP fed samples for Mac-1 KO and WT macrophages were significantly higher than their respective no MP

negative control. For the WT macrophage samples with MPs were significantly lower than the LPS positive control (Figure 2-10). However for the Mac-1 macrophage samples the protein coated MP samples and LPS positive control group were not significantly different (Figure 2-10).

In order to determine the role of RGD-binding integrins in macrophage inflammatory cytokine secretion, we quantified the secretion of TNF-α and IL-6 from WT macrophages upon MP exposure for 24 hours in the presence of 10 mM RGD dissolved in cell media and compared it to unblocked samples. There was a significant decrease in the production of both TNF- α and IL-6 at 24 hours for samples incubated with RGD peptide for all the protein coatings (Figure 2-11 A & B). The decrease in IL-6 secretion was 90% for BSA coated MPs and greater than 98% for all the remaining proteins for RGD blocked samples (Figure 2-11 A) whereas TNF- α levels of blocked samples were below detection limits of the assay (30 pg/mL) (Figure 2-11 B).

UHMWPE MPs Size Distribution

The size distribution of UHMWPE MPs was determined after coating particles with different proteins to verify different protein coated MPs are still in the same size range. It is possible for MPs coated with proteins to form aggregates due to MPs clumping together. Hence, care was taken to ensure that this does not happen to the particle solutions. The MPs coated with different proteins were in the size range of 0.5-5 μm with over 35% of them in the submicron size range (Figure 2-12 A-D). SEM images of the protein coated PE MPs depicts that the MPs are oblong shape and have a rough surface texture (Figure 2-12 E).

Role of Mac-1 Integrins in Macrophage MP Uptake of PE MPs

To explore the role of different ligand-receptor interaction in macrophage particle uptake, PE MPs were coated by adsorption with different opsonizing proteins. Macrophages phagocytosed differential number of particles depending on the protein coated on the MPs with the highest uptake of MPs for fibrinogen coated MPs and lowest uptake of BSA coated MPs for most ratios and time points tested (Figure 2-13 and 2-14).

In order to determine the role of integrin Mac-1 in macrophage MP uptake, we quantified the MP uptake at different cell to MP ratios and different time points for Mac-1 KO macrophages and compared it to macrophages from WT mice. The absence of Mac-1 integrin on macrophage surface down regulates phagocytic uptake of fibrinogen, fibronectin and BSA opsonized PE MPs with MP uptake down to 50-80% as compared to WT controls (Figure 2-13 and 2-14).

Role of Mac-1 Integrins in Macrophage Inflammatory Cytokine Secretion in Response to PE MPs

In order to determine the role of integrin Mac-1 in macrophage inflammatory cytokine secretion, we quantified the secretion of IL-6 and TNF-α upon MP uptake by Mac-1 KO macrophages and compared it to macrophages from WT mice. The inverted culture setup as depicted in the Figure 2-15 was utilized to ensure macrophage contact with the PE MPs as PE MPs are lighter than media and float to the surface. The lack of Mac-1 integrin on macrophage surface down regulates IL-6 secretion upon uptake of BSA opsonized PE MPs with a reduction of 15% as compared to WT control (Figure 2-16 A). The absence of Mac-1 integrin on macrophage surface also down regulates TNF-α secretion upon uptake of Fg, Serum and BSA opsonized PE MPs with a modest

reduction to 80-90% as compared to WT control (Figure 2-16B). There is significant decrease in the secretion of TNF- α and IL-6 by Mac-1 KO macrophages for the positive controls incubated with LPS with secretion reduced to 35% and 75% for TNF-α and IL-6 respectively as compared to WT control (Figure 2-16 A & B). All the MP fed samples for Mac-1 KO and WT macrophages were significantly higher than their respective no MP negative control (Figure 2-16 A & B).

Impact of the Study

Macrophages form the sentinels of the body in response to implanted biomaterials as well as particles generated over time due to wear of these biomaterials [5,152,243]. Macrophages interact with implanted biomaterials, through the layer of physiologic proteins adsorbed on the biomaterial surface and integrin receptors present on macrophage surface [5,14,18,42]. Binding of the integrin receptors initiates a down stream signaling mechanism leading to macrophage activation and release of inflammatory cytokines such as TNF-α, IL-6, IL-1β, prostaglandin-E [152,163,244,245] and chemotactic factors such as MIP-1 β and IL-8 [246]. For non-particulate biomaterials which cannot be phagocytosed by macrophages, macrophages fuse together to form foreign body giant cells which is also an integrin dependent process [82]. Because integrins present on macrophages are involved at the initial stages of material-macrophage interactions, they serve as potential therapeutic targets for modulating the macrophage inflammatory responses to implanted materials. To identify target integrins, we have quantified the role of different macrophage integrins Mac-1 and RGD-binding integrins in inflammatory response to particulate biomaterials using integrin knockout mice and integrin blocking studies.

For the particulate biomaterial system, we first quantified the in vivo osteolysis resulting from implanting polyethylene microparticles on the surface of mouse calvaria. These polyethylene microparticle mimic the wear particles generated from wear of polyethylene liners, one of the apposing components of artificial joint replacements and a major source of wear debris [147,149]. To study the role of RGD binding integrins in the osteolysis response, the particle induced osteolysis was quantified in the presence and absence of RGD peptide eluted from ELVAX™™ polymer discs. The properties of the ELVAX™™ polymer solution and the polymer-drug emulsion were adjusted to achieve release of 70% of the encapsulated peptide within the 1 week of implantation. The area of osteolysis in mice with RGD releasing ELVAX™ discs was 50% as compared to mice with blank ELVAX™ discs. Integrin $\alpha_V\beta_3$ is expressed on activated macrophages [247]. Blocking the macrophage integrin receptors such as $\alpha_5\beta_1$, $\alpha_V\beta_3$ and $\alpha_V\beta_5$ that have an RGD binding site with soluble RGD peptide, prevents interaction and binding of the protein coated MPs (Figure 2-9). When the integrin is bound with a soluble ligand rather than surface-adsorbed ligand, the mechanical resistance required for integrin signaling is insufficient [225]. The cellular signaling molecules that are normally recruited during surface-bound ligand binding are not recruited which affects the strength of the adhesions as well as initiation of other inflammatory signaling pathways [226,248]. This may play a role in the reduction in MP uptake as well as subsequent cytokine secretion upon blocking integrins with RGD peptide (Figure 2-9 & 2-11). Additionally, RGD peptide binds to several integrins present on osteoclasts surface such as $\alpha_V\beta_3$ [174], $\alpha_2\beta_1$ [174] and $\alpha_V\beta_1$ [174]. Osteoclasts actively migrate on the surface of bones and undergo alternating cycles of migration and resorption [171].

Both of these processes involve interaction with extracellular matrix (ECM) which occurs through integrins thus, integrins are key players in the osteoclast resorption process [122]. RGD peptide binding to the integrin receptors is known to disrupts osteoclasts-ECM interaction, prevents binding of osteoclasts to bone surface and prevent formation of a sealing zone which is required for the resorption process [249]. Besides the role of RGD binding integrins in osteoclast functioning, our in vitro data also suggested a major role that these integrins play in macrophage inflammatory response to particulate biomaterials.

The inflammatory response of macrophages has been shown to depend on the size, shape, surface area and texture of the wear particles [223,224] and sizes 0.5-5 μm are shown to be most reactive, [223,224] in the peri-prosthetic osteolysis process. In order to better understand the integrin- protein- microparticle interaction without having to account for changes in size, shape and texture we investigated MPs of a standard size and shape. Hence, the initial experiments were conducted with commercially available fluorescent polystyrene particles Fluoresbrite® YG Microspheres which are spherical and 1 μm in diameter. The PS MPs were coated with different opsonizing proteins in order to study receptor-ligand interactions involved in MP uptake and cytokine secretion. Integrins have a binding specificity to its ligands hence; coating MPs with different opsonizing proteins helps target specific integrin-ligand interactions. We observed ligand specific variations in the uptake of PS MPs with highest uptake for fibrinogen coated MPs and lowest uptake of BSA coated MPs for most ratios and time points tested. Fibrinogen is one of the primary components of plasma deposited on biomaterial surface [17,23], and a ligand for Mac-1 [85], an integrin shown to play a role

in macrophage phagocytosis [94,95]. Upon adsorption onto a hydrophobic biomaterial surface, Fg adopts an energetically favorable conformation thereby exposing the hidden epitopes P1 (γ 190-202) and P2 (γ377-395) which are known to be binding sites for integrin Mac-1 [24].

There have been contradicting reports in the field regarding the role of adsorbed endotoxin on the immunogenicity of the wear particles. Some groups have demonstrated an inflammatory cytokine response with undetectable levels of endotoxin [250,251] where as other have reported a lack of inflammatory cytokine secretion in the absence of detectable endotoxin levels on the MPs used for macrophage phagocytosis [228-230]. Thus, we conducted studies to understand the role of adsorbed endotoxin in our experimental setup. We found that MP uptake does not depend on the level of endotoxin adsorbed on the MPs. However, macrophages that phagocytosed MPs with undetectable levels of endotoxin had undetectable levels of cytokine secretion. . Thus we used a normalized amount (# EU/mL/mg) of LPS adsorbed onto MPs for all the in vitro experiments.

For studying the role of RGD-binding integrins in MP uptake, we blocked RGD receptors using soluble RGD peptide dissolved in cell culture media. At 2 hours after blocking integrin receptors with RGD peptide, the MP uptake was significantly reduced for MPs coated with proteins fibronectin and fibrinogen. At 24 hours, there was significant decrease in MP uptake for all the protein coatings for samples blocked with RGD peptide. A remarkable decrease in the cytokine production at 24 h matching the decreased MP uptake results demonstrates a role of RGD binding integrins in the macrophage inflammatory process. Synthetic peptides containing the RGD sequence

have been shown to compete with adhesive proteins for binding to these integrin receptors, and thus, inhibit integrin-related functions in different cell systems. Along with the MP samples, there was also a complete down regulation in the cytokine secretion from the soluble LPS positive controls when soluble RGD was present. This finding is corroborated by literature showing that integrin α_v is shown to be involved in LPS-induced TLR4 signaling pathways leading to macrophage adhesion and cytokine release [252]. Thus, blocking RGD binding integrins can provide an inflammatory blockade at multiple levels. RGD is the integrin binding site present in several proteins such as fibronectin, fibrinogen, vitronectin and laminin [101] known to adsorb on to biomaterial surfaces. The RGD peptide binds to multiple integrin receptors on macrophage surface such as $\alpha_5\beta_1$, $\alpha_V\beta_3$ and $\alpha_V\beta_5$. Integrin binding by a soluble nature ligand results in an attenuated integrin signal and this may play a role in the reduction in MP uptake and cytokine secretion.

To study the role of Mac-1 integrin in the osteolysis response, the particle-induced osteolysis in Mac-1 KO mice was compared to WT controls. The area of osteolysis in Mac-1 KO mice was 60% lower than WT and not significantly higher than the vehicle control group. The role of Mac-1 integrin in this osteolysis process may be at least two-fold; first through the modulation of macrophage response to wear particles and second through its role in osteoclasts maturation and activation. The integrin Mac-1 has been shown to mediates macrophage adhesion to adsorbed proteins and direct phagocytosis of titanium-alloy wear particles [99]. It has also been reported that blocking the Mac-1 receptor using antibodies against CD11b (α_M) and CD18 (β_2) results in inhibition of osteoclast differentiation in both RAW264.7 cells and bone marrow derived

macrophages upon addition of RANKL [253]. To understand the role of Mac-1 integrin in macrophage response to microparticles, we have further investigated MP uptake as well as subsequent cytokine secretion from macrophages harvested from Mac-1 KO mice and compared it to WT macrophages. The MP uptake and subsequent cytokine secretion upon phagocytosis of PS MPs was initially investigated. The study was then extended to PE MPs as they better mimic the size, shape and material of the wear particles generated in the body from joint implants.

We quantified particle uptake and inflammatory cytokine secretion in response to PS MPs coated with different adhesive proteins and LPS. MP uptake for decreasing cell : MP ratios at various time points starting from 2 hours to 7.5 hours for Mac-1 KO macrophages was compared to WT control. For Fg coated MPs, the MP uptake of Mac-1 KO macrophages is significantly lower than WT (Figure 2-6,2-7 and 2-8). Since fibrinogen is one of the primary components of plasma deposited on biomaterial surface [17], in the absence of integrin Mac-1, a Fg receptor [85], macrophage adhesion is disrupted leading to reduced particle uptake. MPs coated with fibronectin and vitronectin, other Mac-1 ligands [86,88], showed decreased particle uptake for certain ratios and time points tested (Figure 2-6,2-7 and 2-8). Along with Fg, Fn and VN serum coated MPs also showed decreased particle uptake for Mac-1 KO macrophages as compared to WT for ratio 1:20 and 1:40 beyond 3.5 hours as well as for ratio 1:10 at 7.5 hours similar to FN and VN (Figure 2-6,2-7 and 2-8). Fibronectin and vitronectin present in the serum adsorb on to MPs and in the absence of Mac-1 which binds to both fibronectin and vitronectin MP uptake is reduced. BSA coated MPs did exhibit reduced MP uptake for Mac-1 KO macrophages as compared to WT for ratio 1:10 however for

higher ratios this relationship was unexpectedly inversed although the differences were small (Figure 2-7). The differences in the Mac-1 and WT macrophage particle uptake although small, are indicative of differences in the kinetics of macrophage phagocytosis in the absence of Mac-1 integrin. These differences in kinetics may play a role in the recruitment of signaling molecules and contribute to differences in cell signaling and functioning.

We studied the role of integrin Mac-1 in inflammatory cytokine secretion in response to PS MPs at 24 hours upon particle exposure. Similar to the trends seen in MP uptake, TNF-α and IL-6 secretion from Mac-1 KO macrophages is lower than WT for FN, serum and VN coated MPs. IL-6 secretion from Mac-1 KO macrophages is lower than WT for Fg coated MPs. Additionally we see that, TNF-α and IL-6 secretion from Mac-1 KO macrophages is lower than WT for the positive control of soluble LPS. This may be explained by the finding that integrin Mac-1 is shown to form a receptor complex with CD-14 and TLR-4 in response to LPS which is required for expression of the full spectrum of genes [254]. CD-14 does not have a transmembrane component [255] and requires a signaling co-receptor for intracellular signaling.

We conducted experiments similar to PS MPs with PE MPs as PE better represent the wear particles generated in vivo. However, we see that the results of the PS and PE MPs experiments do not follow the same trend for the all the opsonizing proteins. The biggest difference between the results of PS and PE MPs experiments was seen for BSA coated MPs. For PS MPs, the MP uptake and subsequent cytokine secretion was higher for Mac-1 KO macrophages as compared to WT. However, for PE MP this inequality was reversed and MP uptake as well as cytokine secretion from Mac-1 KO

macrophages was lower than WT controls. The uptake of fibrinogen and fibronectin coated MPs was lower than WT for some of the conditions tested however the reduction was not as effective as seen with PS MPs. Cytokine secretion from Mac-1 KO macrophages was reduced as compared to WT for some protein coatings however similar to uptake experiments the reduction was a modest 10-15%. These differences in the response to PS and PE MPs can be attributed to the differences in the material properties, size and shape of the two MP types. The concentration and confirmation of proteins adsorbed on biomaterial surface depend on the surface properties [18]. Upon adsorption proteins can undergo conformational changes to reduce surface energy and thus expose different ligand binding sites thus creating bioactive sites for the interaction of cells with biomaterials [18]. The PE MPs are extremely hydrophobic as compared to PS MPs and it has been shown that proteins that adsorb onto extremely hydrophobic surfaces such as UHMWPE, undergo extensive denaturation/unfolding [14,39,77]. This denturation may result in differences binding sites being exposed on the PE MPs as compared to PS MPs. Integrin Mac-1 is shown to mediate adhesion to denatured proteins [42]. Thus we observe a reduction in the PE MP uptake as well as cytokine secretion for Mac-1 KO macrophages as compared to WT macrophages for BSA opsonized MPs.

Thus we have identified integrins that play a role in the in-vivo osteolytic response which is mediated by osteoclasts but is initiated by macrophage response to particulate wear debris particles. We have further elucidated the mechanisms and ligand-receptor interaction involved in this process by studying MP uptake and subsequent cytokine secretion from macrophages with the integrin knocked out or blocked using peptides.

Thus Mac-1 and RGD-binding integrins can serve as therapeutic target for design of anti-integrin therapies to mitigate peri-implant osteolysis.

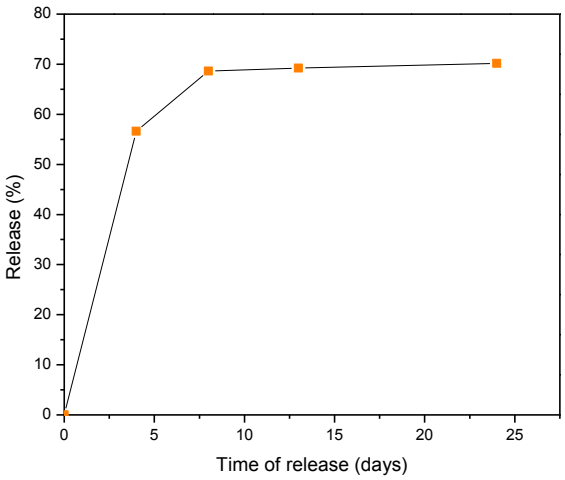

Figure 2-1. Release kinetics of RGD from ELVAX™ polymer disc. Release kinetics were studied at 37ºC in PBS (pH = 7.4) with continuous shaking. Each point represents the mean of 3 samples. The standard deviation was <10% of the respective values.

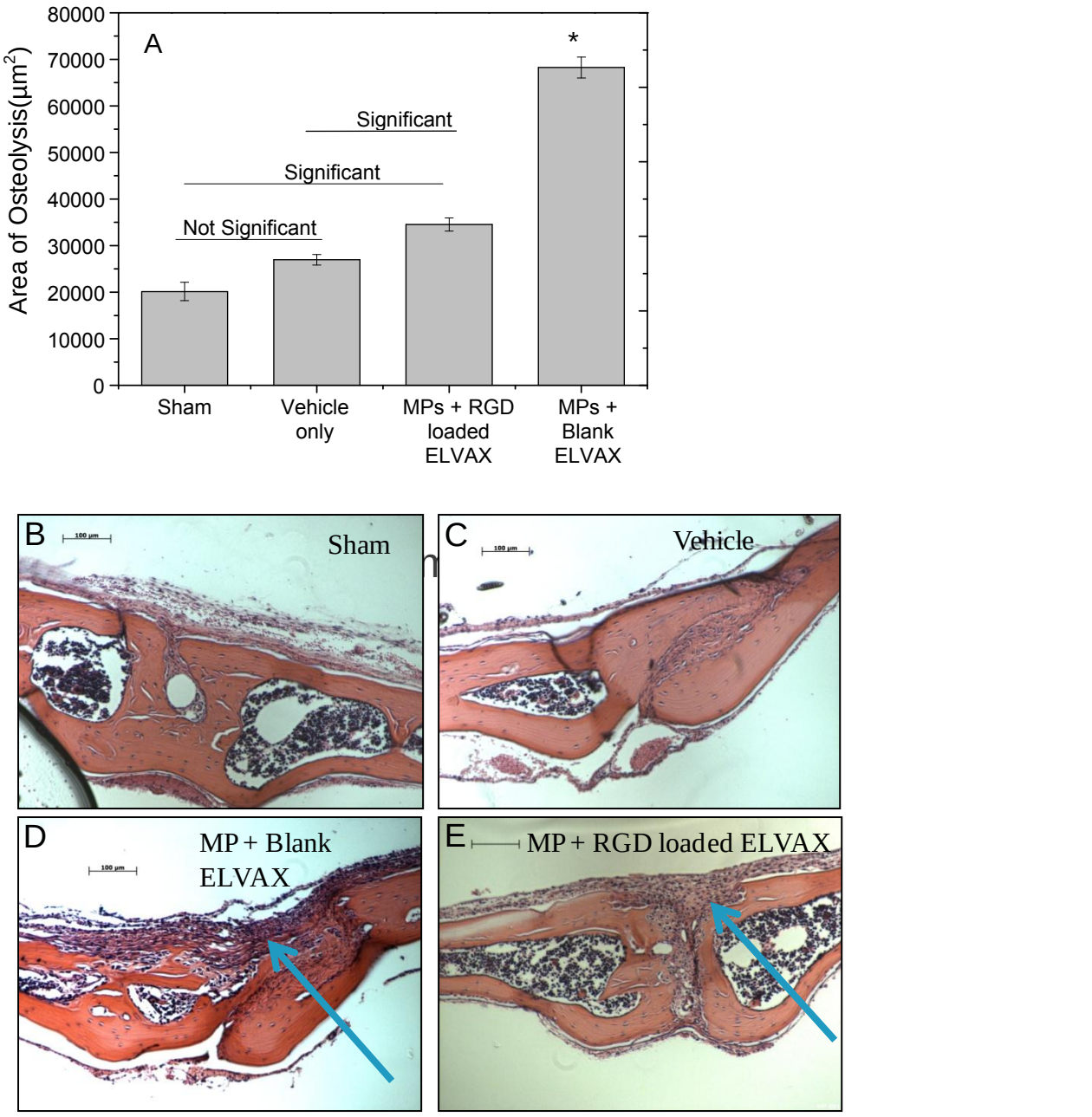

Figure 2-2. RGD-binding integrins modulates osteolysis in response to particulate biomaterials. A) The area of osteolysis around the midline suture (1.5 mm) was quantified at 7 days. The average area of osteolysis was quantified by pooling data from 10 sample points per mouse and 6 mice per group. Plotted are mean and standard error. (* indicates statistically significant difference ($p < 0.05$) from all other groups. Decalcified calvaria were sectioned and stained with Hematoxylin and Eosin for osteolysis measurement. Representative images of calvaria from B) Sham and C) Vehicle D) MP + Blank ELVAX™ and E) MP + RGD loaded ELVAX™ are shown to depict the difference in area of osteolysis. Area of osteolysis is shown with blue arrows

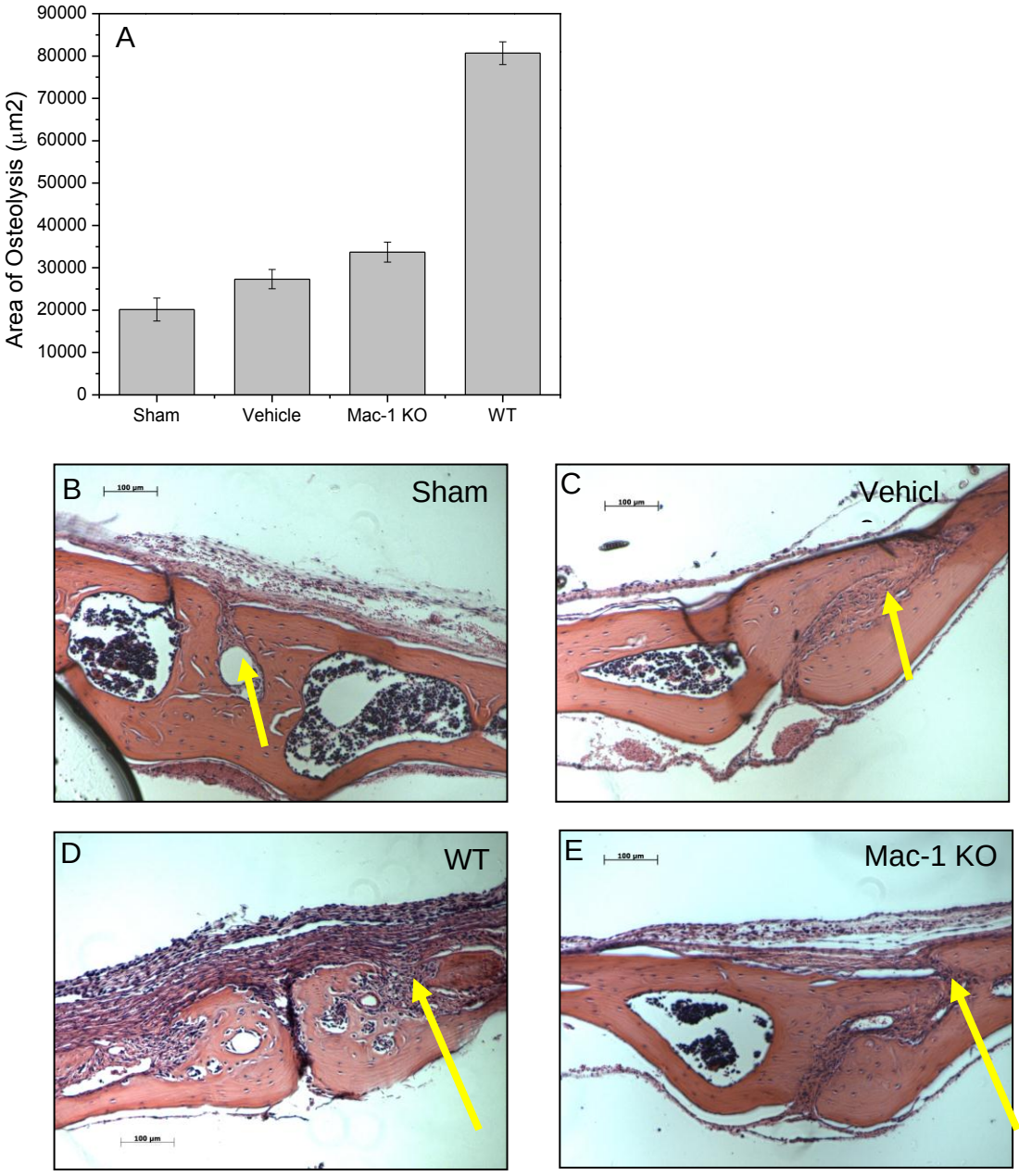

Figure 2-3. Mac-1 integrin modulates osteolysis in response to particulate biomaterials. A) The area of osteolysis around the midline suture (1.5 mm) was quantified at 7 days. The average area of osteolysis was quantified by pooling data from 10 sample points per mouse and 6 mice per group. Plotted are mean and standard error. (* indicates statistically significant difference ($p < 0.05$) from all other groups. Decalcified calvaria were sectioned and stained with Hematoxylin and Eosin for osteolysis measurement. Representative images of calvaria from B) Sham and C) Vehicle D) WT and E) Mac-1 KO are shown to depict the difference in area of osteolysis. Area of osteolysis is shown with yellow arrows

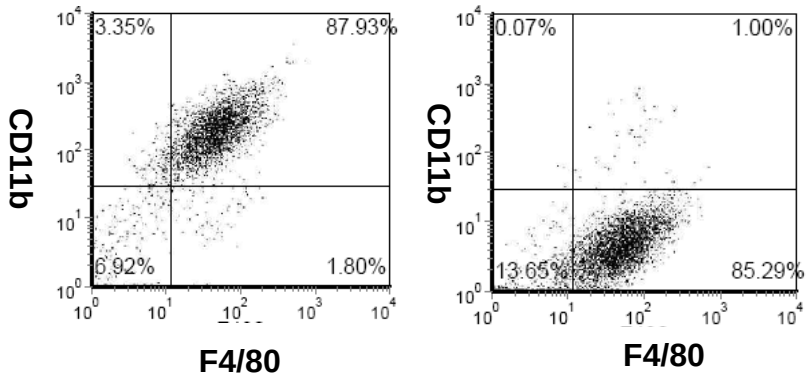

Figure 2-4. A) Purity of the macrophage culture was determined to be ~90% as determined by immunofluorescent quantification of F4/80 and CD11b, murine macrophage markers by flow cytometric analysis. B) The deficiency of Mac-1 receptor on macrophages from the Mac-1 KO mouse was verified by staining for CD11b (α chain of Mac-1). The percentage of cells expressing CD11b was determined to be ~1%

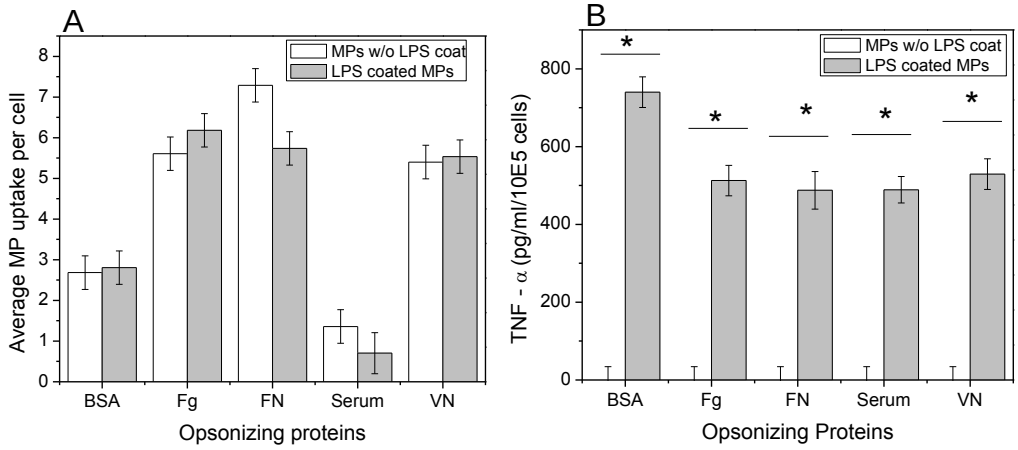

.

Figure 2-5. Presence of endotoxin plays a role in cytokine production upon phagocytosis of LPS coated PS MPs however it does not play a role in MP uptake. A) After feeding PS MPs at cell:MP ratio of 1:20, the MP uptake at 7.5 hours was quantified for MPs coated with or without LPS(100EU/20 million MPs/mL). The average number of MPs taken up by macrophages was quantified by pooling data from at least 9 samples from 3 separate runs. Plotted are mean and standard error. B) Quantification of TNF-α secretion from WT macrophages upon exposure to MPs coated with or without LPS and different opsonizing proteins for 24 hours. The cytokine concentration was quantified by pooling data from 4 samples. Plotted are mean and standard error. (* indicates statistically significant difference ($p < 0.05$) between MPs coated with or without LPS for the same protein coating).

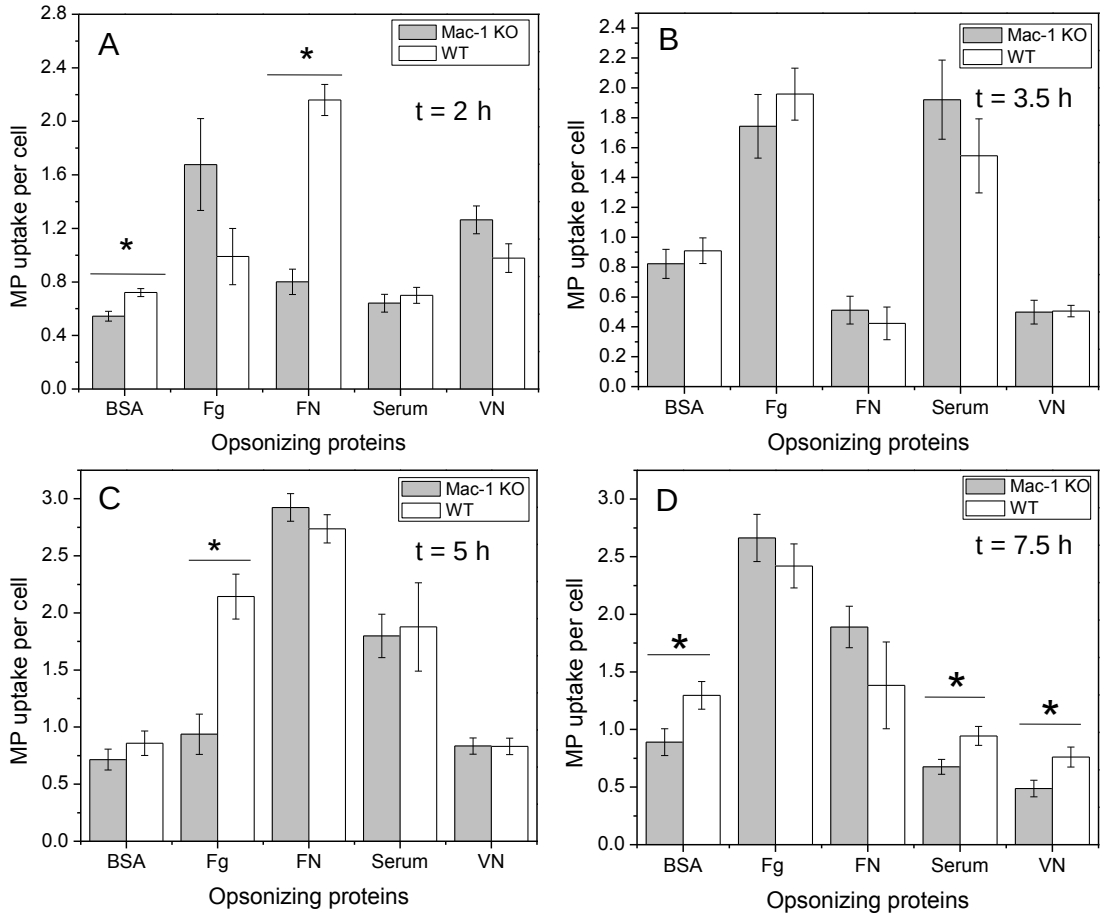

Figure 2-6. Integrin Mac-1 modulates phagocytosis of protein opsonized PS MPs by macrophages. After feeding PS MPs at cell:MP ratio of 1:10, the MP uptake at A) 2 hours B) 3.5 hours C) 5 hours D) 7.5 hours was quantified in Mac-1 KO macrophages and compared to WT control. The average number of MPs taken up by macrophages was quantified by pooling data from at least 15 samples from 5 separate runs. Plotted are mean and standard error. (* indicates statistically significant difference ($p < 0.05$) between Mac-1 KO and WT control samples for the protein coating)

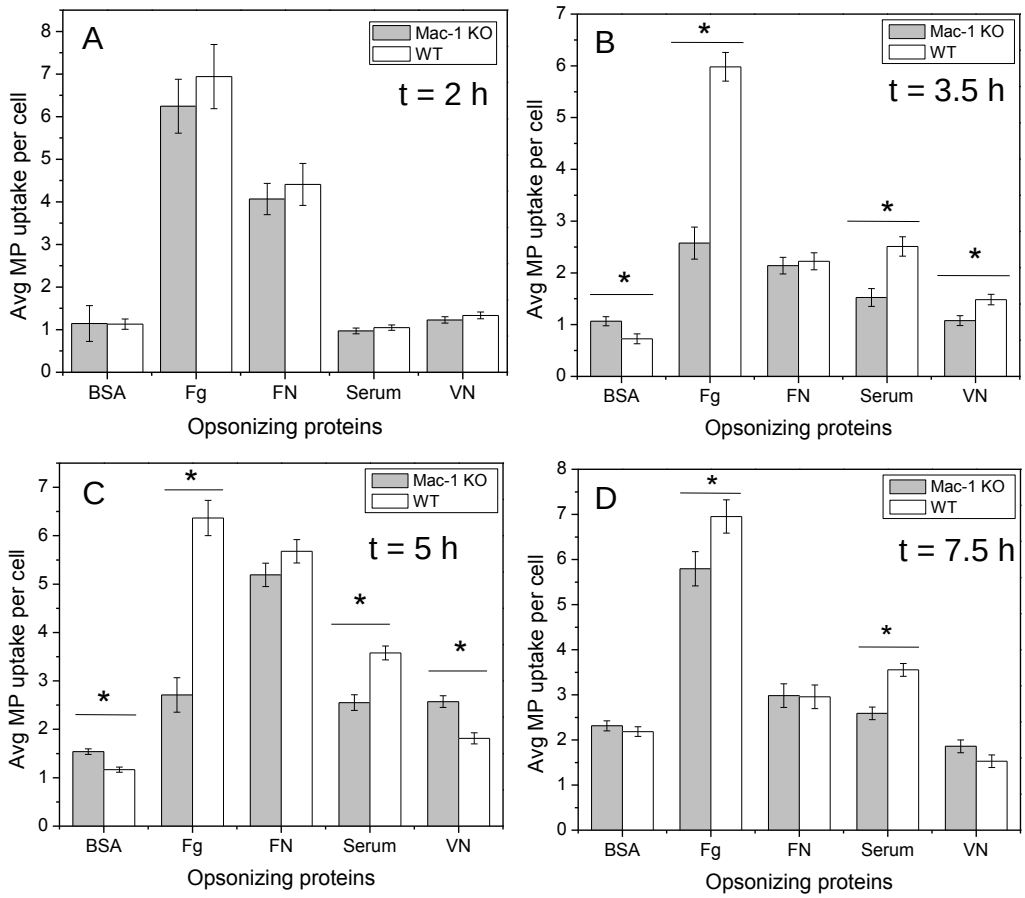

Figure 2-7. Integrin Mac-1 modulates phagocytosis of protein opsonized PS MPs by macrophages. After feeding LPS (100EU/20 million MPs/mL) and different protein coated PS MPs at cell : MP ratio of 1:20, the MP uptake at A) 2 hours B) 3.5 hours C) 5 hours D) 7.5 hours was quantified in Mac-1 KO macrophages and compared to WT control, The average number of MPs taken up by macrophages was quantified by pooling data from at least 15 samples from 5 separate runs. Plotted are mean and standard error. (* indicates statistically significant difference ($p < 0.05$) between Mac-1 KO and WT control samples for the protein coating)

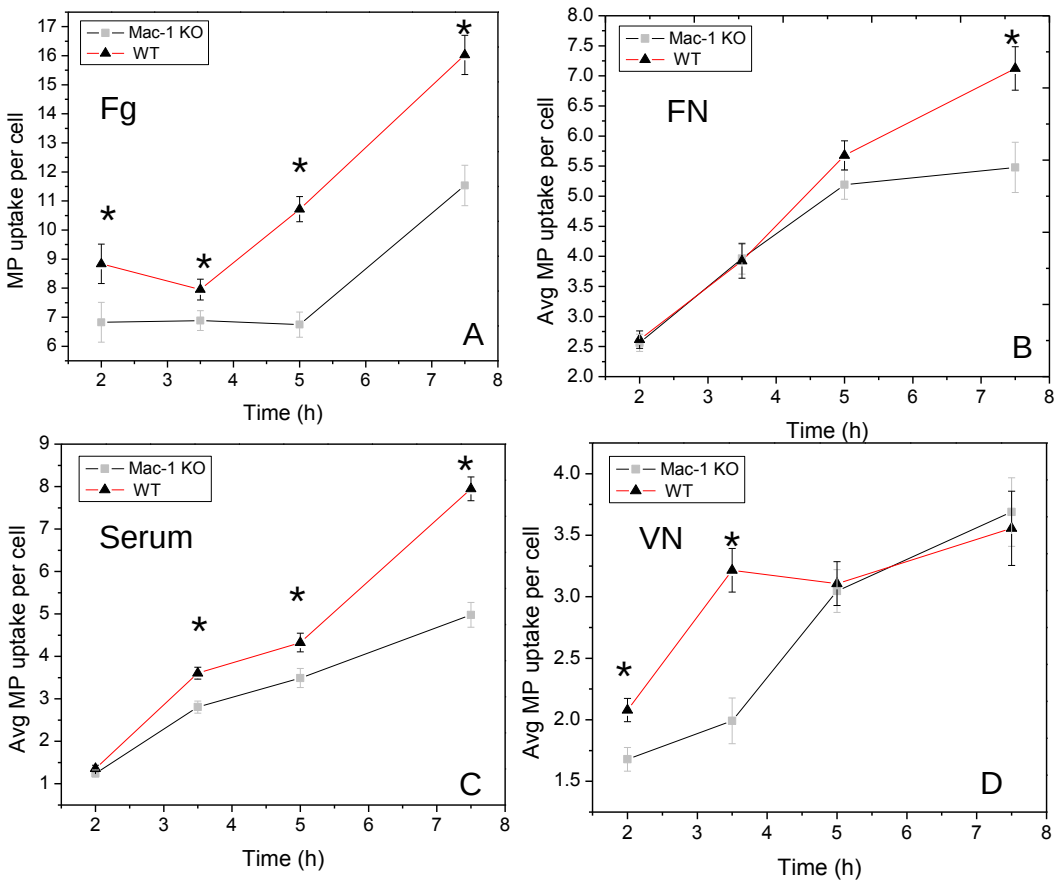

Figure 2-8. Integrin Mac-1 modulates phagocytosis of protein opsonized PS MPs by macrophages. After feeding LPS (100EU/20 million MPs/mL) and different protein coated PS MPs at cell : MP ratio of 1:40, the MP uptake for A) Fg B) FN C) Ser D) VN was quantified in Mac-1 KO macrophages and compared to WT control, The average number of MPs taken up by macrophages from 2-7.5 hours was quantified by pooling data from at least 15 samples from 5 separate runs. Plotted are mean and standard error. (* indicates statistically significant difference ($p < 0.05$) between Mac-1 KO and WT control samples for the protein coating)

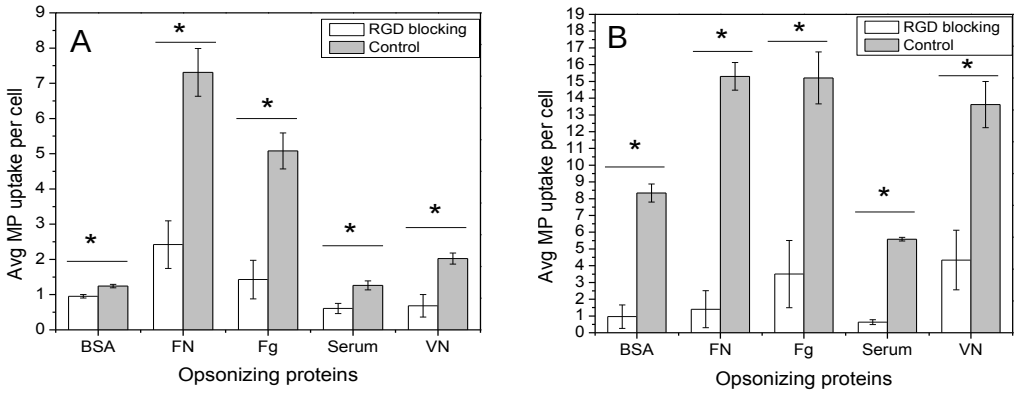

Figure 2-9. Phagocytosis of protein opsonized PS MPs by macrophage is modulated by blocking RGD-binding integrins with soluble RGD peptide. A) MP uptake of LPS (100EU/20 million MPs/mL) and different protein coated MPs at 2 hours after blocking with 1 mM RGD peptide. The average number of MPs taken up by WT macrophages was quantified by pooling data from 18 samples from 6 separate runs. B) MP uptake at 24 hours after blocking with 10 mM RGD peptide. The average number of MPs taken up by WT macrophages was quantified by pooling data from 8 samples from 2 separate runs. Plotted are mean and standard error. (* indicates statistically significant difference ($p < 0.05$) between samples incubated with RGD peptide and control samples for the same protein coating)

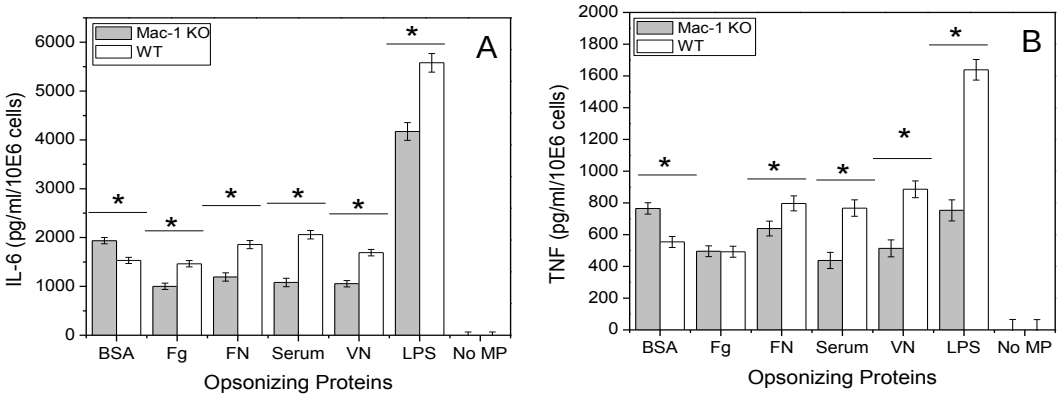

Figure 2-10. Integrin Mac-1 modulates inflammatory cytokine secretion from macrophages upon exposure to protein and LPS coated PS MPs. A) Quantification of IL-6 secretion from Mac-1 KO and WT macrophages upon exposure to LPS(100EU/20 million MPs/mL) and protein coated PS MPs for 24 hours. B) Quantification of TNF-α secretion from Mac-1 KO and WT macrophages upon exposure to protein coated PS MPs for 24 hours. The cytokine concentration was quantified by pooling data from 30 samples from 5 separate runs. Plotted are mean and standard error. (* indicates statistically significant difference ($p < 0.05$) between Mac-1 KO and WT control samples for the same protein coating)

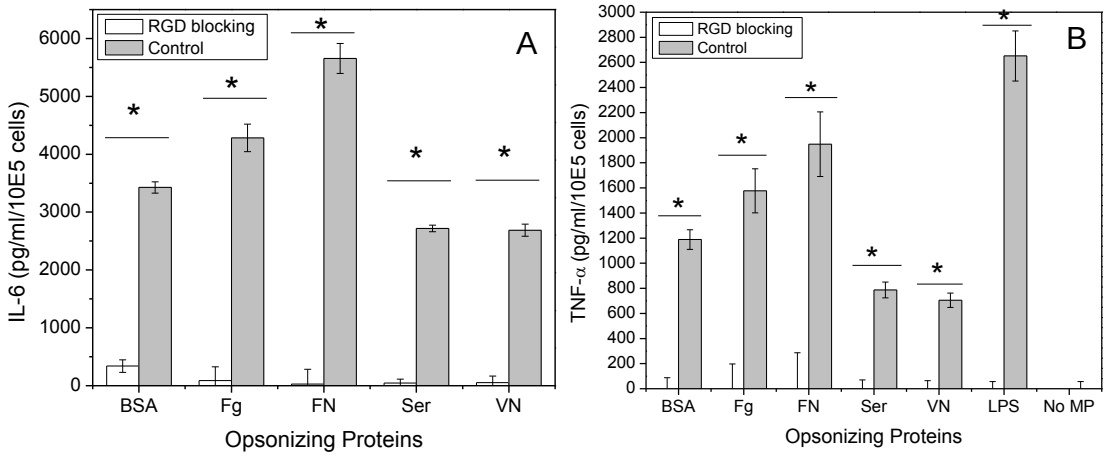

Figure 2-11. Macrophage cytokine secretion upon exposure to protein coated PS MPs is modulated by blocking RGD-binding integrins. A) Quantification of IL-6 secretion from WT macrophages upon blocking RGD receptors by soluble RGD (10 mM) and exposure to LPS(100EU/20 million MPs/mL) and different protein coated PS MPs for 24 hours. B) Quantification of TNF-α secretion from WT macrophages upon blocking RGD receptors by soluble RGD (10 nM) and exposure to LPS and protein coated PS MPs for 24 hours. The cytokine concentration was quantified by pooling data from 6 samples from 2 separate runs. Plotted are mean and standard error. (* indicates statistically significant difference ($p < 0.05$) between RGD peptide and control samples for the protein coating)

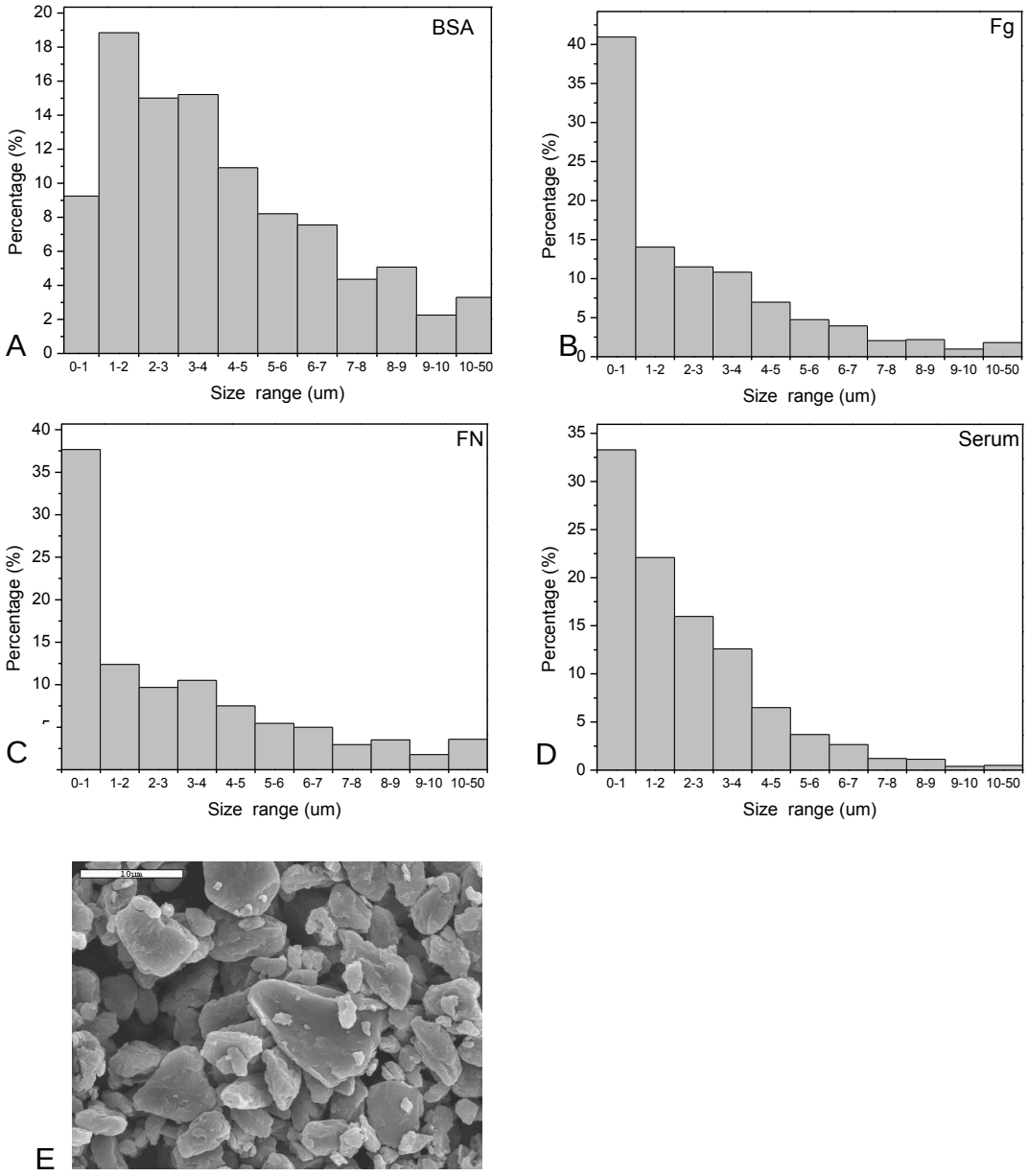

Figure 2-12. Particle size distribution of protein coated UHMWPE MPs. MPs coated with A) BSA B) Fg C) FN and D)Serum were analyzed for size distribution using Coulter counter. E) SEM image of BSA coated PE MP (scale bar = 10 µm) showing the size distribution, shape and surface texture of the PE MPs.

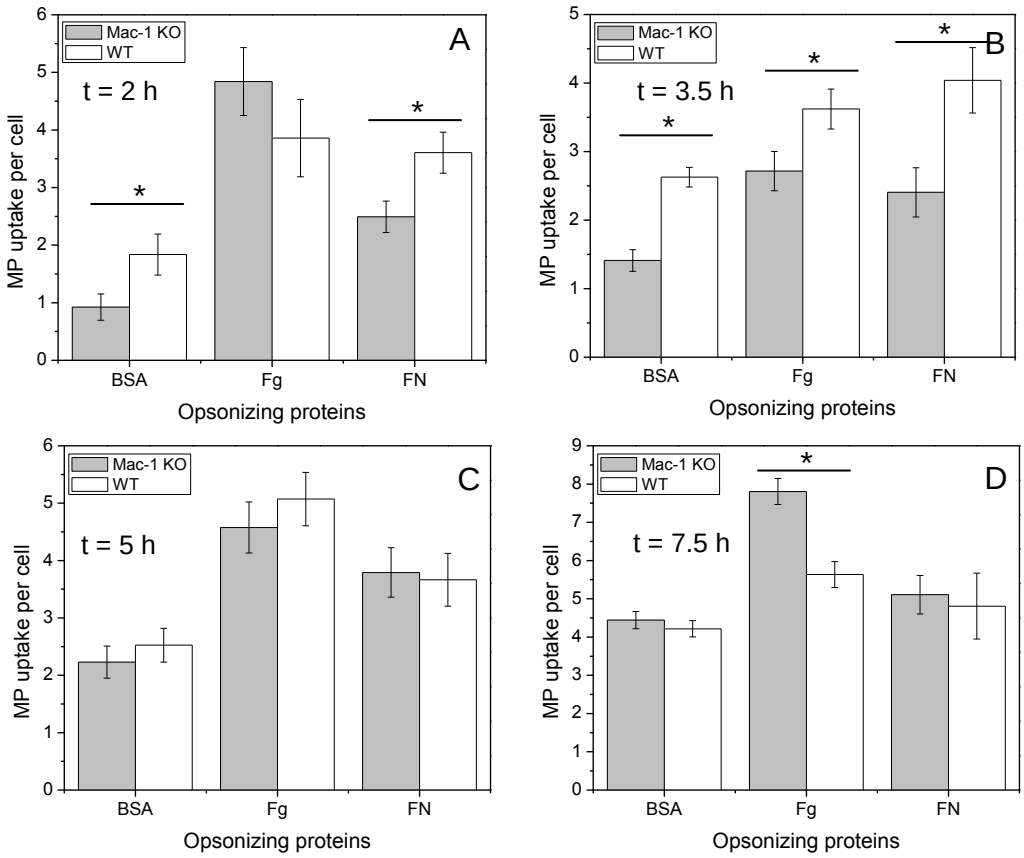

Figure 2-13. Integrin Mac-1 modulates phagocytosis of protein opsonized PE MPs by macrophages. After feeding LPS (100EU/20 million MPs/mL) and different protein coated PE MPs at cell : MP ratio of 1:20, the MP uptake at A) 2 hours B) 3.5 hours C) 5 hours D) 7.5 hours was quantified in Mac-1 KO macrophages and compared to WT control, The average number of MPs taken up by macrophages was quantified by pooling data from at least 24 samples from 4 separate runs. Plotted are mean and standard error. (* indicates statistically significant difference ($p < 0.05$) between Mac-1 KO and WT control samples for the protein coating)

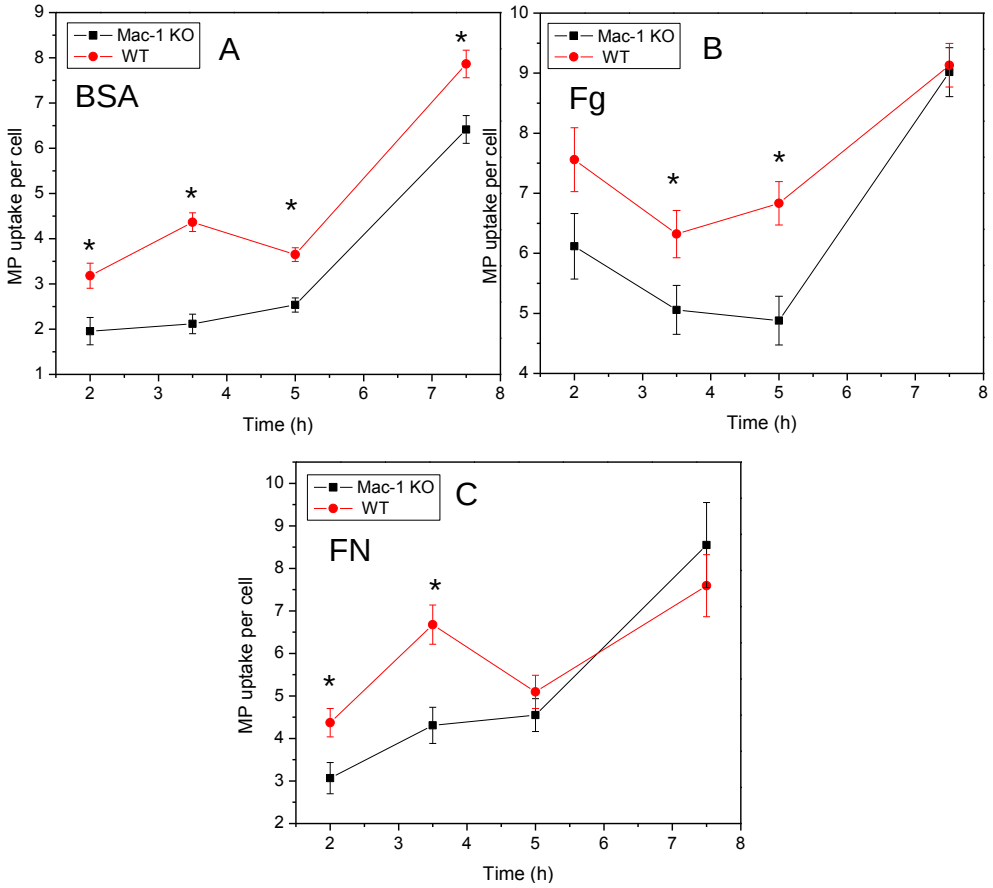

Figure 2-14. Integrin Mac-1 modulates phagocytosis of protein opsonized PS MPs by macrophages. After feeding LPS (100EU/20 million MPs/mL) and different fluorescently labeled protein coated PE MPs at cell : MP ratio of 1:40, the MP uptake for A) BSA B) Fg C) FN was quantified in Mac-1 KO macrophages and compared to WT control, The average number of MPs taken up by macrophages from 2-7.5 hours was quantified by pooling data from at least 24 samples from 4 separate runs. Plotted are mean and standard error. (* indicates statistically significant difference ($p < 0.05$) between Mac-1 KO and WT control samples for the protein coating)

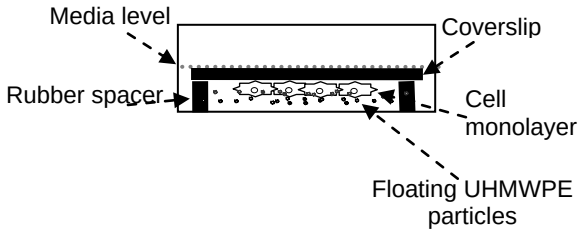

Figure 2-15. Detail of a single well for inverted culture phagocytosis assay. The less dense UHMWPE particles float to the surface of the media where they establish contact with macrophages on the coverslip inverted on Viton O-rings. Such a setup ensures free interaction between cells and particles similar to the interaction in the joint space in the body.

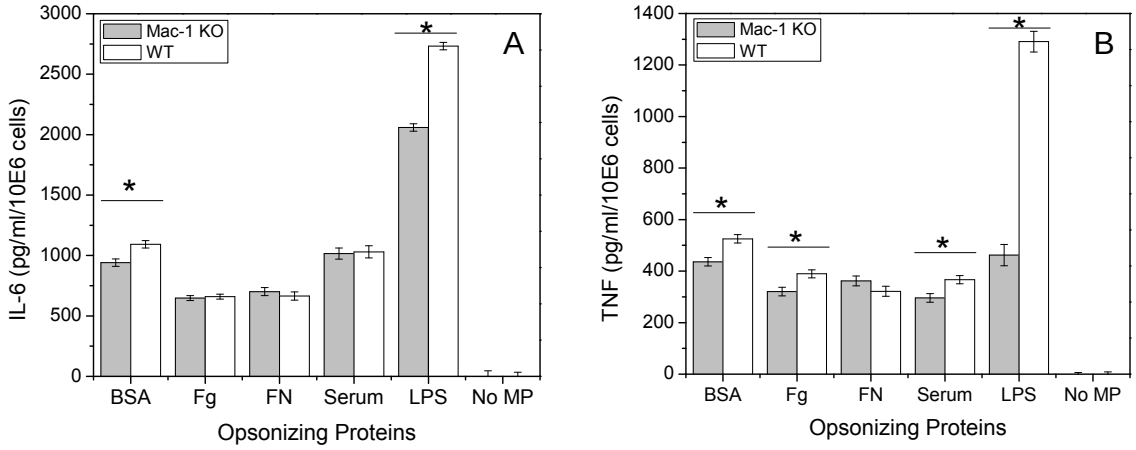

Figure 2-16. Integrin Mac-1 modulates inflammatory cytokine secretion from macrophages upon exposure to protein and LPS coated UHMWPE MPs. A) Quantification of IL-6 secretion from Mac-1 KO and WT macrophages upon exposure to LPS(100EU/20 million MPs/mL) and protein coated PE MPs for 24 hours. B) Quantification of TNF-α secretion from Mac-1 KO and WT macrophages upon exposure to protein coated PE MPs for 24 hours. The cytokine concentration was quantified by pooling data from 24 samples from 6 separate runs. Plotted are mean and standard error. (* indicates statistically significant difference ($p < 0.05$) between Mac-1 KO and WT control samples for the same protein coating)

CHAPTER 3
INTEGRIN-DIRECTED MODULATION OF MACROPHAGE RESPONSE TO BULK BIOMATERIALS

Background

Following the implantation of a biomaterial within the body a series of host immune responses termed as foreign body response ant it which attempt to eliminate or isolate the foreign body [39]. Macrophages play a major role in this foreign body response as they form majority of the cell type recruited to the site of biomaterial implantation and they secrete various cytokines and signaling molecules that lead to material degradation [39]. If the implant is too big for the macrophages to phagocytose, macrophages fuse to form foreign body giant cells (FBGCs) which release reactive oxygen intermediates (ROIs), degradative enzymes, and acid into the space between the cell membrane and biomaterial surface and is shown to mediate degradation of biomaterial surfaces [5,8]. The macrophages and FBGCs along with recruited fibroblasts lead to fibrous encapsulation of the implant [5]. This fibrous encapsulation severely limits the functional performance of several implanted biomaterial such as pacemaker leads, glucose sensors [256], electrodes in vivo [257] and drug delivery devices [11]. For these applications, it is particularly important to have uninterrupted exchange of nutrients and cellular byproducts with the surrounding medium and the fibrous capsule prevents this free exchange. Hence various research groups have been investigating several surface modification approaches for reducing fibrous capsule formation. These techniques focus on reducing protein adsorption on the biomaterial surface, one of the primary and critical steps of the foreign body response. It is critical because macrophages interact with biomaterials through the interface of the adsorbed proteins and cell surface receptors called integrins [5,14,77]. The modification approaches to reduce protein adsorption

include self=assembled monolayers [258], polymer brushes [259] and nanotopographic structures [260]. It is also possible to reduce the fibrous capsule formation by modulating the macrophage response as macrophages play a central role in this process.

Macrophages have integrin receptors on its surface which direct various cell functions such as adhesion to extracellular matrix (ECM) proteins, adhesion and signaling to other cell types, cell migration and spreading as well as phagocytosis [83]. Since integrins present on macrophages direct various processes that are involved in the inflammatory response, they serve as ideal therapeutic targets for modulating the macrophage inflammatory response. Fibrinogen is one of the primary components of plasma deposited on biomaterial surface mediating the acute inflammatory response through phagocyte recruitment to implanted material [17,23]. Mac-1, a leukocyte integrin present on macrophages and neutrophils functions as a fibrinogen receptor and this receptor-mediated interaction between Mac-1 and fibrinogen has been shown to direct macrophage adhesion and activation [222]. Additionally integrin Mac-1 mediates cell adhesion to a number of other proteins that adsorb out of physiologic fluids onto synthetic materials including complement factor fragment C3bi, albumin, vitronectin, and fibronectin [5,48,261]. As integrin Mac-1 present on macrophages direct various inflammatory processes, it may serve as ideal therapeutic target for modulating the macrophage inflammatory response [94-96,221].

Among the mileu of proteins that adsorb onto the biomaterial surface, majority of them such as fibrinogen, fibronectin and vitronectin, contain a tripeptide, Arg-Gly-Asp (RGD), that serves as the recognition sequence for integrins [101]. Hence, RGD

mimetics that target integrins on the macrophage surface may competitively bind to the integrins thus disrupting its binding to the protein adsorbed on biomaterial surfaces. This may arrest the macrophage inflammatory response at the very first step of adhesion. Echistatin, a 49-residue protein purified from the venom of the saw-scaled viper Echis carinatus contains the RGD sequence which is much more potent than the tetrapeptide Arg-Gly-Asp-Phe [125] and binds to integrins such as $\alpha_V ß_3$ through this RGD binding site. Echistatin is shown to inhibit osteoclastic bone resorption in vitro and in vivo by binding to $\alpha_V ß_3$, which is known to modulate osteoclast function [127]. Through its RGD binding site, echistatin can serve as an effective integrin targeted therapy.

In this paper, we have studied the role of the integrins in foreign body response to subcutaneously implanted biomaterials. For subcutaneous implantation of bulk biomaterials, we have used a common biomaterial polyethylene terephthalate which is used in several medical applications such as vascular grafts [262], surgical mesh [263] and sutures. To investigate the role of integrin Mac-1 in the foreign body response (FBR) to implanted biomaterials we implanted PET discs in Mac-1 KO mice and WT controls. The thickness of the collagenous capsule formed around the disc seven days after implantation was used as a measure to quantify FBR. Similarly, to investigate RGD-binding integrins for their role in FBR, we coat the PET discs with ethylene vinyl acetate (ELVAX™) polymer loaded with echistatin which is slowly released by diffusion from the polymer matrix. ELVAX™ is a non-inflammatory and non-biodegradable polymer that has been investigated for slow and sustained release of compounds into the brain [132] as well as tooth space [134]. Once the role of these integrin receptors in

the foreign body response is delineated, they can serve as a therapeutic target for integrin-targeted therapies.

Experimental Procedure

Biomaterial Implantation and Analysis

Discs (7 mm diameter, 0.5 mm thick) were cut from PET sheets, washed, and sterilized by washing in 70% ethanol for 48 hours. At the end of 48 hours the endotoxin level on the discs was determined using Chromo-LAL™ assay and the endotoxin levels on the disc were determined to be below the recommended maximum FDA level. (0.5 EU/mL) Discs were implanted subcutaneously on the mouse's back (n = 4-5 samples/group) in accordance with protocol approved by the University of Florida IACUC committee. The wounds were closed with wound clips, which were removed at day 7 after implantation. PET discs were explanted at 14 days, formalin-fixed and paraffin-embedded. Histological sections (5 μm thick) were stained with hematoxylin eosin stain for nuclei (dark blue) and collagen (pink) and the thickness of the capsule surrounding the disc was determined by bright field microscopy. For studying the role of Mac-1 integrin, discs were implanted in Mac-1 KO mice and WT control mice. For the RGD blocking experiments, echistatin a nonpeptide RGD mimetics was loaded into ELVAX™ polymer. Polymer/ drug coatings were prepared from an emulsion of ELVAX™ copolymer beads (5% by weight) and echistatin (final conc. = 50 μg/mL) in a ratio of 9:1 (ELVAX™: drug) in dichloromethane in sealed glass vessels. This solution was agitated vigorously for 15 min followed by sonication in a water bath at 25°C for 15 min. Approximately 20 μL of solution was then pipetted onto each PET disc and discs were allowed to dry overnight under mild vacuum to remove solvent by evaporation. Control discs with only ELVAX™ coatings were prepared similarly.

Foreign Body Giant Cell (FBGC) Formation

Fusion was induced in expanded macrophages obtained at the end of 10 day culture protocol described in Chapter 2. The macrophages were lifted and replated onto non tissue culture treated 24-well plates with 10E6 cells per well. Fusion was induced by addition of 10 ng/mL recombinant mouse (rm) GM-CSF (R&D Systems) and 10 ng/mL rm IL-4 (R&D Systems) to macrophage growth medium depleted of LCCM. Complete media in the wells was replaced on day 3 and 5 and fusion was analyzed on day 7. Cells with 3 or more nuclei were counted as FBGC as cells with 2 nuclei could be a dividing cell.

Determination of Loading and Release Kinetics of Echistatin from ELVAX™ Coating around PET Discs

To study the loading efficiency of the echistatin into the ELVAX™ polymer, the coating around the PET discs was dissolved in methylene chloride. Water was added in order to extract the echistatin in the aqueous phase and this solution was agitated vigorously for 15 min followed by sonication in a water bath at 25°C for 15 min. The solution was then centrifuged at 10000 g for 10 min in order to separate out the oil and water phase of the emulsion. The water was collected and spectrophotometric analysis was used to determine the concentration of echistatin encapsulated around each disc.

To study the release kinetics of the encapsulated echistatin from the prepared discs, the discs were placed on a shaker in PBS (pH=7.4) at 37°C. The supernatant was collected and replenished with fresh water every alternate day. Using spectrophotometric analysis, the concentration of echistatin in the supernatant was determined and the release was plotted as a percentage of loaded echistatin over a span of 3 weeks.

Statistical Analysis

Statistical analyses were performed using general linear nested model ANOVA, using Systat (Version 12, Systat Software, Inc., San Jose, CA). Pair-wise comparisons were made between the different groups separately for each protein using Tukey's Honestly-Significant-Difference Test with p-values of less than or equal to 0.05 were considered to be significant.

Results

Role of Mac-1 in Foreign Body Response to Implanted Biomaterial

In order to study the role of Mac-1 in foreign body response to implanted biomaterial, we performed subcutaneous implantation of PET discs in Mac-1 KO and WT mice. One of the standard methods to evaluate chronic inflammation to synthetic materials is measurement of fibrous capsule thickness following subcutaneous implantation. PET discs were implanted subcutaneously for 14 days after which a smooth acellular fibrous capsule was formed around the implant as part of the foreign body response that the body mounts against implanted foreign materials. The thickness of the capsule formed around the PET discs implanted in Mac-1 KO mice was significantly thinner as compared to WT controls for the body wall side of the disc as well as the average of both sides (Figure 3-1). The capsule thickness was 40% thinner on the body wall side and 15% thinner on the side facing the skin in Mac-1 KO mice as compared to WT controls (Figure 3-1 A). Overall the capsule thickness in Mac-1 KO mice was 27% thinner as compared to WT controls (Figure 3-1 A). Hematoxylin and eosin stained sections of the disc with the fibrous capsule are depicted for the purpose of visualizing and understanding the difference in the capsule formed around the two groups (Figure 3-1 B).

Role of Mac-1 in Foreign Body Giant Cell Formation

Since the fibrous capsule is composed of macrophages, FBGCs and fibroblast, we investigated the role of Mac-1 integrin in FBGC formation by studying fusion of macrophages to form FBGC and comparing the percentage of fusion to WT controls. There was no significant difference in the percentage of fusion between Mac-1 and WT controls (Figure 3-2).

Loading and Release Kinetics of Echistatin from ELVAX™ Discs

In order to determine the loading efficiency of echistatin into the ELVAX™ coating on the PET discs and determine the amount of echistatin loaded per disc, the polymer coating on PET discs was dissolved in methylene chloride. Echistatin was then extracted into water phase of the emulsion by sonication. The loading efficiency of echisatin into the ELVAX™ disc was 95%, with 12 µg echistatin encapsulated in the polymer around each disc. Next, the release of echistatin from the disc was characterized over 3 weeks to estimate the echistatin that may be released into the implant site. There is burst of echistatin from the discs in the first 2 days, releasing about 20% of the encapsulated echistatin (Figure 3-3). This is followed by a gradual release of 7-10 % of the encapsulated echistatin every 2 days in the next 10 days. After 10 days, there is a plateau phase during the next 7 days when the release echistatin falls to 3-5% every 2 days (Figure 3-3).

Role of RGD-binding Integrins in Foreign Body Response to Implanted Biomaterial

In order to study the role of RGD-binding integrins in foreign body response to implanted biomaterial we performed subcutaneous implantation of PET discs coated with ELVAX™ polymer loaded with RGD-mimetic echistatin. The thickness of the

capsule formed around the echistatin coated PET discs was 15% thinner as compared to only ELVAX™ coated control discs (Figure 3-4).

Impact of the Study

Biomaterial-adherent macrophages are central mediators of the foreign body response, which in some cases results in the isolation and degradation of implanted materials. For many biomedical devices such as sensors, drug delivery devices and implanted electrodes, the foreign body reaction limits implant efficacy [11,256,257]. Since macrophages play such a central role in the response to implanted materials various studies have explored modulating macrophage response using different approaches such as surface chemistry and surface roughness to modulate macrophage adhesion to biomaterials [57-61]. Some of these techniques reduce macrophage adhesion by making anti-fouling surfaces which resist protein adsorption which results in abrogating macrophage interaction with the surface [60]. Nanotopographic surfaces which have features in the nanometer size range have also been explored to modulate macrophage adhesion and function [62,63]. Another link between the macrophages and biomaterial surface are the integrin receptors that bind to the adsorbed protein. Binding of integrins to their ligands leads to integrin clustering and downstream signaling that may result in alteration cell growth, differentiation, migration, attachment and spreading [68]. Macrophages interact with adhesion proteins via integrins, which is evident from the decrease in cell attachment observed in the presence of anti-integrin antibodies [69]. Since integrins play such an important role in macrophage adhesion and activation, we have investigated the role of Mac-1 and RGD-binding integrins in the in-vivo FBR to subcutaneously implanted bioamaterials. The thickness of the foreign body capsule formed around the implant was used as a metric for comparing the FBR. We

saw a 30% reduction in the thickness of capsule formed around discs implanted in Mac-1 KO mice as compared to that implanted in WT mice. Fibrinogen is one of the primary components of plasma deposited on biomaterial surface [17]. Hence, in the absence of integrin Mac-1, a Fg receptor [85], macrophage adhesion to the biomaterial surface may be abrogated. Reduced macrophage adhesion may be one of the reasons for the reduced capsule thickness in the Mac-1 KO mice. Our results from the previous chapter have also demonstrated that integrin Mac-1 plays a role in macrophage activation and cytokine secretion. These cytokines secreted by macrophages at the site of implant signal the recruitment and activation of other cells such as lymphocytes, fibroblasts, endothelial cells, and smooth muscle cells that participate in the various stages of the foreign body response [5]. The reduced cytokine secretion from Mac-1 KO macrophages may result in stunted signaling to other cells that form the fibrous capsule that results in a thinner capsule.

Another cell type that participates in the fibrous capsule formation is FBGC, which is formed by the fusion of macrophages [5]. We have investigated the role of Mac-1 integrin in FBGC formation and there was no significant difference in the percentage of fusion between the Mac-1 and WT macrophages. Thus FBGC formation may be ruled out as a factor contributing to the difference in the capsule thickness.

We observed a 15% reduction in the thickness of fibrous capsule formed around discs secreting echistatin which contains the RGD sequence [125]. Echistatin binds to integrins such as $\alpha_V ß_3$ through this RGD binding site. Blocking the macrophage integrin receptors such as $\alpha_5\beta_1$, $\alpha_V\beta_3$ and $\alpha_V\beta_5$ that have an RGD binding site with echistatin can disrupt macrophage binding to the biomaterial surface. In the previous chapter, we have

reported that RGD-binding plays a major role in the macrophage response to particulate biomaterials. Blocking the RGD-binding integrins with soluble RGD peptide resulted in a 98% decrease in cytokine production by macrophages upon phagocytosis of microparticles. A similar effect can be expected in the macrophage response to bulk biomaterials. The cytokines secreted by macrophages at the site of implant play a major role in recruitment of other cell types that play a role in the foreign body response [5]. The reduced cytokine secretion from macrophages upon blocking RGD-binding integrins with Echistatin may result in altered signaling to other cells that form the fibrous capsule and results in a thinner capsule.

We have identified integrins that play a role in the foreign body response and fibrous capsule formation to subcutaneously implanted biomaterials. Thus Mac-1 and RGD-binding integrins can serve as therapeutic target for design of anti-integrin therapies to reduce fibrous capsule formation.

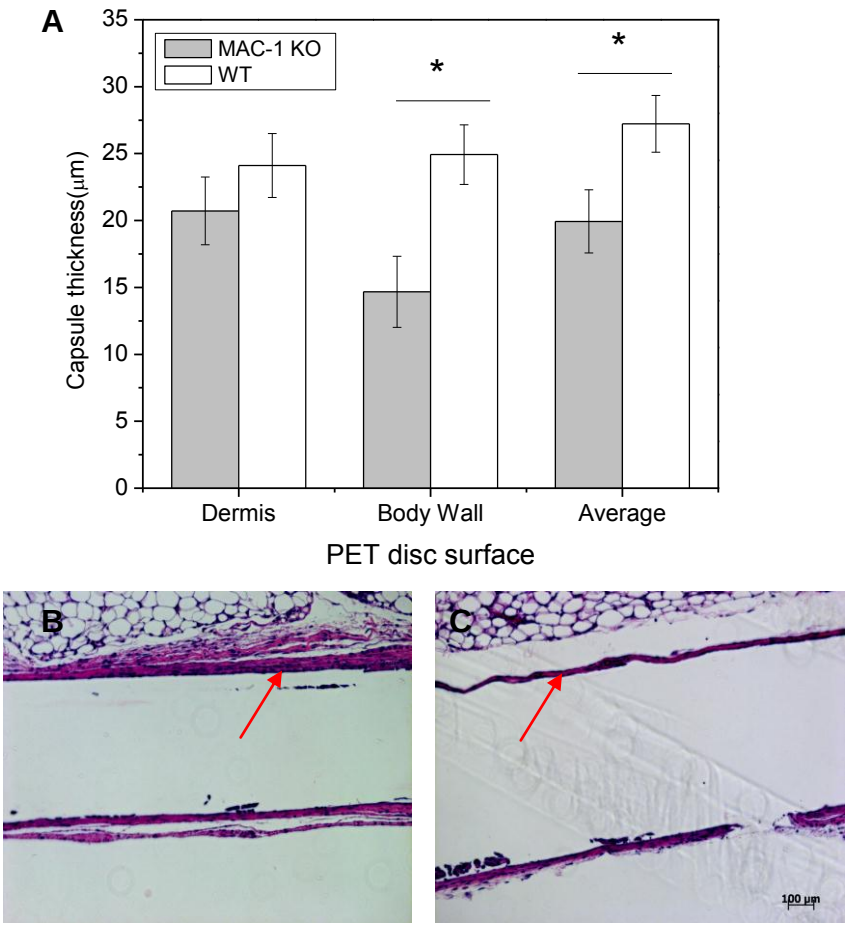

Figure 3-1. Integrin Mac-1 modulates foreign body response to subcutaneously implanted biomaterials. A) The capsule thickness around the implanted PET discs was quantified at 2 weeks for both the dermis side and body wall side of the disc. B and C) Hematoxylin and Eosin stained sections (collagen pink;cell nuclei:dark blue) of tissue response to implanted PET discs. Discs implanted in Mac-1 KO mice (C) had a thinner capsule (indicated by arrow) as compared to WT control(B).

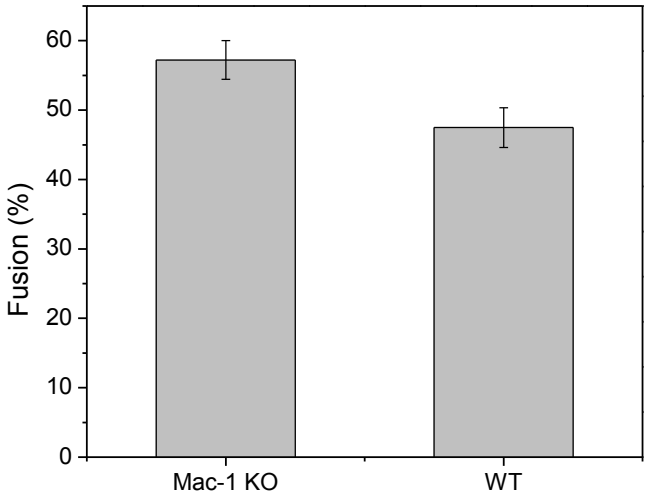

Figure 3-2. Integrin Mac-1 does not play a role in fusion of macrophages to form foreign body giant cells. Macrophage fusion was quantified as the percentage of giant cell nuclei relative to the total number of nuclei. The fusion percentage was quantified by pooling data from 12 samples from 3 separate runs. Plotted are mean and standard error. (* indicates statistically significant difference ($p < 0.05$) between Mac-1 KO and WT control samples

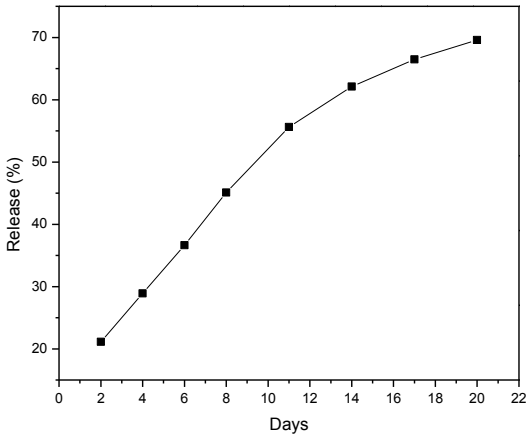

Figure 3-3. Release kinetics of Echistatin from ELVAX™ polymer coating on PET discs. Release kinetics were studied at 37ºC in PBS (pH = 7.4) with continuous shaking. Each point represents the mean of 3 samples. The standard deviation was <10% of the respective values.

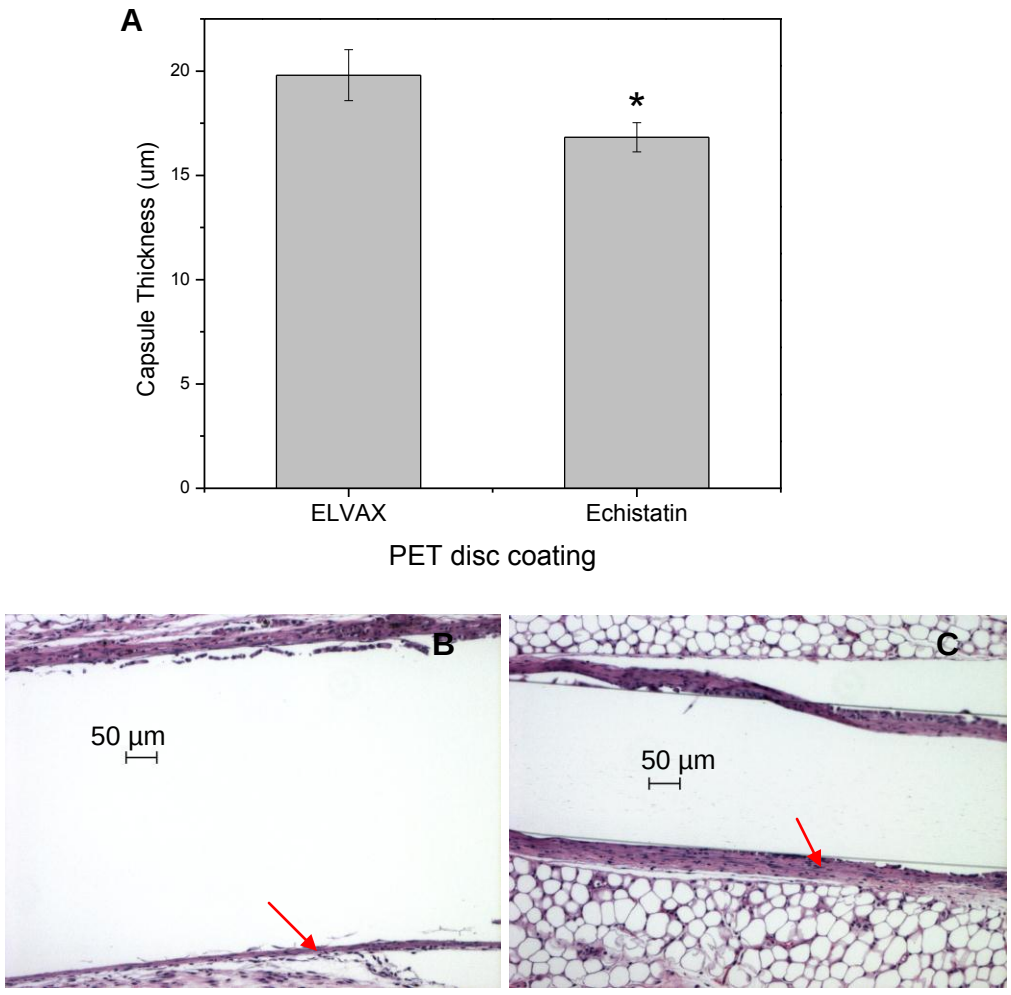

Figure 3-4. RGD-binding integrins modulates foreign body response to subcutaneously implanted biomaterials. A) The capsule thickness around the implanted PET discs was quantified at 2 weeks. Echistatin coated discs had a thinner capsule (indicated by arrow) as compared to ELVAX™ control. B and C) Hematoxylin and Eosin stained sections (collagen pink;cell nuclei:dark blue) of tissue response to implanted PET discs. Discs coated with Echistatin loaded ELVAX™ (B) had a thinner capsule (indicated by arrow) as compared to only ELVAX™ coated controls (C).

CHAPTER 4
CONTRIBUTIONS OF SURFACE TOPOGRAPHY AND CYTOTOXICITY TO THE MACROPHAGE RESPONSE TO ZINC OXIDE NANORODS

Background

Nanostructured materials, whose structural elements have dimensions in the range of 1–100 nm, exhibit unique properties compared to the bulk material due to small dimensions and large surface area relative to volume [182]. These nanostructured materials are being investigated for use in an increasing number of applications such as microelectronics, sensor technology, semiconductors and cosmetics as well as medical applications such as biosensors, tissue engineering and drug delivery vehicles [183]. Because biological systems operate in the nanmeter size range, nanostructured materials present possibilities for unique biological interactions. For example, increased osteoblast adhesion and mineralization has been demonstrated on nanostructured surfaces of both titanium dioxide and zinc oxide (ZnO), as compared to micron-sized surface topographies [65]. Interestingly, different cell types have been demonstrated to elicit differential responses to a given nanostructured material. For example, carbon nanotubes have been shown to promote adhesion of osteoblasts [66] whereas they inhibit adhesion of other cells such as fibroblasts, [184] chondrocytes, [184] smooth muscle cells [184] as well as macrophages [63]. In particular, altered cell adhesion and viability of fibroblasts, umbilical vein endothelial cells and capillary endothelial cells has been reported on ZnO nanorods as compared to ZnO flat substrates [185].

Zinc oxide has unique optical, semiconducting, piezoelectric and magnetic properties hence, it is used for different applications in fields such as semiconductors, biosensors and piezoelectrics [186]. Furthermore, ZnO is also used in a number of both exploratory and well-established biomedical applications. For example, ZnO nanorods

grown on high electron mobility transistors devices have been shown to be highly sensitive for glucose detection, [187] while ZnO has long been used as a component in various biomedical applications such as dental filling materials (e.g., temporary fillings) [188] and sunscreens [189]. Additionally, ZnO has been investigated as a component in topical wound healing ointments [190-192] and is used in commercially available products for the treatment of venous ulcers [193] and acne [194]. Nanoparticles of ZnO are also known for their anti-bacterial activity against both gram-negative and gram-positive bacteria [65,195,196].

Due to various biological applications of ZnO, especially as nanoparticles, a number of groups have investigated the cytotoxicity of ZnO. Cell type-specific results have been reported. Zinc oxide was reported to not be toxic to cultured human dermal fibroblasts [197] and T-cells [196] whereas it exhibited toxicity to neuroblastoma cells [198] and vascular endothelial cells [199].

In this work, we evaluate the response of macrophages to ZnO nanorod surfaces which have previously been shown to modulate adhesion and viability of fibroblasts and endothelial cells [185]. We investigate macrophage adhesion and viability on ZnO nanorod surfaces compared to sputtered ZnO as a relatively flat substrate in order to gauge effects due to surface topography and those intrinsic to the material. Our goal is to explore the potential for nano-structured surfaces to modulate macrophage responses. As macrophage adhesion to biomaterial surface is one of the early steps of the inflammatory response to an implanted material, [5,178,179] a surface which modulates macrophage adhesion may serve to direct the foreign body response.

Experimental Procedure

Fabrication of ZnO Nanorods

ZnO nanorods were made by a solution-based hydrothermal growth method [185,264]. First, ZnO nanoparticles were prepared by mixing 10 mM zinc acetate dehydrate (Sigma Aldrich, St. Louis, MO) with 30 mM of NaOH (Sigma Aldrich, St. Louis, MO) at 58°C for 2 hours. Next, ZnO nanoparticles were spin-coated onto the substrate several times and then post-baked on a hot plate at 150°C to promote adhesion. Seeded substrates were then suspended face down in a Pyrex glass dish filled with an aqueous nutrient solution. The growth rate was approximately 1 μm/h with 100 mL aqueous solution containing 20 mM zinc nitrate hexahydrate and 20 mM hexamethylenetriamine (Sigma Aldrich, St. Louis, MO). To arrest the nanorod growth, the substrates were removed from solution, rinsed with de-ionized water and dried in air at room temperature. For relatively “flat” control samples, ZnO was deposited using a Kurt Lesker CMS-18 Multi Target Sputter Deposition system. In order to compare topographical features, scanning electron microscopy and atomic force microscopy images of substrates were obtained using Raith 150 E-Beam writer and AFM Dimension 3100.

Macrophage Generation

Bone marrow-derived macrophages were generated from 7-10 week-old C57BL6/J mice using a 10 day culture protocol [234,235] as described in Chapter 2.

Substrate Preparation and Macrophage Culture

The two ZnO substrates were grown on 22 mm square glass coverslips (Fisherbrand, Fisher Scientific) which were also was used as glass reference substrates. Prior to cell seeding, the ZnO substrates were sterilized by ethanol wash for

15 min followed by UV treatment for 15 min. The glass coverslips were O_2 plasma etched using a Plasma Preen–II 862 plasma etcher followed by ethanol wash and UV treatment.

In order to examine dynamic behavior of macrophages on nanorods using time-lapse video microscopy, macrophages were cultured overnight on ZnO nanorods. Macrophages were seeded on the nanorod substrate and allowed to adhere for 1 hour after which a time lapse video of individual cells was taken in order to study the change in spread area of the cell over time. Phase contrast imaging of single cells was performed overnight using a Nikon TE 2000 microscope. Images were collected every 1 min for 13 h, using a 40x objective. Cells were stained for actin using rhodamine phalloidin (Molecular Probes, Inc., Eugene, OR) [265].

Adhesion and viability studies were performed using macrophages pre-loaded with calcein [266]. Briefly, macrophages were loaded with 1 µg/mL calcein-AM (AnaSpec Inc, San Jose,CA) in 2 mM dextrose solution by incubating it at 37°C for 20 min, pelleted and resuspended in macrophage culture media. Macrophages in this cell suspension were counted by hemocytometer and 500,000 cells in 3 mL media were seeded onto substrates for 16 hours. The number of cells adherent on the surfaces was quantified at 3 hours and 16 hours post-seeding. At the time of quantification, media was aspirated from the wells and 7-AAD (Beckman Coulter, Fullerton, CA) in 1% BSA was added to the wells as per manufacturer's instruction. Adherent cells that retained calcein and did not stain with 7-AAD were counted as live while 7-AAD positively-stained cells were counted as dead. Three non-overlapping fields were imaged per sample for the purpose of quantifying the total adherent, live and dead cells. Data was

averaged from 6-8 replicates obtained from 3 separate runs. In order to quantify the amount of zinc dissolved in the media due to dissolution of ZnO from the substrates, supernatants were collected at 3 hours and 16 hours of cell culture. Supernatants were analyzed for Zn content using Perkin-Elmer Plasma 3200 Inductively Coupled Plasma Mass Spectroscopy (ICP) system. Data was averaged from three separate samples.

In order to verify whether the cell death was due to apoptosis or necrosis, cells were immunofluorescently stained using antibodies specific to active caspase-3, a marker for cells undergoing apoptosis [267]. The cells were first fixed with 3.7% formaldehyde for 15 min at 4°C. The cells then were permeabalized with 0.5% Triton-X in PBS for 15 min at room temperature. Cells were blocked with 1% goat serum for 1 hour at room temperature followed by incubation with rabbit polyclonal to active caspase-3 (Abcam Inc, MA) for 1 h at room temperature. Cells were then incubated with alkaline phosphatase-conjugated goat anti-rabbit antibody for 45 min at room temperature, washed and then incubated for 20 min with Vector® Red substrate. Vector® Red substrate is cleaved by alkaline phosphatase to produce a red reaction product, visible in bright field microscopy. The number of cells stained red was quantified from images taken from 3 non-overlapping fields to determine the percentage of cell population which was apoptotic at 3 hours and 16 hours.

In order to test the non-contact based toxicity of ZnO substrates, 2 million macrophages per well, in 6-well plates, were exposed to the three substrates placed face-down on top of sterilized Viton O-rings used as spacers to separate the substrates from the cells (Figure 2.5 A). The substrates were maintained in the cultures in this configuration for 7 days, with media change every alternate day. At day 7, the

substrates were removed and 7-AAD was added to the wells in order to stain the dead cells. Phase contrast and fluorescence images of 3 non-overlapping fields per well were taken in order to quantify the number of viable cells adherent on the wells. The data was collected and averaged from 8 replicates obtained from 2 separate runs.

In-vivo Response to ZnO Nanorod Coating

In order to determine the foreign body response mounted against ZnO nanorod-coated biomaterials, polyethylene terephthalate (PET) discs coated with ZnO nanorods and sputtered ZnO were implanted subcutaneously in mice on the dorsal side of the thorax in accordance with a protocol approved by the University of Florida IACUC committee. Uncoated PET discs served as a reference. Two discs were implanted per mouse and there were two animals in each experimental group. Discs (7 mm diameter, 0.5 mm thick) were cut from PET sheets and ZnO nanorods were grown on its surface as described in fabrication of ZnO nanorod section. Prior to implantation, the nanorod coated and uncoated discs were sterilized by washing in 70% ethanol. The wounds were closed with wound clips which were removed at day 7 after implantation. PET discs were explanted at 14 days, formalin-fixed and paraffin-embedded. Histological sections (5 μm thick) were stained with hemotoxylin and eosin stain for nuclei (dark blue) and collagen (pink) and examined by phase-contrast microscopy.

Statistical Analysis

Statistical analyses were performed using general linear nested model ANOVA and Pearson’s correlation, as appropriate, using Systat (Version 12, Systat Software, Inc., San Jose, CA). Pair-wise comparisons were made using Tukey's Honestly-Significant-Difference Test with p-values of less than or equal to 0.05 considered to be significant. The Pearson’s correlation value between live cells at 7 days and zinc

concentration in the cell media was calculated using zinc concentration values at 16 h, for the purpose of simplifying the analysis as media was changed every alternate day during the 7 day culture period.

Results

ZnO Substrate Characterization

Surface topography of the two ZnO substrates was characterized by scanning electron microscopy (Figure 4-1). The nanorods were found to be approximately 50 nm in diameter and 500 nm in height. Furthermore, atomic force microscopy of the sputtered ZnO revealed root mean squared roughness value of 31 nm, while glass substrate had a mean squared roughness value of 0.3 nm. Comparing the length scale of topographical features normal to the surface for the ZnO substrates, the sputtered ZnO length scale is an order of magnitude less than the nanorod length scale (nanorod height), indicating that sputtered ZnO substrates can be used for comparison as a relatively smooth ZnO surface.

Macrophage Adhesion, Spreading and Viability on ZnO Nanorods

In order to qualitatively determine the influence of surface topography on macrophage spreading and adhesion, macrophage spreading on ZnO nanorods was examined by time lapse video microscopy. Macrophages were allowed to adhere for 1 hour on the nanorod substrate following which, a time lapse videos were taken to observe cell spreading over time. Images of a representative cell from the 13 hour time interval are shown (Figure 4-2). At 1.5 hours, the macrophage was well spread however, at 2 hours there was retraction of lamellopodia and at 3 hours the cell was completely rounded. At 6.5 hours protrusions from the well-rounded cell became evident. These protrusions grew in size up to 9 hours after which they remain constant

in size and cellular movement ceased. Further investigation revealed that these protrusions contain actin (data not shown) suggesting cytoplasmic leakage. Compared to the ZnO nanorods, macrophages on the glass substrate remained well spread over the 13 hours time-span (data not shown).

In order to quantify the extent to which ZnO nanorod substrates were able to modulate macrophage adhesion, the adherent number and viability of macrophages on ZnO nanorod surface were compared to that on sputtered ZnO substrates (as a relatively flat ZnO surface) and glass substrates as a reference. The sum of the live and dead cells was computed for total adherent cell number. The most salient feature is that for both 3 hours and 16 hours of culture, the number of viable cells adherent on both nanorod and sputtered ZnO substrates was reduced compared to glass, with the ZnO nanorod substrates supporting the lowest cell numbers (Figure 4-3).

In more detail, at 3 hours there was no difference between the total number of adherent cells on sputtered ZnO and glass; in contrast, the total number of adherent cells on ZnO nanorods was 50% of the total adherent number on glass substrates (Figure 4-3)**.** Furthermore, at 3 hours the number of live cells adherent on sputtered ZnO and ZnO nanorods was 75% and 50% of the number of live cells adherent on glass, respectively. Lastly at 3 hours, the number of adherent dead cells on the sputtered ZnO substrate was 3-fold higher compared to glass while dead cell numbers on the ZnO nanorods and glass were comparable.

At 16 hours the total number of adherent cells on sputtered ZnO was 50% compared to glass, while the total number of adherent cells on ZnO nanorod was 30% compared to glass (Figure 4-3). The number of live cells adherent on sputtered ZnO

and ZnO nanorods was 52% and 12%, respectively, compared to the number of live cells adherent on glass at 16 hours. Finally, at 16 hours the number of dead cells adherent on the sputtered ZnO substrate was 1.3-fold greater than the number of dead cells on glass, while the dead cell number on the ZnO nanorods was 1.6-fold greater than on glass.

In order to investigate the mechanism of macrophage death, cells were immunostained against activated caspase-3, which is expressed by cells undergoing apoptosis [267]. The percentage of total cells positively stained for activated caspase-3 was <1%, indicating the lack of apoptosis and attributing cell death to necrosis. All together, these data suggest that although substrates presenting nanorod topography demonstrated a dramatic reduction in the number of adherent macrophages compared to the control substrates, which could indicate a role for nanotopography– the sputtered ZnO substrates, lacking such nanotopographical features, also exhibited a significant reduction in macrophage adhesion, which strongly suggests that material toxicity of ZnO is a factor in this response.

Dissolved Levels of Zn and Non-contact Based Toxicity of ZnO

A mechanism by which ZnO substrates could induce cell toxicity is through dissolution of zinc into cell culture media followed by cellular internalization. In fact, dissolved zinc has been shown to induce cell toxicity in a cell type-dependent manner via production of reactive oxygen species and disruption of energy metabolism [268,269]. In order to further explore this prospect, we quantified the amount of dissolved Zn present in cell culture media when macrophages were cultured on the substrates for 3 hours and 16 hours, using Inductively Coupled Plasma- Mass spectroscopy (ICP) (Figure 4-4). The amount of dissolved Zn in the cell culture media

was measured to be ~150 μM at both 3 hours and 16 hours for the sputtered ZnO substrate. In contrast, the amount of dissolved Zn in the cell culture media was ~300 μM at 3 hours and 430 μM at 16 hours for the ZnO nanorod substrate. Notably, the level of dissolved Zn in the culture media presents the trend ZnO nanorod > ZnO sputtered > glass, which is the inverse trend of adherent cell viability; glass > ZnO sputtered > ZnO nanorod.

In order to ascertain if ZnO substrates can modulate macrophage numbers through substrate dissolution in the absence of direct contact between cells and substrates, the substrates were incubated 7 days in shared media with macrophages cultured on tissue culture plastic. Substrates were inverted above macrophage cultures by placing substrates on top of O-rings serving as spacers and media was exchanged with fresh media every other day (Figure 4-5 A). The number of viable cells after 7 days of culture in media shared with both sputtered ZnO and nanorod ZnO substrates was approximately 50% the number of viable cells cultured with glass substrates (Figure 2-5 B). Significant differences in viable cell numbers were not detected between sputtered ZnO and nanorod ZnO substrates. These data demonstrate that ZnO substrate dissolution occurs and those dissolution products modulate viable macrophage numbers.

Foreign Body Response to Zinc Nanorod Coated PET

Although in vitro analysis provides valuable insight into adhesion, viability and toxicity to ZnO substrates, it cannot adequately represent the body's response to an implanted material. Furthermore, the use of ZnO in current medical applications motivated additional in vivo analysis. Histological analysis of fibrous capsule formation subsequent to subcutaneous implantation was performed as an established means to

evaluate chronic inflammation to implanted materials [5,270]. Polyethylene terephthalate (PET) discs were coated with ZnO by sputtering or through growth of ZnO nanorods (Figure 4-6 A) and uncoated PET discs were utilized as reference. Coated and uncoated PET discs were implanted subcutaneously for 14 days. Histological analysis of explanted discs demonstrated that the uncoated PET discs implanted subcutaneously had a smooth acellular fibrous capsule (Figure 4-6 B). In contrast, surrounding the discs coated both with sputtered ZnO and ZnO nanorods there was an elevated number of accumulated leukocytes and a lack of a continuous fibrous capsule (Figure 4-6 C & D), representing unresolved inflammation, likely a result of cell necrosis indicated from in vitro studies.

Impact of the Study

Nanotopography has previously been shown to modulate cell adhesion and function [62,65,66,184,185,198,271-273]. Depending on the cell type, the effect of nanoparticles or nanostructures such as nanoposts, nanopits, nanotubes and nanoislands varies from enhanced cell function [65,66] to toxicity [198,272]. In particular, ZnO nanorods, nanowires, and nanotubes are attractive for biosensing applications, given their chemical stability, high specific surface area, and electrochemical activity [186,274-277]. Furthermore, engineering ZnO nanorods with well-controlled aspect ratio and spacing has been demonstrated [278]. Our interest in ZnO nanorods was to investigate their potential as a well-controlled nanotopography model system to modulate macrophage adhesion and subsequent responses. Biomaterial-adherent macrophages are central mediators of the foreign body reaction, which results in the isolation and degradation of implanted materials. For many biomedical devices such as sensors, drug delivery devices and implanted electrodes,

the foreign body reaction limits implant efficacy. Biomaterial surface engineering approaches to modulate cell adhesive responses have precedent in general [30,31,266,279-281] and for macrophages in particular [282]. Furthermore, ZnO nanorods have previously been reported to modulate cell adhesion and anchorage-dependent viability in a cell type-dependent fashion [185].

Our investigation of macrophage adhesion demonstrated the ability of ZnO nanorods to dissuade macrophage adhesion. At the earlier time point of 3 hours, the number of adherent macrophages on ZnO nanorods was half that of glass and this reduction in adhesion furthered by 16 hours. Additionally, at 3 hours, the number of dead cells on the ZnO nanorod was low, equivalent to that of glass, although this number increased 30% by 16 hours. Taken in isolation, these data could be viewed optimistically as a feasible means to modulate macrophage adhesion with ZnO nanorod coatings. In fact, if macrophage death were to occur through apoptotic mechanisms, then even this cell death could represent a reasonable approach for biomaterial coating to limit foreign body reaction, as has been suggested previously [282]. However, reviewing the cell adhesion and viability results from the flat ZnO (sputtered) control clearly indicates the limitation of substrates formed from ZnO – the material itself possesses toxicity resulting in non-apoptotic (necrotic) cell death. Furthermore, given the reduced adherent cell numbers on sputtered ZnO compared to glass, this toxicity itself may provide some inhibition of cellular adhesion. Unfortunately, this confounds the ability to attribute modulation of macrophage adhesion to nanotopography as opposed to toxicity, and clearly indicates that investigation in nanotopography-directed modulation of macrophages will require an alternative base material. Furthermore,

these data indicate that ZnO is not an ideal biomaterial coating, in particular for applications where long-term macrophage-biomaterial contact is expected such as soft tissue-residing implanted devices. This notion is underscored by the observed unresolved inflammation when ZnO-coated substrates were implanted subcutaneously in mice.

Pearson's correlations between viable adherent macrophage number and the concentration of solubilized Zn (measured via ICP mass spectroscopy) revealed moderate negative correlations of -0.4 and -0.5 for both 3 hours and 16 hours, respectively (Figure 4-7). Additionally, Pearson's correlation of viable macrophage numbers when not in contact with substrates versus Zn concentration in the shared media revealed a moderate negative correlation (-0.4) as well (Figure 4-7). This indicates correlation between an increase in zinc concentration and a decrease in the number of live cells, for which there is clear precedent. Zinc has been shown to induce cellular toxicity via production of reactive oxygen species [268] and disruption of energy metabolism [269] at concentrations as low as 60 μM [283,284].

However, there are still informative points to consider. It is noteworthy that the strength of these Pearson's correlations indicates only a moderate strength of association between viable cell number and amount of soluble Zn, allowing for a possible role of nanotopography influencing the observed decrease in cell adhesion and viability. In fact, there are a number of reasons to suspect such a contribution of nanotopography-driven modulation of cell adhesion and function. For example, a recent study that conformally coated ZnO nanorods with SiO2 to prevent the leaching of ZnO into the solution demonstrated reduced adhesion and survival of endothelial cells and

fibroblasts, which was attributed to a lack of sustainable adhesive complexes on nanorod substrates [273]. Since macrophages are also adhesion-dependent cells, they may be driven to undergo cell death due to a lack of adhesive cues, termed anoikis, [285] a form of programmed cell death, or apoptosis. However, for macrophages seeded on the bare ZnO substrate system examined here, this is not likely the case, given the fact that the macrophages adherent to the ZnO nanorods did not express activated caspase-3. Another possibility is cell penetration by nanorods. Given the dimensions (50 nm in diameter, 500 nm in height), it is possible that a large number of these ZnO nanorods may pierce the cell membrane and lead to a loss of membrane integrity, which could drive cell death.

Thus, while we originally set out to investigate the role of nanotopography on modulating macrophage adhesive responses, this work indicates that use of ZnO nanorods for this goal does not represent a tenable approach for macrophages. Although our results cannot rule out the effects of nanotopography, interpretation is intractably confounded by the dissolution and inherent toxicity of Zn from these substrates. Future efforts in this vein will need to focus on use of nontoxic approaches.

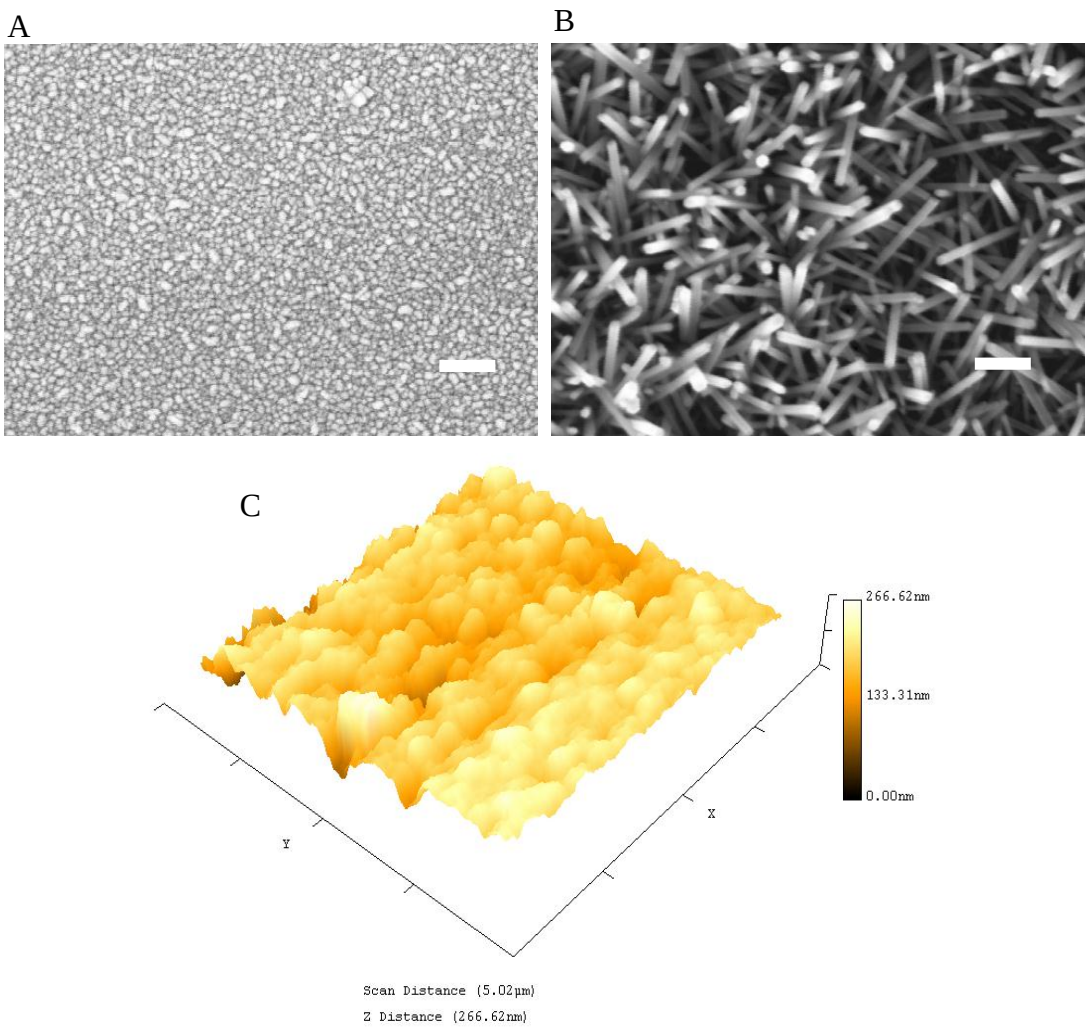

Figure 4-1. Surface topography of sputtered ZnO and ZnO nanorods. A.) SEM image of sputtered ZnO. Scale bar is 200 nm. B.) SEM images of ZnO nanorods indicating upright growth of nanorods. Nanorod diameter of is ~50 nm and height is ~500 nm. Scale bar is 200 nm. C.) AFM image of sputtered ZnO substrate. The surface roughness is approximately 31 nm, which is an order of magnitude less than the height of nanorods, validating selection as a relatively smooth surface compared to ZnO nanorods.

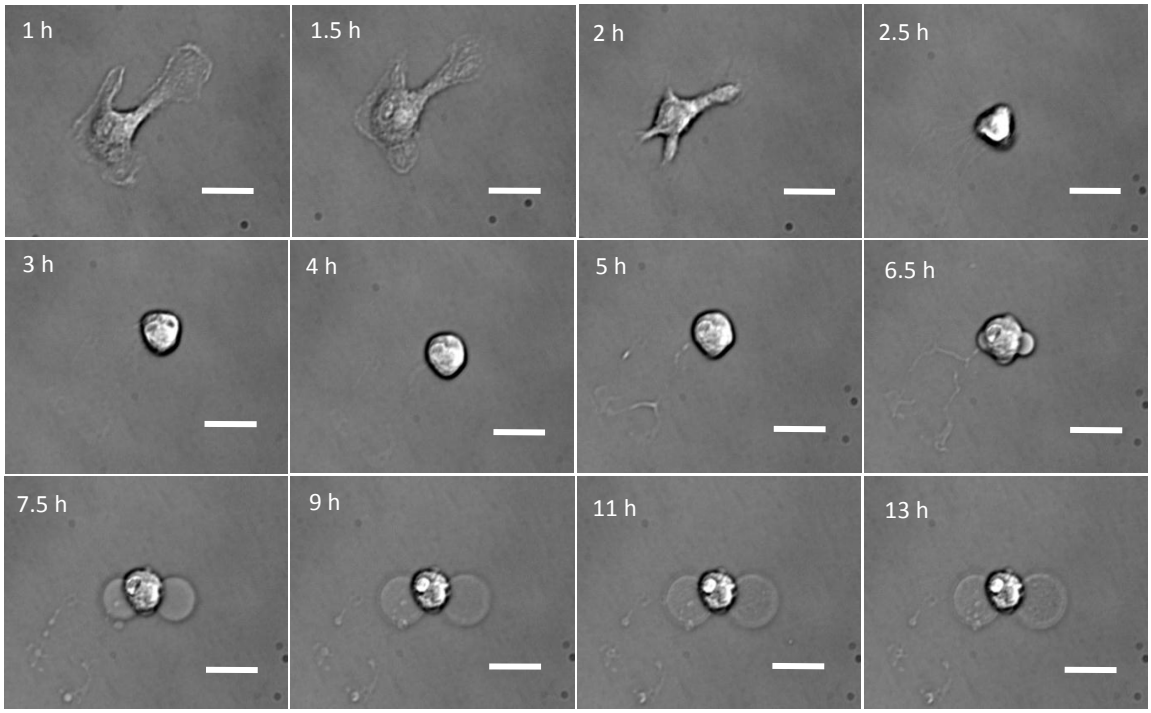

Figure 4-2. Time-lapse images of adherent macrophage seeded on ZnO nanorods demonstrating initial adhesion followed by contraction and apparent cytoplasm leakage. Macrophages on ZnO nanorod surface were imaged for 13 hours in culture and images from a representative cell are shown. Scale bar is 20 um.

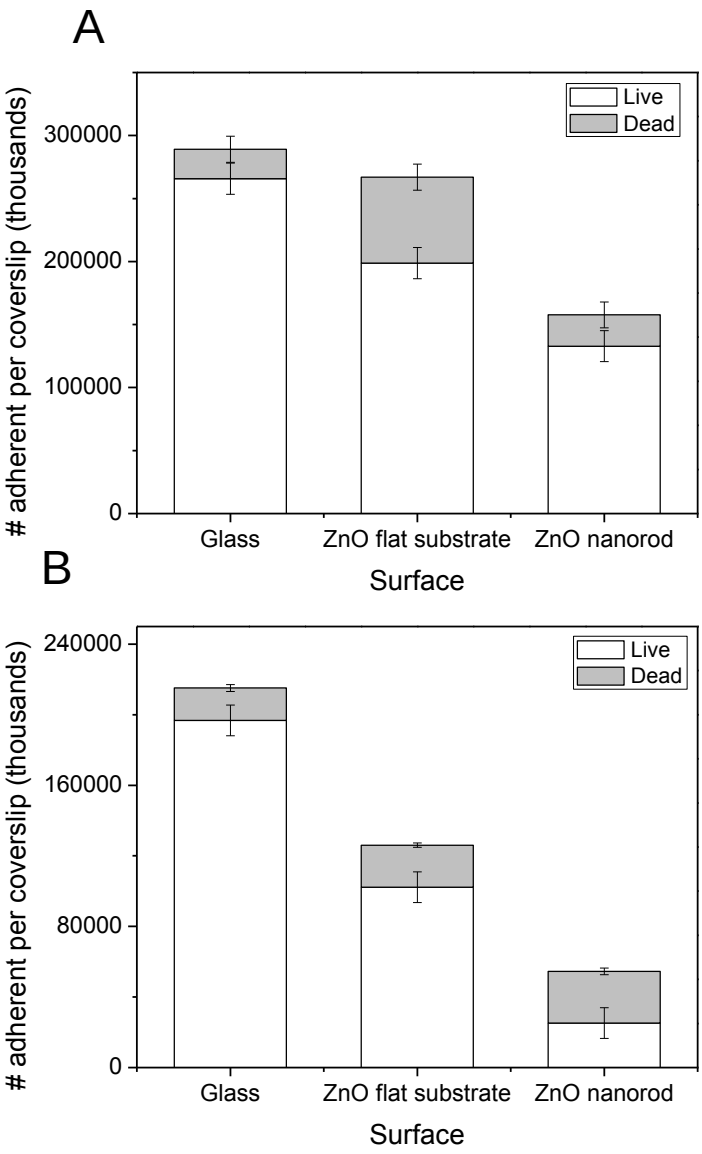

Figure 4-3. Macrophage adhesion and viability on ZnO substrates. Macrophage number – live, dead and total on the 3 substrates – glass, sputtered ZnO and ZnO nanorords was quantified at A) 3 hours and B) 16 hours post-seeding. Average numbers of live and dead macrophages on substrates were quantified by pooling data from 6 samples from 3 separate runs. Three images were taken per sample. Plotted are mean and standard error. (* indicates statistically significant difference ($p < 0.05$) from all other conditions in the same category (i.e. live, dead, total)).

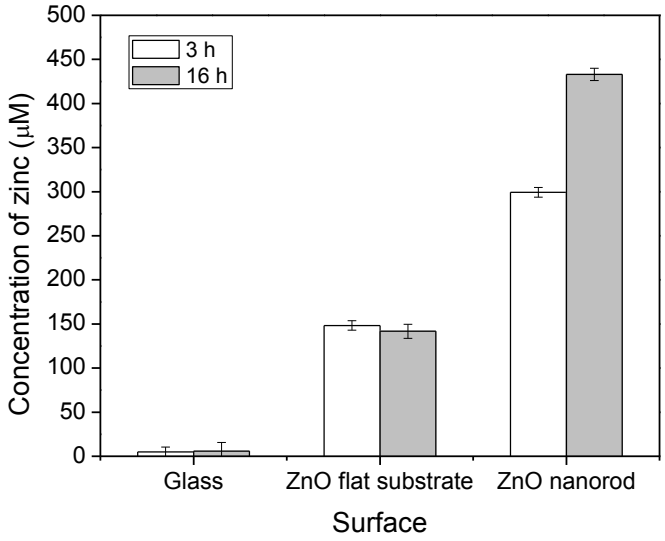

Figure 4-4. Dissolved levels of zinc in culture media when macrophages are cultured on zinc oxide substrates. Zinc concentration in the cell culture media was quantified at 3 hours and 16 hours with macrophages cultured on the glass, sputtered ZnO and ZnO nanorod substrates using Inductively Coupled Plasma-mass spectroscopy. (* indicates statistically significant difference ($p < 0.05$) from all other conditions in the same category (i.e., 3 hours and 16 hours)).

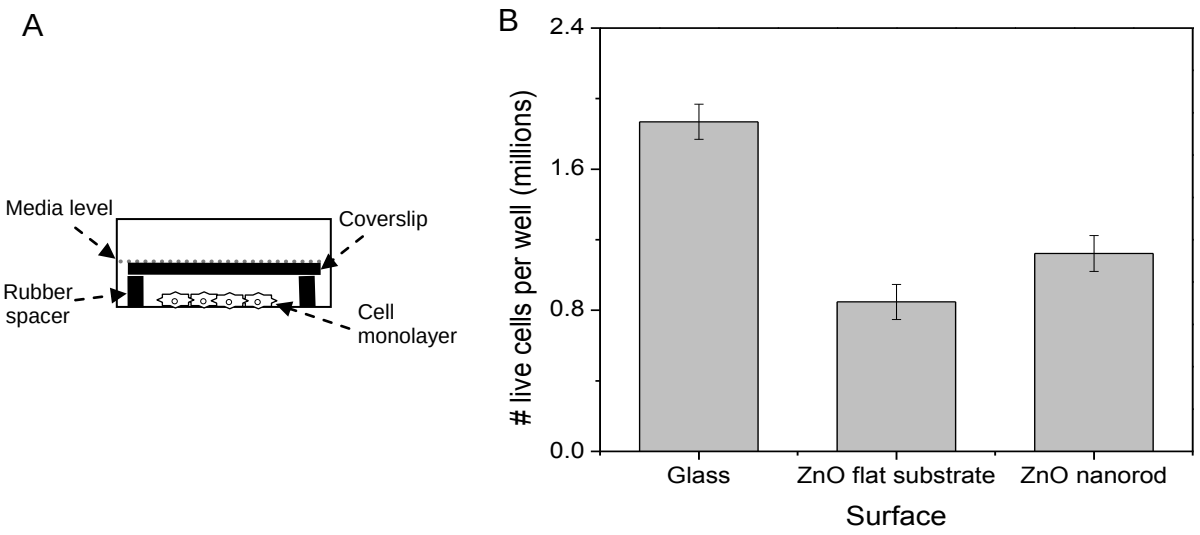

Figure 4-5. A) Setup to determine cytotoxicity of ZnO when cells are not present in contact with the substrates. B) Viability of macrophages when ZnO substrates are present in the same media but not in direct contact with cells. Cells are cultured at the bottom of a 6 well plate and substrates are inverted in the well as shown with the help of Viton O-rings in order to provide shared culture media. The average number of live adherent cells on glass, sputtered ZnO and ZnO nanorod substrates was quantified by pooling data from 8 replicates from 2 separate runs. Three images were taken per replicate. Plotted are mean and standard error. (* indicates statistically significant difference ($p < 0.05$) from all other conditions.)

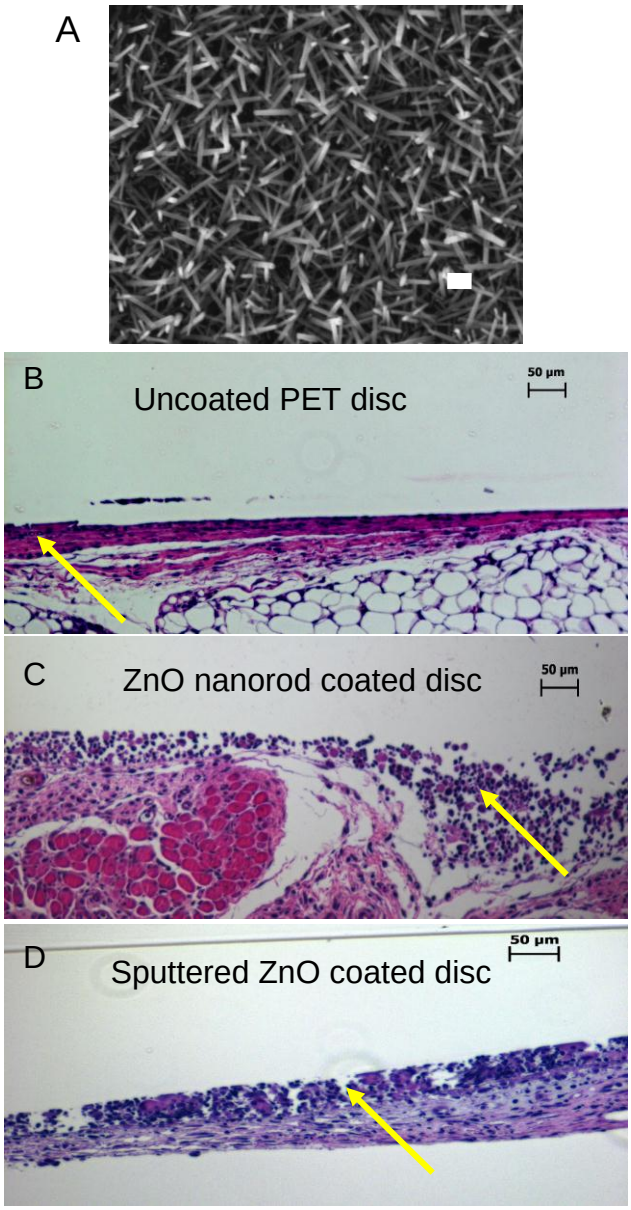

Figure 4-6. Foreign body response to zinc oxide coated PET discs implanted subcutaneously in mice. Zinc oxide coatings on implanted discs prevent formation of acellular fibrous capsule around discs, indicative of unresolved inflammation. A.) SEM image of ZnO nanorods coated on the PET discs. (Scale bar is 200 nm) H & E section of tissue response to implanted biomaterials B) Uncoated PET C) ZnO nanorod coated PET D) Sputtered ZnO coated PET

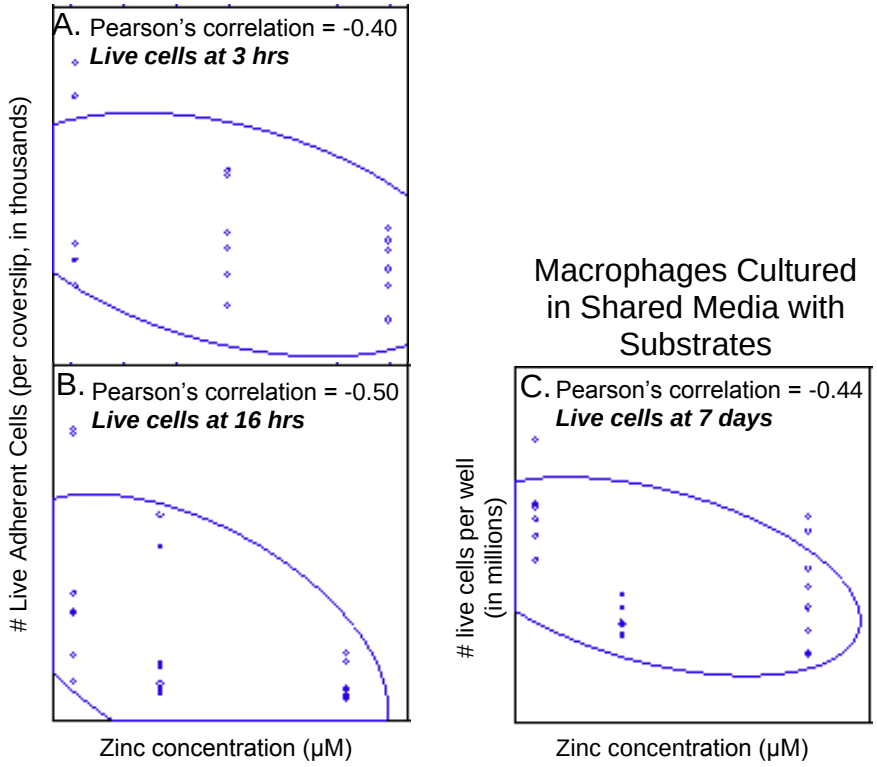

Figure 4-7. Correlation between dissolved zinc levels in media and macrophage viability. Macrophage viability has a moderate negative correlation with dissolved Zn concentration in the media. The number of live cells adherent on substrates at both 3 and 16 hours and the number of live cells adherent on the well bottom at 7 days with inverted substrates negatively correlates with zinc concentration in the media. A.) Pearson's correlation coefficient between live substrate-adherent macrophages and zinc concentration at 3 h is -0.40, demonstrating moderate correlation. B.) Pearson's correlation coefficient between live substrate-adherent macrophages and zinc concentration at 16 hours is -0.50, demonstrating moderate correlation. This indicates that as Zn concentration increases, number of live cells decreases. C.) Pearson's correlation coefficient for live macrophages at 7 days with inverted substrates and zinc concentration was -0.44, demonstrating moderate correlation.

CHAPTER 5
ANTIBACTERIAL EFFECTS OF ZINC OXIDE NANOROD SURFACES

Background

The US medical device industry is a $30 billion industry and medical implant demand is predicted to rise 9.3 percent annually through 2011 [286]. Medical implants are being extensively used in every organ of the human body, with success in replacing or repairing physiologic functions. However, a major impediment is implant-associated infections caused by bacterial adhesion to biomaterials, which necessitate implant removal, extended care and prolonged antibiotic treatment [200-202]. This additional care significantly contributes to health care costs. For example, of the 2.6 million orthopedic devices implanted annually in the US, approximately 112,000 (4.3%) become infected [203]. The most common cause of infection is the generally non-pathogenic and ubiquitous bacteria S. epidermidis which is normally found on human skin and under normal circumstances is well tolerated by the immune system [205,206]. However, when adherent to implanted surfaces, bacteria develop a protective biofilm resistant to immune and antibiotic attack and can develop multiple resistance to antibiotics [207,208]. Many implant-associated infections therefore require surgical removal of the implant. Estimated costs of implant-associated infections exceeds $3 billion annually in the US [203].

In order to address this problem, implant coating strategies have been developed with the goal to eliminate initial bacterial adhesion and/or kill adherent bacteria. Various strategies have been investigated. For example, surface coatings which support low levels of protein adsorption, termed non-fouling, including surfaces modified with polyethylene glycol, polyethylene oxide brushes and hydrophilic polyurethanes,

demonstrate resistance to bacterial adhesion [211,212]. However, the effectiveness of these coatings toward resisting biofilm formation is limited and results vary depending on bacterial species [213]. A more recent approach is the use of “active” coatings which provide continuous release of bactericidal agents [214-217]. Complimentarily, nanotechnologies can provide orthogonal approaches which have the potential to be combined with both non-fouling and active release strategies.

Nanostructured materials, whose structural elements have dimensions in the range of 1–100 nm, exhibit unique properties compared to the bulk material due to small dimensions and large surface area relative to volume [182]. These nanomaterials are used in an over broadening array of applications such as microelectronics, sensor technology, semiconductors, cosmetics as well as medical applications such as biosensors, tissue engineering and drug delivery vehicles [183]. Formation of nano-scale rod-like structures, “nanorods” has recently been accomplished and is being investigated to coat complex implant surfaces [185,260,264]. These nano-scale coatings approach provides increased stability compared to nanoscale powders and avoids health and stability issues associated with nanoparticulates [287]. Notably, nanoparticles of zinc oxide (ZnO) have demonstrated bactericidal effectiveness for various bacterial strains such as B. atrophaeus [288], E. coli [288,289], S. agalactiae [195], S. aureus [195] and S. epidermidis [65], suggesting ZnO as a promising material for use in antimicrobial coatings. Furthermore, nanotopographic surfaces have been reported to modulate bacterial adhesion [290]. These facts motivated us to investigate the potential of ZnO nanorod surfaces to resist to bacterial adhesion and possess bactericidal activity.

Experimental Procedure

Fabrication of ZnO Nanorods

ZnO nanorods were made by a solution-based hydrothermal growth method as described in Chapter 4.

Bacterial Culture

Bacterial adhesion and viability experiments were performed using P. aeruginosa and S. epidermidis. These represent the most common strains in device related infections, exhibit increased resistance to antibiotics when associated with device-related infections and have structural differences in their cell walls (being Gram-negative and Gram-positive, respectively). Bacteria were cultured in Luria Broth consisting of 10 g Bacto tryptone, 5 g yeast extract and 5 g sodium chloride per liter of sterile water. This blend has been shown to inhibit extracellular polysaccharide production by bacteria and therefore biofilm production [291]. By scraping the surface of the frozen bacteria stock with a sterile 1 µL loop a small amount of bacteria were transferred into the Erlenmeyer flask containing 50 mL of Luria Broth. The mixture was agitated for approximately 16h in an incubator-shaker at 37°C and 225 rpm. The bacterial optical density (OD) was assessed in a Nanodrop® Spectrophotometer ND-1000. The optical density (OD) of the culture was converted to bacteria concentration based on standard curve generated by plotting OD versus bacteria number, obtained by direct bacterial enumeration. The culture was diluted in Luria Broth to obtain 500,000 cells/mL.

Substrate Preparation and Bacterial Adhesion Studies

Before seeding bacteria, substrates were cleaned and sterilized by washing in 95% ethanol for 1 min and then rinsing with phosphate buffered saline (PBS). This

procedure was repeated three times with a final ethanol rinse. The substrates were then left to dry. Substrates were then placed in 35 mm x 10 mm cell culture dishes (Corning Inc. Lowell, MA) and $1x10^6$ bacteria in suspension were seeded. Bacteria were allowed to adhere for 2 h in a bacterial incubator at 37°C. After incubation all substrates were rinsed twice with PBS to remove non-adherent bacteria and placed in new 35 mm x 10 mm cell culture dishes. Next, 2 mL of PBS were added to each dish and they were then incubated at 37°C for another 22 h.

Fluorescence Staining and Imaging

After 22 h of culture, non-adherent cells were removed by two gentle washes with PBS. Total adherent bacteria were then stained with Hoechst 33258, (Invitrogen) a membrane-permeable DNA-binding dye, by incubating for 1 h followed by PBS wash. Dead bacteria were incubated for 30 min with 7-Aminoactinomycin D (7-AAD) (BD Pharmingen) a membrane-impermeable DNA-binding dye, which stains bacteria only when the bacterial cell wall is compromised. Images were obtained with a fluorescence microscope (Nikon TE 2000) and analyzed using Axiovision software 4.7.2 (Carl Zeiss Imaging Solution) to determine total adherent and dead bacteria cell counts. At least three images were taken per sample; samples were prepared at least in triplicate and repeated at least three times. The average number and standard error of adherent and dead bacterial cells on the substrates were computed.

Statistics

Statistical analyses were performed using ANOVA, using Systat (Version 12, Systat Software, Inc., San Jose, CA). Pair-wise comparisons were made using Tukey's Honestly-Significant-Difference, with p values of less than or equal to 0.05 considered to be significant.

Results

In order to quantify the extent to which ZnO nanorod substrates were able to modulate bacterial adhesion, the adherent number and viability of bacteria on ZnO nanorod substrates were compared to that on sputtered ZnO substrates and glass as a reference. Overall, the most salient feature is that for both bacterial strains cultured, the number of dead bacteria on ZnO nanorod substrates was much higher compared to glass, and for S. epidermidis higher compared to sputtered ZnO substrates (Figures 5-1 B and 5-3 B).

For P. aeruginosa, ZnO substrates demonstrated some ability to resist adhesion, where total numbers of adherent bacteria on ZnO substrates was reduced compared to glass. Representative images of stained P. aeruginosa on the three substrates are shown in the Figure 5-2, which is an overlay of fluorescence images with DNA stained blue for all adherent bacteria and red for the dead bacteria. The images clearly demonstrate the reduction of adherent bacteria and the increased number of dead bacteria on the ZnO surfaces. Pooled data was analyzed by ANOVA and the mean and standard error plotted for each substrate. Overall, groups were found to be significant by ANOVA (p-value < 0.04), and the total adherent bacteria number on both ZnO substrates was found to be significantly less than on glass substrates (50% of the total adherent number on ZnO nanorods, and 65% of the total adherent number on sputtered ZnO, compared to glass) (Figure 5-1 A) Total adherent numbers were not significantly different between the two ZnO substrates, however ($p = 0.16$).

In order to determine the antimicrobial potential of substrates for P. aeruginosa, the numbers of killed bacteria were compared. Overall, groups were found to be significant by ANOVA (p-value $< 1x10\text{-}3$). Notably, ZnO nanorod substrates

demonstrated enhanced antimicrobial efficiency compared to sputtered ZnO and glass, with the number of killed P. aeruginosa on ZnO nanorods (19% killed) being 2.5-fold higher than glass (7.5% killed) and 1.5-fold higher than ZnO sputtered (13% killed) (Figure 5-1 B). The numbers of killed P. aeruginosa were not significantly different between the sputtered ZnO and glass substrates, however ($p = 0.1$).

In order to determine the effects of ZnO substrates on bacteria with a different cell wall structure, adhesion and viability experiments were repeated using S. epidermidis. In contrast, to the Gram-negative P. aeruginosa, the Gram-positive S. epidermidis demonstrated a number of adherent bacteria on the ZnO nanorod substrate that was equivalent to glass. Furthermore, the number of adherent S. epidermidis on sputtered ZnO was higher than the other substrates. Although adherent bacteria numbers did not follow the same trend, the ratio of killed S. epidermidis on the substrates followed the same general trend as P. aeruginosa. Representative images of stained S. epidermidis bacteria on the substrates are shown in the Figure 5-4, which is an overlay fluorescence images with DNA stained blue for all adherent bacteria and red for the dead bacteria. The images show a slightly increased adhesion on sputtered ZnO and a higher number of dead bacteria on the ZnO substrates. Pooled data was analyzed by ANOVA and the mean and standard error plotted for each substrate. Overall, groups were found to be significant by ANOVA (p-value < 0.05). The total numbers of adherent S. epidermidis on ZnO nanorod and glass substrates were equivalent, while the number of adherent S. epidermidis on sputtered ZnO was 15% higher than the ZnO nanorod and glass substrates (Figure 5-3 A).

Next, to determine the antimicrobial potential of substrates for S. epidermidis, the numbers of killed bacteria were compared. Overall, groups were found to be significant by ANOVA (p-value < 1x10-10). Notably, ZnO nanorod substrates demonstrated enhanced antimicrobial efficiency compared to sputtered ZnO and glass substrates (Figure 5-3 B), with the number of killed bacteria on ZnO nanorods (16%) being 30-fold higher than glass (0.5%). The number of killed bacteria on ZnO nanorods was 1.5-fold higher than on sputtered ZnO, while the number of killed bacteria on sputtered ZnO (11%) was 20-fold higher than glass.

Impact of the Study

ZnO nanorods, nanowires, and nanotubes have been explored for various biomedical applications because of their attractive properties such as electrochemical activity, high specific surface area and chemical stability [183]. We have recently reported that ZnO nanorod surfaces are capable of modulating adhesion and viability of multiple mammalian cell types [185,260]. Relevant work with ZnO nanoparticles has reported a bactericidal effect on numerous gram-positive and gram-negative bacterial strains [65,195,288,289]. Proposed mechanisms for the anti-bacterial activity of ZnO nanoparticles include the induction of H_2O_2, a strong oxidizing agent [292-295], disruption of cell membrane and leakage of its cytoplasmic contents [288,289], as well as internalization of the nanoparticles [289]. Hence our interest in investigating ZnO nanorod surface, a well-controlled nanotopography model system to evaluate bacterial adhesion and viability and explore its potential as an antibacterial implants coating. In this study the antibacterial activity of ZnO nanorods and sputtered ZnO substrates for bacterial strains P. aeruginosa and S. epidermidis has been investigated. Antibacterial surface coatings should possess activity against a wide range of bacteria as the type of

bacteria found in different implants varies greatly [201]. We selected both gram-positive as well as gram-negative strains of bacteria in order to study the effect of nanorods on bacteria with different cell wall structures. Importantly, S. epidermidis is the strain that is most associated with device-related infection, while the nocosomial-associated P. aeruginosa is also involved in device-related infection, with the ability to develop antibiotic resistance [296].

Fewer P. aeruginosa adhered on ZnO substrates, with ZnO nanorods and sputtered ZnO supporting 65% and 50% of the total number adherent on the reference glass substrate. The ZnO nanorod substrate killed the most P. aeruginosa, with a 1.5-fold and 2.5-fold increase compared to sputtered ZnO and glass, respectively. These anti-adhesive and cytotoxic effect are in line with previously published data on effect of ZnO nanorod surfaces on mammalian cells [185,260] as well as other bacterial strains [195,288] Notably, the anti-adhesive effect of the ZnO substrates on the gram-positive S. epidermidis bacteria was not as profound as the gram-negative P. aeruginosa bacteria. In fact, the sputtered ZnO had the highest adherent bacteria numbers with approximately 15% more adherent bacteria as compared to glass and ZnO nanorod substrates. The decrease in bacteria viability followed the same trend for both strains with the highest number of killed bacteria on ZnO nanorod substrates. However, while there was a 30-fold increase over the number of dead bacteria on glass for S. epidermidis, there was only a 2.5-fold increase for P. aeruginosa. The difference in activity against the two types of bacteria could be attributed to differences in their cell walls. Specifically, gram positive bacteria have a thick layer of peptidoglycans and a cytoplasmic membrane, whereas the gram-negative bacterial wall consists of a thin

layer of peptidoglycan between the cytoplasmic membrane and the outer membrane [297,298] The structural differences in the bacterial cell wall of these strains may differentially interact with the ZnO nanorods through strain-specific differences in non-specific electrostatic and van der Waals interactions.

Recent work by Tam et al. also reported antimicrobial activity of ZnO nanorod surfaces using the bacterial strains E. coli and Bacillus atrophaeus [288]. They determined that for these strains, the antibacterial activity of the ZnO nanorods was attributed to damage of the cell membranes, which caused leakage of cell contents and cell death [288]. Although the exact cause of the membrane damage in the current work requires additional investigation, the release of Zn2+ ions is a plausible reason for the antibacterial activity of ZnO substrates. ZnO is known to be unstable in solution and breaks down to produce Zn2+ ions. Zinc ions can penetrate cell membranes, disrupt the cell's metal ion homeostasis and can be toxic when the concentrations are high enough [299]. Previously we have shown that the amount of Zn dissolved in cell culture media is significantly higher for ZnO nanorod substrates (450 µM) compared to sputtered ZnO substrates (150 µM) [260]. Another possibility is direct penetration of the bacterial cell wall by nanorods and this loss of membrane integrity can result in cell death. Even though bacteria are relatively small, a large number of ZnO nanorods are estimated to be in contact with a single bacteria (estimated ~250-500 nanorods; with a nanorod surface density of 126 nanorods per μm^2 for our substrates [185]). Although in this work we used ZnO nanorods of one set length, these antimicrobial mechanisms could potentially be differentially modulated by different nanorod lengths and optimized in the future. Although approaches using timed-release antibiotic coatings reportedly achieve

higher levels of bactericidal efficacy in earlier time points, low levels of antibiotic release at later time points raise concerns of developing antibiotic resistance for chronic or recurring infections [300]. All together these findings support the continued investigation of ZnO nanorod coatings as complimentary, orthogonal antimicrobial coating approaches with potential to both reduce bacterial adhesion and viability.

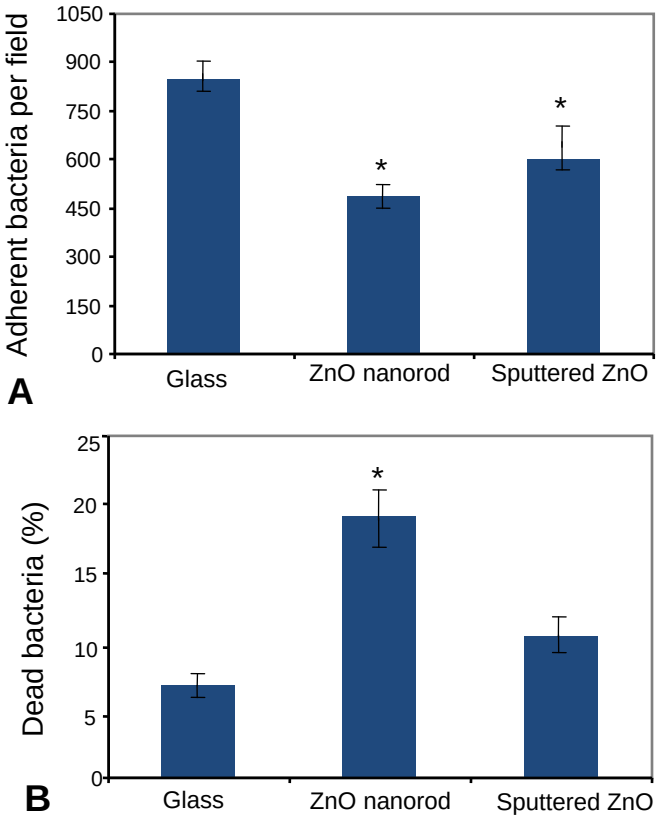

Figure 5-1. *Pseudomonas aeruginosa* adhesion and viability is reduced on ZnO nanorod substrates. Bacterial cell numbers: total (A), and dead (B) on glass, sputtered ZnO and ZnO nanorod substrates were quantified at 24 h post-seeding. Mean and standard error are plotted for the number of adherent and dead bacteria on substrates, with a sample number, n = 22, from 3 separate runs. (A) * indicates significant difference from glass. (B) * indicates significant difference from all other surfaces.

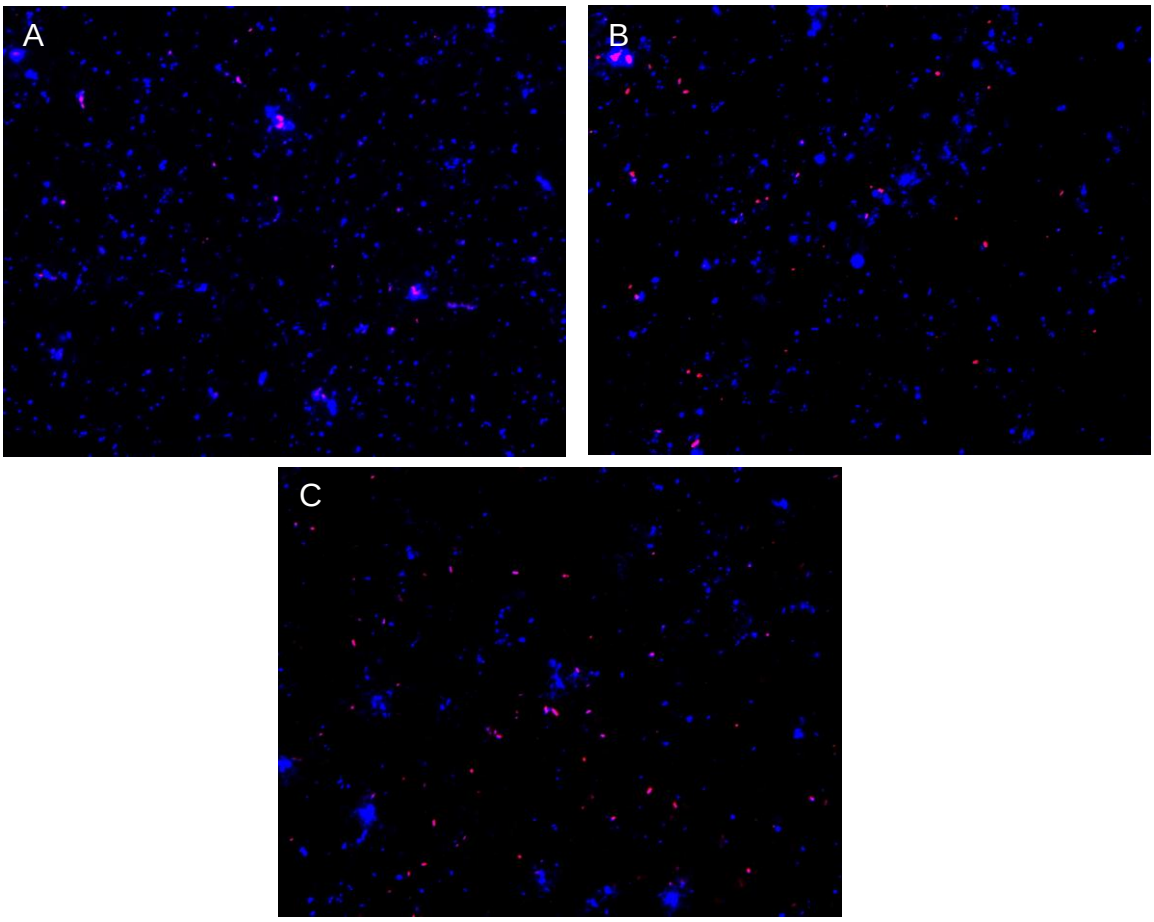

Figure 5-2. Pseudomonas aeruginosa demonstrate decreased adhesion and viability of bacteria on ZnO nanorod. Bacteria on substrates: glass (A), ZnO nanorods (B) and sputtered ZnO (C) were stained after 24 h of culture. Fluorescence images of Hoechst staining (blue) represent total adherent bacteria and staining with 7-AAD (red) represent dead bacteria.

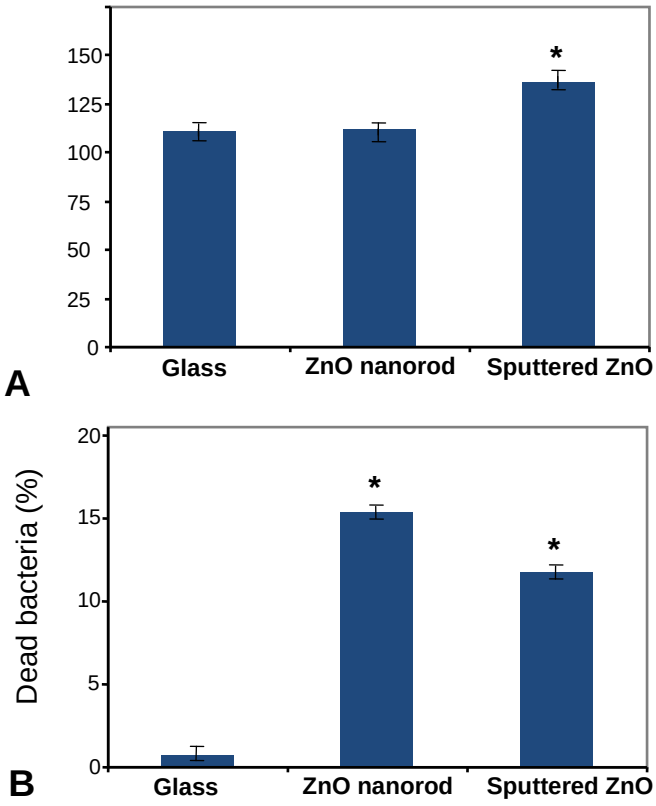

Figure 5-3. *Staphylococcus epidermidis* viability is reduced on ZnO substrates. Bacterial cell numbers: total (A), and dead (B) on glass, sputtered ZnO and ZnO nanorod substrates were quantified at 24 h post-seeding. Mean and standard error are plotted for the number of adherent and dead bacteria on substrates, with a sample number, n = 12, from 4 separate runs. * indicates significant difference from all other surfaces.

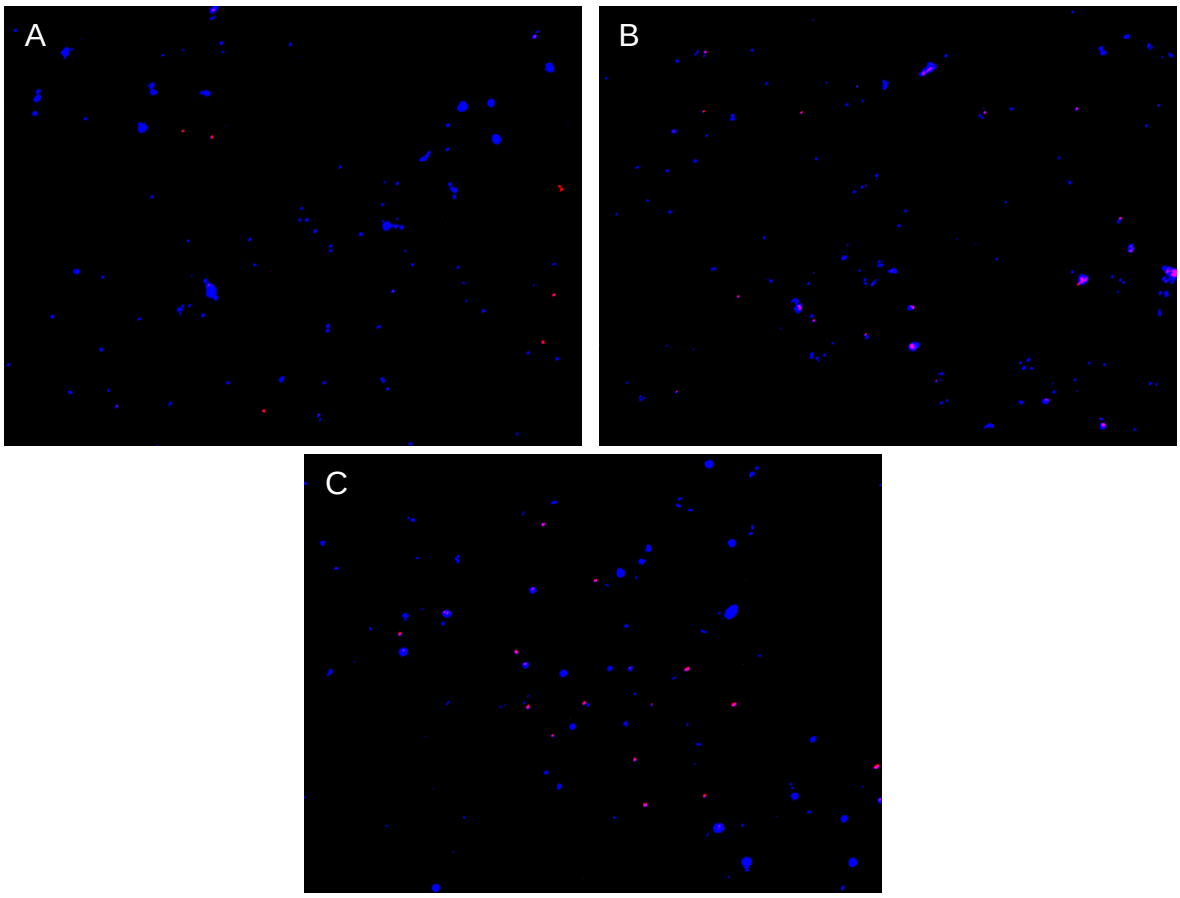

Figure 5-4. Staphylococcus epidermidis demonstrate decreased viability, but comparable adhesion on ZnO nanorod. Bacteria on substrates: glass (A), ZnO nanorods (B) and sputtered ZnO (C) were stained after 24 h of culture. Fluorescence images of Hoechst staining (blue) represent total adherent bacteria and staining with 7-AAD (red) represent dead bacteria.

CHAPTER 6
CONCLUSIONS AND FUTURE DIRECTIONS

The goal of my research was to modulate macrophage response to biomaterials in order to mitigate the foreign body response, which has been shown to limit the functioning, performance and lifetime of implanted biomaterials. I have explored two approaches to achieve this end goal- integrin targeting as well as exploring nanotopographic surfaces as anti-adhesion surface. My work focused mainly on understanding the role of the integrins in the various biomaterial-related inflammatory processes such as peri-prosthetic osteolysis, fibrous encapsulation of biomaterials and more specifically the role of integrins in macrophage response to particulate and bulk biomaterials. Through a series of experiments, I demonstrated the role of integrin Mac-1 and RGD-binding integrins in these inflammatory processes. The role of these integrins varied from a major player to some modulation depending on the process and integrin being studied. Recommendations for future experiments include many interesting avenues. During my research, I explored the role of integrins in the in vivo processes and then further investigated the mechanisms involved in these processes using in-vitro experiments focusing on macrophages. However other cell types are also involved in the host response to implanted materials and studying the role of integrins in osteoclasts and neutrophils functioning is a research topic worth exploring.

In order to study the role of Mac-1 integrin, I used a Mac-1 KO mouse for all the experiments. However in order to move towards a therapeutic approach, functional antibody blocking experiments could be carried out by delivering the antibodies to the site of implant only. The Mac-1 KO mice have the integrin knocked out from all the cell types such as neutrophils and osteoclasts, which express this receptor. Thus, the

effects seen in the in-vivo experiments are a compound effect of the absence on integrin on several cell types and thus we see an enhanced effect of absence of Mac-1 in vivo as compared to the in vitro responses. Mac-1 integrin play a role in different macrophage functions. Hence the functional blocking studies will have to focus on titrating the dosage as well as the temporal release of the antibodies into the implant site.

Most in-vivo experiments conducted were based on established animal models however; they involved very small times of implantation ranging from 1-2 weeks. However implants are required to stay in the body for much longer periods of time in most applications. Hence experiments involving longer implantation times need to be conducted to study long term effects of integrin blocking on response to implants. The properties of the ELVAX™ controlled release system and the dose of RGD/echistatin will need to be modified to match the time of implantation. Other RGD-antagonists such as Abciximab and tirofiban which have been approved for clinical use in the United States can also be explored as therapeutic approaches to mitigate peri-implant osteolysis and fibrous capsule formation. Abciximab is shown to bind to integrin αvβ3 as well as Mac-1 integrin.

The ZnO nanorod surface exhibited toxicity towards macrophages due to the dissolved Zn, making result interpretation regarding the role of nanotopography challenging. Nanorod surface made from other materials such as titanium shown to be non-toxic and used in several orthopedic implants can be explored to study the role of nanotopography without confounding toxicity issues. The length scale of the nanorods

can also be varied to study the role of height of nanotopographic features in adhesion modulation.

My research primarily focused on understanding the role of integrins and nanotopogrpahy in modulating macrophage response to biomaterials. Based on the insight gained through this work, future work in this direction can focus on translating this understanding to a therapeutic approach.

LIST OF REFERENCES

[1] NIH Consens Statement. In Clinical Applications of Biomaterials.198; 4(5): 1-19.

[2] Global Biomaterial Market (2009-2014). 2009. MarketsandMarkets. Accessed on 10-11-2010. Available at http://www.reportlinker.com/p0148007/Global-Biomaterial-Market.html.

[3] Ratner BD. Biomaterial Science : An Interdisciplinary endeavor. In Biomaterials Science: An introduction to materials in medicine. 2010. p 1-9.

[4] Williams DF. On the mechanisms of biocompatibility. Biomaterials 2008;29:2941-2953.

[5] Anderson JM. Biological responses to materials. Annu Rev Mater Res 2001;31:81-110.

[6] Archibeck MJ, Jacobs JJ, Roebuck KA, Glant TT. The basic science of periprosthetic osteolysis. Instr Course Lect 2001;50:185-195.

[7] Bauer TW, Schils J. The pathology of total joint arthroplasty.II. Mechanisms of implant failure. Skeletal Radiol 1999;28:483-497.

[8] Zhao Q, Topham N, Anderson JM, Hiltner A, Lodoen G, Payet CR. Foreign-body giant cells and polyurethane biostability: in vivo correlation of cell adhesion and surface cracking. J Biomed Mater Res 1991;25:177-183.

[9] Gordon M, Bullough PG. Synovial and osseous inflammation in failed silicone-rubber prostheses. J Bone Joint Surg Am 1982;64:574-580.

[10] Smahel J. Foreign material in the capsules around breast prostheses and the cellular reaction to it. Br J Plast Surg 1979;32:35-42.

[11] Anderson JM, Niven H, Pelagalli J, Olanoff LS, Jones RD. The role of the fibrous capsule in the function of implanted drug-polymer sustained release systems. J Biomed Mater Res 1981;15:889-902.

[12] Luttikhuizen DT, Harmsen MC, van Luyn MJA. Cellular and molecular dynamics in the foreign body reaction. Tissue Eng 2006;12:1955-1970.

[13] Anderson JM. Inflammatory response to implants. ASAIO Trans 1988;34:101-107.

[14] Ratner BD, Bryant SJ. Biomaterials: Where we have been and where we are going. Annu Rev Biomed Eng 2004;6:41-75.

[15] Engelhardt E, Toksoy A, Goebeler M, Debus S, Brocker EB, Gillitzer R. Chemokines IL-8, GROalpha, MCP-1, IP-10, and Mig are sequentially and differentially expressed during phase-specific infiltration of leukocyte subsets in human wound healing. Am J Pathol 1998;153:1849-1860.

[16] Anderson JM. Biocomapatibility and Bioresponse to Biomaterials. In Atala, A., editors. Principles of Regenerative Medicine. Elsevier, 2010. p 704-722.

[17] Tang LP, Eaton JW. Fibrin(Ogen) Mediates Acute Inflammatory Responses to Biomaterials. J Exp Med 1993;178:2147-2156.

[18] Latour RA. Biomaterials: Protein-Surface Interactions. In New York, N.Y: Taylor & Francis, 2005. p

[19] Babensee JE, Cornelius RM, Brash JL, Sefton MV. Immunoblot analysis of proteins associated with HEMA-MMA microcapsules: human serum proteins in vitro and rat proteins following implantation. Biomaterials 1998;19:839-849.

[20] Fabrizius-Homan DJ, Cooper SL. A comparison of the adsorption of three adhesive proteins to biomaterial surfaces. J Biomater Sci Polym Ed 1991;3:27-47.

[21] Jenney, C. R. and Anderson, J. M.Adsorbed serum proteins responsible for surface dependent human macrophage behavior.Journal of Biomedical Materials Research1999;49:

[22] Xu LC, Siedlecki CA. Effects of surface wettability and contact time on protein adhesion to biomaterial surfaces. Biomaterials 2007;28:3273-3283.

[23] Shen MC, Horbett TA. The effects of surface chemistry and adsorbed proteins on monocyte/macrophage adhesion to chemically modified polystyrene surfaces. J Biomed Mater Res 2001;57:336-345.

[24] Hu WJ, Eaton JW, Ugarova TP, Tang L. Molecular basis of biomaterial-mediated foreign body reactions. Blood 8-15-2001;98:1231-1238.

[25] Altieri DC, Agbanyo FR, Plescia J, Ginsberg MH, Edgington TS, Plow EF. A unique recognition site mediates the interaction of fibrinogen with the leukocyte integrin Mac-1 (CD11b/CD18). J Biol Chem 7-25-1990;265:12119-12122.

[26] Ugarova TP, Solovjov DA, Zhang L, Loukinov DI, Yee VC, Medved LV, Plow EF. Identification of a novel recognition sequence for integrin alphaM beta2 within the gamma-chain of fibrinogen. J Biol Chem 8-28-1998;273:22519-22527.

[27] Garcia AJ. Get a grip: integrins in cell-biomaterial interactions. Biomaterials 2005;26:7525-7529.

[28] Brodbeck WG, Colton E, Anderson JM. Effects of adsorbed heat labile serum proteins and fibrinogen on adhesion and apoptosis of monocytes/macrophages on biomaterials. J Mater Sci Mater Med 2003;14:671-675.

[29] Collier TO, Thomas CH, Anderson JM, Healy KE. Surface chemistry control of monocyte and macrophage adhesion, morphology, and fusion. J Biomed Mater Res 2000;49:141-145.

[30] Keselowsky BG, Collard DM, Garcia AJ. Integrin binding specificity regulates biomaterial surface chemistry effects on cell differentiation. Proc Natl Acad Sci U S A 4-26-2005;102:5953-5957.

[31] Keselowsky BG, Collard DM, Garcia AJ. Surface chemistry modulates focal adhesion composition and signaling through changes in integrin binding. Biomaterials 2004;25:5947-5954.

[32] Ademovic Z, Holst B, Kahn RA, Jorring I, Brevig T, Wei J, Hou X, Winter-Jensen B, Kingshott P. The method of surface PEGylation influences leukocyte adhesion and activation. J Mater Sci Mater Med 2006;17:203-211.

[33] Brevig T, Holst B, Ademovic Z, Rozlosnik N, Rohrmann JH, Larsen NB, Hansen OC, Kingshott P. The recognition of adsorbed and denatured proteins of different topographies by beta2 integrins and effects on leukocyte adhesion and activation. Biomaterials 2005;26:3039-3053.

[34] Shen M, Garcia I, Maier RV, Horbett TA. Effects of adsorbed proteins and surface chemistry on foreign body giant cell formation, tumor necrosis factor alpha release and procoagulant activity of monocytes. J Biomed Mater Res A 9-15-2004;70:533-541.

[35] Shive MS, Brodbeck WG, Colton E, Anderson JM. Shear stress and material surface effects on adherent human monocyte apoptosis. J Biomed Mater Res 2002;60:148-158.

[36] Brodbeck WG, Shive MS, Colton E, Nakayama Y, Matsuda T, Anderson JM. Influence of biomaterial surface chemistry on the apoptosis of adherent cells. J Biomed Mater Res 6-15-2001;55:661-668.

[37] Collier TO, Anderson JM. Protein and surface effects on monocyte and macrophage adhesion, maturation, and survival. J Biomed Mater Res 6-5-2002;60:487-496.

[38] Tang LP, Jennings TA, Eaton JW. Mast cells mediate acute inflammatory responses to implanted biomaterials. Proc Natl Acad Sci U S A 7-21-1998;95:8841-8846.

[39] Anderson JM, Rodriguez A, Chang DT. Foreign body reaction to biomaterials. Semin Immunol 2008;20:86-100.

[40] DeFife KM, Jenney CR, McNally AK, Colton E, Anderson JM. Interleukin-13 induces human monocyte/macrophage fusion and macrophage mannose receptor expression. J Immunol 4-1-1997;158:3385-3390.

[41] McNally AK, Anderson JM. Interleukin-4 induces foreign body giant cells from human monocytes/macrophages. Differential lymphokine regulation of macrophage fusion leads to morphological variants of multinucleated giant cells. Am J Pathol 1995;147:1487-1499.

[42] Sun DH, Trindade MCD, Nakashima Y, Maloney WJ, Goodman SB, Schurman DJ, Smith RL. Human serum opsonization of orthopedic biomaterial particles: Protein-binding and monocyte/macrophage activation in vitro. J Biomed Mater Res A 2003;65A:290-298.

[43] DeFife KM, Hagen KM, Clapper DL, Anderson JM. Photochemically immobilized polymer coatings: effects on protein adsorption, cell adhesion, and leukocyte activation. J Biomater Sci Polym Ed 1999;10:1063-1074.

[44] DeFife KM, Shive MS, Hagen KM, Clapper DL, Anderson JM. Effects of photochemically immobilized polymer coatings on protein adsorption, cell adhesion, and the foreign body reaction to silicone rubber. J Biomed Mater Res 3-5-1999;44:298-307.

[45] Horbett TA. Principles underlying the role of adsorbed plasma proteins in blood interactions with foreign materials. Cardiovasc Pathol 1993;2:137S-148S.

[46] Brodbeck WG, Nakayama Y, Matsuda T, Colton E, Ziats NP, Anderson JM. Biomaterial surface chemistry dictates adherent monocyte/macrophage cytokine expression in vitro. Cytokine 6-21-2002;18:311-319.

[47] Berton G, Lowell CA. Integrin signalling in neutrophils and macrophages. Cell Signal 1999;11:621-635.

[48] Tang L, Ugarova TP, Plow EF, Eaton JW. Molecular determinants of acute inflammatory responses to biomaterials. J Clin Invest 3-1-1996;97:1329-1334.

[49] Anderson JM, Jones JA. Phenotypic dichotomies in the foreign body reaction. Biomaterials 2007;28:5114-5120.

[50] Dagtekin G, Schiffer R, Klein B, Jahnen-Dechent W, Zwadlo-Klarwasser G. Modulation of angiogenic functions in human macrophages by biomaterials. Biomaterials 2003;24:3395-3401.

[51] Amiji M, Park K. Surface Modification of Polymeric Biomaterials with Poly(Ethylene Oxide), Albumin, and Heparin for Reduced Thrombogenicity. Journal of Biomaterials Science-Polymer Edition 1993;4:217-234.

[52] Bridges AW, Singh N, Burns KL, Babensee JE, Lyon LA, Garcia AJ. Reduced acute inflammatory responses to microgel conformal coatings. Biomaterials 2008;29:4605-4615.

[53] Zhong Y, Bellamkonda RV. Controlled release of anti-inflammatory agent alpha-MSH from neural implants. J Control Release 9-2-2005;106:309-318.

[54] Hong YJ, Jeong MH, Kim W, Lim SY, Lee SH, Hong SN, Kim JH, Ahn YK, Cho JG, Park JC, Cho DL, Kim H, Kang JC. Effect of abciximab-coated stent on in-stent intimal hyperplasia in human coronary arteries. Am J Cardiol 10-15-2004;94:1050-1054.

[55] DeFranco AL, Locksley RM, Robertson M. Overview of the Immune System. In Immunity: the immune response in infectious and inflammatory disease. New Science Press, 2007. p 1-20.

[56] Rousche PJ, Normann RA. Chronic recording capability of the Utah Intracortical Electrode Array in cat sensory cortex. J Neurosci Methods 7-1-1998;82:1-15.

[57] Bota PC, Collie AM, Puolakkainen P, Vernon RB, Sage EH, Ratner BD, Stayton PS. Biomaterial topography alters healing in vivo and monocyte/macrophage activation in vitro. J Biomed Mater Res A 2010;95:649-657.

[58] Lee S, Choi J, Shin S, Im YM, Song J, Kang SS, Nam TH, Webster TJ, Kim SH, Khang D. Analysis on migration and activation of live macrophages on transparent flat and nanostructured titanium. Acta Biomater 1-11-2011;

[59] Irwin EF, Saha K, Rosenbluth M, Gamble LJ, Castner DG, Healy KE. Modulus-dependent macrophage adhesion and behavior. J Biomater Sci Polym Ed 2008;19:1363-1382.

[60] Shen M, Pan YV, Wagner MS, Hauch KD, Castner DG, Ratner BD, Horbett TA. Inhibition of monocyte adhesion and fibrinogen adsorption on glow discharge plasma deposited tetraethylene glycol dimethyl ether. J Biomater Sci Polym Ed 2001;12:961-978.

[61] Collier TO, Anderson JM, Brodbeck WG, Barber T, Healy KE. Inhibition of macrophage development and foreign body giant cell formation by hydrophilic interpenetrating polymer network. J Biomed Mater Res A 6-15-2004;69:644-650.

[62] WojciakStothard B, Curtis A, Monaghan W, Macdonald K, Wilkinson C. Guidance and activation of murine macrophages by nanometric scale topography. Experimental Cell Research 1996;223:426-435.

[63] Kim JY, Khang D, Lee JE, Webster TJ. Decreased macrophage density on carbon nanotube patterns on polycarbonate urethane. J Biomed Mater Res A 2009;88:419-426.

[64] Balasundaram G, Webster TJ. Increased osteoblast adhesion on nanograined Ti modified with KRSR. J Biomed Mater Res A 3-1-2007;80:602-611.

[65] Colon G, Ward BC, Webster TJ. Increased osteoblast and decreased Staphylococcus epidermidis functions on nanophase ZnO and TiO2. Journal of Biomedical Materials Research Part A 2006;78A:595-604.

[66] Elias KL, Price RL, Webster TJ. Enhanced functions of osteoblasts on nanometer diameter carbon fibers. Biomaterials 2002;23:3279-3287.

[67] Rice JM, Hunt JA, Gallagher JA, Hanarp P, Sutherland DS, Gold J. Quantitative assessment of the response of primary derived human osteoblasts and macrophages to a range of nanotopography surfaces in a single culture model in vitro. Biomaterials 2003;24:4799-4818.

[68] Guan JL, Trevithick JE, Hynes RO. Fibronectin/integrin interaction induces tyrosine phosphorylation of a 120-kDa protein. Cell Regul 1991;2:951-964.

[69] Kao WJ, Lee D, Schense JC, Hubbell JA. Fibronectin modulates macrophage adhesion and FBGC formation: the role of RGD, PHSRN, and PRRARV domains. J Biomed Mater Res 2001;55:79-88.

[70] Hynes RO. Integrins - Versatility, Modulation, and Signaling in Cell-Adhesion. Cell 1992;69:11-25.

[71] Hynes RO. Integrins: Bidirectional, allosteric signaling machines. Cell 2002;110:673-687.

[72] Geiger B, Bershadsky A, Pankov R, Yamada KM. Transmembrane extracellular matrix-cytoskeleton crosstalk. Nature Reviews Molecular Cell Biology 2001;2:793-805.

[73] Xing BD, Jedsadayanmata A, Lam SCT. Localization of an integrin binding site to the C terminus of talin. Journal of Biological Chemistry 2001;276:44373-44378.

[74] Faull RJ, Ginsberg MH. Inside-out signaling through integrins. J Am Soc Nephrol 1996;7:1091-1097.

[75] Diamond MS, Garciaaguilar J, Bickford JK, Corbi AL, Springer TA. The I-Domain Is a Major Recognition Site on the Leukocyte Integrin Mac-1 (Cd11b/Cd18) for 4 Distinct Adhesion Ligands. Journal of Cell Biology 1993;120:1031-1043.

[76] Danen EH, Sonnenberg A. Integrins in regulation of tissue development and function. J Pathol 2003;201:632-641.

[77] Flick MJ, Du XL, Degen JL. Fibrin(ogen)alpha(M)beta(2) interactions regulate leukocyte function and innate immunity in vivo. Experimental Biology and Medicine 2004;229:1105-1110.

[78] Broberg M, Eriksson C, Nygren H. GpIIb/IIIa is the main receptor for initial platelet adhesion to glass and titanium surfaces in contact with whole blood. J Lab Clin Med 2002;139:163-172.

[79] Gonzalez AL, El-Bjeirami W, West JL, McIntire LV, Smith CW. Transendothelial migration enhances integrin-dependent human neutrophil chemokinesis. J Leukoc Biol 2007;81:686-695.

[80] Luscinskas FW, Kansas GS, Ding H, Pizcueta P, Schleiffenbaum BE, Tedder TF, Gimbrone MA, Jr. Monocyte rolling, arrest and spreading on IL-4-activated vascular endothelium under flow is mediated via sequential action of L-selectin, beta 1-integrins, and beta 2-integrins. J Cell Biol 1994;125:1417-1427.

[81] McNally AK, Anderson JM. Complement C3 participation in monocyte adhesion to different surfaces. Proc Natl Acad Sci U S A 10-11-1994;91:10119-10123.

[82] McNally AK, Anderson JM. Beta1 and beta2 integrins mediate adhesion during macrophage fusion and multinucleated foreign body giant cell formation. Am J Pathol 2002;160:621-630.

[83] Brown, E. J.Integrins of Macrophages and Macrophage-Like Cells.The Macrophage as Therapeutic Target2003;

[84] Arnaout MA. Structure and Function of the Leukocyte Adhesion Molecules Cd11 Cd18. Blood 1990;75:1037-1050.

[85] Lishko VK, Podolnikova NP, Yakubenko VP, Yakovlev S, Medved L, Yadav SP, Ugarova TP. Multiple binding sites in fibrinogen for integrin alpha(M)beta(2) (Mac-1). Journal of Biological Chemistry 2004;279:44897-44906.

[86] Lishko VK, Yakubenko VP, Ugarova TP. The interplay between integrins alpha(M)beta(2) and alpha(5)beta(1), during cell migration to fibronectin. Experimental Cell Research 2003;283:116-126.

[87] Walzog B, Schuppan D, Heimpel C, Hafezimoghadam A, Gaehtgens P, Ley K. The Leukocyte Integrin Mac-1 (Cd11b/Cd18) Contributes to Binding of Human Granulocytes to Collagen. Experimental Cell Research 1995;218:28-38.

[88] Kanse SM, Matz RL, Preissner KT, Peter K. Promotion of leukocyte adhesion by a novel interaction between vitronectin and the beta(2) integrin Mac-1 (alpha(M)beta(2), CD11b/CD18). Arteriosclerosis Thrombosis and Vascular Biology 2004;24:2251-2256.

[89] Yang HY, Yu JP, Fu G, Shi XL, Xiao L, Chen YZ, Fang XH, He C. Interaction between single molecules of Mac-1 and ICAM-1 in living cells: An atomic force microscopy study. Experimental Cell Research 2007;313:3497-3504.

[90] Beller DI, Springer TA, Schreiber RD. Anti-Mac-1 Selectively Inhibits the Mouse and Human Type 3 Complement Receptor. Journal of Experimental Medicine 1982;156:1000-1009.

[91] Altieri DC, Edgington TS. The Saturable High-Affinity Association of Factor-X to Adp-Stimulated Monocytes Defines A Novel Function of the Mac-1 Receptor. Journal of Biological Chemistry 5-25-1988;263:7007-7015.

[92] DiScipio RG, Daffern PJ, Schraufstatter IU, Sriramarao P. Human polymorphonuclear leukocytes adhere to complement factor H through an interaction that involves alpha(M)beta(2) (CD11b/CD18). Journal of Immunology 1998;160:4057-4066.

[93] Diamond MS, Alon R, Parkos CA, Quinn MT, Springer TA. Heparin Is an Adhesive Ligand for the Leukocyte Integrin Mac-1 (Cd11b/Cd18). Journal of Cell Biology 1995;130:1473-1482.

[94] Coxon A, Rieu P, Barkalow FJ, Askari S, Sharpe AH, vonAndrian UH, Arnaout MA, Mayadas TN. A novel role for the beta 2 integrin CD11b/CD18 in neutrophil apoptosis: A homeostatic mechanism in inflammation. Immunity 1996;5:653-666.

[95] Ehlers MRW. CR3: a general purpose adhesion-recognition receptor essential for innate immunity. Microbes and Infection 2000;2:289-294.

[96] Lu, H. F., Smith, C. W., Perrard, J., Bullard, D., Tang, L. P., Shappell, S. B., Entman, M. L., Beaudet, A. L., and Ballantyne, C. M.LFA-1 is sufficient in mediating neutrophil emigration in Mac-1-deficient mice.Journal of Clinical Investigation1997;99:1340.

[97] Sisco M, Chao JD, Kim I, Mogford JE, Mayadas TN, Mustoe TA. Delayed wound healing in Mac-1-deficient mice is associated with normal monocyte recruitment. Wound Repair and Regeneration 2007;15:566-571.

[98] Davis GE. The Mac-1 and p150,95 beta 2 integrins bind denatured proteins to mediate leukocyte cell-substrate adhesion. Exp Cell Res 1992;200:242-252.

[99] Nakashima Y, Sun DH, Trindade MCD, Maloney WJ, Goodman SB, Schurman DJ, Smith RL. Signaling pathways for tumor necrosis factor-alpha and interleukin-6 expression in human macrophages exposed to titanium-alloy particulate debris in vitro. Journal of Bone and Joint Surgery-American Volume 1999;81A:603-615.

[100] Pierschbacher MD, Ruoslahti E. Cell attachment activity of fibronectin can be duplicated by small synthetic fragments of the molecule. Nature 5-3-1984;309:30-33.

[101] Ruoslahti E. RGD and other recognition sequences for integrins. Annual Review of Cell and Developmental Biology 1996;12:697-715.

[102] Pytela R, Suzuki S, Breuss J, Erle DJ, Sheppard D. Polymerase chain reaction cloning with degenerate primers: homology-based identification of adhesion molecules. Methods Enzymol 1994;245:420-451.

[103] Massia SP, Hubbell JA. Covalent surface immobilization of Arg-Gly-Asp- and Tyr-Ile-Gly-Ser-Arg-containing peptides to obtain well-defined cell-adhesive substrates. Anal Biochem 1990;187:292-301.

[104] Massia SP, Hubbell JA. Covalently attached GRGD on polymer surfaces promotes biospecific adhesion of mammalian cells. Ann N Y Acad Sci 1990;589:261-270.

[105] Garcia AJ, Schwarzbauer JE, Boettiger D. Distinct activation states of alpha 5 beta 1 integrin show differential binding to RGD and synergy domains of fibronectin. Biochemistry 2002;41:9063-9069.

[106] Cornejo CJ, Winn RK, Harlan JM. Anti-adhesion therapy. Advances in Pharmacology 1997;99-142.

[107] Curley GP, Blum H, Humphries MJ. Integrin antagonists. Cellular and Molecular Life Sciences 1999;56:427-441.

[108] Jaeschke H, Farhood A, Bautista AP, Spolarics Z, Spitzer JJ, Smith CW. Functional Inactivation of Neutrophils with a Mac-1 (Cd11b/Cd18) Monoclonal-Antibody Protects against Ischemia-Reperfusion Injury in Rat-Liver. Hepatology 1993;17:915-923.

[109] Bhaskar V, Fox M, Breinberg D, Wong MHL, Wales PE, Rhodes S, DuBridge RB, Ramakrishnan V. Volociximab, a chimeric integrin alpha5beta1 antibody, inhibits the growth of VX2 tumors in rabbits. Investigational New Drugs 2008;26:7-12.

[110] Targan SR, Feagan BG, Fedorak RN, Lashner BA, Panaccione R, Present DH, Spehlmann ME, Rutgeerts PJ, Tulassay Z, Volfova M, Wolf DC, Hernandez C, Bornstein J, Sandborn WJ. Natalizumab for the Treatment of Active Crohn's Disease: Results of the ENCORE Trial. Gastroenterology 2007;132:1672-1683.

[111] Kamata T, Wright R, Takada Y. Critical Threonine and Aspartic-Acid Residues within the I-Domains of Beta-2 Integrins for Interactions with Intercellular-Adhesion Molecule-1 (Icam-1) and C3bi. Journal of Biological Chemistry 1995;270:12531-12535.

[112] McGuire SL, Bajt ML. Distinct Ligand-Binding Sites in the I-Domain of Integrin Alpha(M)Beta(2) That Differentially Affect a Divalent Cation-Dependent Conformation. Journal of Biological Chemistry 1995;270:25866-25871.

[113] Rosen H, Gordon S. Monoclonal-Antibody to the Murine Type-3 Complement Receptor Inhibits Adhesion of Myelomonocytic Cells-Invitro and Inflammatory Cell Recruitment Invivo. Journal of Experimental Medicine 1987;166:1685-1701.

[114] Rosen H, Gordon S. The Role of the Type-3 Complement Receptor in the Induced Recruitment of Myelomonocytic Cells to Inflammatory Sites in the Mouse. American Journal of Respiratory Cell and Molecular Biology 1990;3:3-10.

[115] Springer T, Galfre G, Secher DS, Milstein C. Mac-1 - Macrophage Differentiation Antigen Identified by Monoclonal Antibody. European Journal of Immunology 1979;9:301-306.

[116] Anderson DC, Miller LJ, Schmalstieg FC, Rothlein R, Springer TA. Contributions of the Mac-1 Glycoprotein Family to Adherence-Dependent Granulocyte Functions - Structure-Function Assessments Employing Subunit-Specific Monoclonal-Antibodies. Journal of Immunology 1986;137:15-27.

[117] Dunne JL, Collins RG, Beaudet AL, Ballantyne CM, Ley K. Mac-1, but not LFA-1, uses intercellular adhesion molecule-1 to mediate slow leukocyte rolling in TNF-alpha-induced inflammation. Journal of Immunology 2003;171:6105-6111.

[118] Graham IL, Gresham HD, Brown EJ. An Immobile Subset of Plasma-Membrane Cd11b/Cd18 (Mac-1) Is Involved in Phagocytosis of Targets Recognized by Multiple Receptors. Journal of Immunology 1989;142:2352-2358.

[119] Moyle, M., Muchowski, P., Chang, E., Soule, H. R., Plow, E. F., and Zhang, L.Neutrophil Inhibitor Factor (Nif), a Leukocyte Antagonist from the Hookworm, Binds the I-Domain of Cd11b/Cd18.Circulation1994;90:

[120] Zhang L, Plow EF. Identification and reconstruction of the binding site within alpha(M)beta(2) for a specific and high affinity ligand, NIF. Journal of Biological Chemistry 1997;272:17558-12564.

[121] Barnard JW, Biro MG, Carozza M, Nagpala P, Moyle M, Soule HR, Malik AB. Nif (Neutrophil Inhibitory Factor) Blocks Tnf-Alpha-Dependent Lung Vascular Injury by Preventing Neutrophil Adherence. Faseb Journal 1995;9:963.

[122] Duong LT, Lakkakorpi P, Nakamura I, Rodan GA. Integrins and signaling in osteoclast function. Matrix Biology 2000;19:97-105.

[123] Gailit J, Clarke C, Newman D, Tonnesen MG, Mosesson MW, Clark RAF. Human Fibroblasts Bind Directly to Fibrinogen at RGD Sites through Integrin [alpha]v[beta]3. Experimental Cell Research 1997;232:118-126.

[124] Tseng YL, Peng HC, Huang TF. Rhodostomin, a disintegrin, inhibits adhesion of neutrophils to fibrinogen and attenuates superoxide production. Journal of Biomedical Science 2004;11:683-691.

[125] Gan ZR, Gould RJ, Jacobs JW, Friedman PA, Polokoff MA. Echistatin - a Potent Platelet-Aggregation Inhibitor from the Venom of the Viper, Echis-Carinatus. Journal of Biological Chemistry 1988;263:19827-19832.

[126] Kumar CC, Nie HM, Rogers CP, Malkowski M, Maxwell E, Catino JJ, Armstrong L. Biochemical characterization of the binding of echistatin to integrin alpha(v)beta(3) receptor. Journal of Pharmacology and Experimental Therapeutics 1997;283:843-853.

[127] Nakamura I, Tanaka H, Rodan GA, Duong LT. Echistatin inhibits the migration of murine prefusion osteoclasts and the formation of multinucleated osteoclast-like cells. Endocrinology 1998;139:5182-5193.

[128] Rezwan K, Chen QZ, Blaker JJ, Boccaccini AR. Biodegradable and bioactive porous polymer/inorganic composite scaffolds for bone tissue engineering. Biomaterials 2006;27:3413-3431.

[129] Jiang W, Gupta RK, Deshpande MC, Schwendeman SP. Biodegradable poly(lactic-co-glycolic acid) microparticles for injectable delivery of vaccine antigens. Adv Drug Deliv Rev 1-10-2005;57:391-410.

[130] Langer R. Implantable controlled release systems. Pharmacol Ther 1983;21:35-51.

[131] Langer R, Moses M. Biocompatible controlled release polymers for delivery of polypeptides and growth factors. J Cell Biochem 1991;45:340-345.

[132] Bix GJ, Clark GD. ELVAX™ as a slow-release delivery agent for a platelet-activating factor receptor agonist and antagonist. J Neurosci Methods 11-7-1997;77:67-74.

[133] Tamargo RJ, Myseros JS, Epstein JI, Yang MB, Chasin M, Brem H. Interstitial chemotherapy of the 9L gliosarcoma: controlled release polymers for drug delivery in the brain. Cancer Res 1-15-1993;53:329-333.

[134] Dolce C, Vakani A, Archer L, Morris-Wiman JA, Holliday LS. Effects of echistatin and an RGD peptide on orthodontic tooth movement. J Dent Res 2003;82:682-686.

[135] Saltzman WM, Langer R. Transport rates of proteins in porous materials with known microgeometry. Biophys J 1989;55:163-171.

[136] Wyatt T, Saltzman W. Protein Delivery from Nondegradable Polymer Matrices. In Sander, L and Hendren, R, editors. Protein Delivery. Springer,US, 2002. p 119-137.

[137] The facts about Arthritis.http://www.arthritis.org/resources/gettingstarted/default.asp 2010.

[138] Cost Statistics for Arthritis. 2011. 2-5-2011. Available at http://www.cdc.gov/arthritis/data_statistics/cost.htm.

[139] Borigini, M. J.Arthritis.http://www.nlm.nih.gov/medlineplus/ency/article/001243.htm 2010.

[140] Hip Implants.http://orthoinfo.aaos.org/topic.cfm?topic=A00355&return_link=0 2007.

[141] Elsharkawy K, Higuera CA, Klika AK, Barsoum WK. Evolution of bearing surfaces in total hip arthroplasty: a review. Current Orthopaedic Practice 2010;21:198-208.

[142] Garellick G, Malchau H, Herberts P, Hansson E, Axelsson H, Hansson T. Life expectancy and cost utility after total hip replacement. Clin Orthop Relat Res 1998;141-151.

[143] Patient Statistics.http://www.aaos.org/Research/stats/patientstats.asp 2007.

[144] Crawford RW, Murray DW. Total hip replacement: indications for surgery and risk factors for failure. Ann Rheum Dis 1997;56:455-457.

[145] The American Joint Replacement Registry Fact sheet.http://orthodoc.aaos.org/ajrr/AJRR%20Fact%20Sheet_AJRR.pdf 2010.

[146] Harris WH. The problem is osteolysis. Clin Orthop Relat Res 1995;46-53.

[147] Doorn PF, Campbell PA, Amstutz HC. Metal versus polyethylene wear particles in total hip replacements. Clinical Orthopaedics and Related Research 1996;206-216.

[148] Oparaugo PC, Clarke IC, Malchau H, Herberts P. Correlation of wear debris-induced osteolysis and revision with volumetric wear-rates of polyethylene - A survey of 8 reports in the literature. Acta Orthopaedica Scandinavica 2001;72:22-28.

[149] Wooley PH, Schwarz EM. Aseptic loosening. Gene Therapy 2004;11:402-407.

[150] Edidin AA, Kurtz SM. Influence of mechanical behavior on the wear of 4 clinically relevant polymeric biomaterials in a hip simulator. Journal of Arthroplasty 2000;15:321-331.

[151] Margevicius KJ, Bauer TW, McMahon JT, Brown SA, Merritt K. Isolation and characterization of debris in membranes around total joint prostheses. J Bone Joint Surg Am 1994;76:1664-1675.

[152] Ingham E, Fisher J. The role of macrophages in osteolysis of total joint replacement. Biomaterials 2005;26:1271-1286.

[153] Pollice PF, Rosier RN, Looney RJ, Puzas JE, Schwarz EM, O'Keefe RJ. Oral pentoxifylline inhibits release of tumor necrosis factor-alpha from human peripheral blood monocytes : a potential treatment for aseptic loosening of total joint components. J Bone Joint Surg Am 2001;83-A:1057-1061.

[154] Schwarz EM, Looney RJ, O'Keefe RJ. Anti-TNF-alpha therapy as a clinical intervention for periprosthetic osteolysis. Arthritis Res 2000;2:165-168.

[155] Schwarz EM, Campbell D, Totterman S, Boyd A, O'Keefe RJ, Looney RJ. Use of volumetric computerized tomography as a primary outcome measure to evaluate drug efficacy in the prevention of peri-prosthetic osteolysis: a 1-year clinical pilot of etanercept vs. placebo. J Orthop Res 2003;21:1049-1055.

[156] Iwase M, Kim KJ, Kobayashi Y, Itoh M, Itoh T. A novel bisphosphonate inhibits inflammatory bone resorption in a rat osteolysis model with continuous infusion of polyethylene particles. J Orthop Res 2002;20:499-505.

[157] Shanbhag AS, Hasselman CT, Rubash HE. The John Charnley Award. Inhibition of wear debris mediated osteolysis in a canine total hip arthroplasty model. Clin Orthop Relat Res 1997;33-43.

[158] Amstutz HC, Campbell P, Kossovsky N, Clarke IC. Mechanism and Clinical-Significance of Wear Debris-Induced Osteolysis. Clinical Orthopaedics and Related Research 1992;7-18.

[159] Boynton E, Waddell JP, Morton J, Gardiner GW. Aseptic Loosening in Total Hip Implants - the Role of Polyethylene Wear Debris. Canadian Journal of Surgery 1991;34:599-605.

[160] Mabrey JD, Afsar-Keshmiri A, Engh GA, Sychterz CJ, Wirth MA, Rockwood CA, Agrawal CM. Standardized analysis of UHMWPE wear particles from failed total joint arthroplasties. Journal of Biomedical Materials Research 2002;63:475-483.

[161] McKellop HA, Campbell P, Park SH, Schmalzried TP, Grigoris P, Amstutz HC, Sarmiento A. The Origin of Submicron Polyethylene Wear Debris in Total Hip-Arthroplasty. Clinical Orthopaedics and Related Research 1995;3-20.

[162] Goodman SB. Wear particles, periprosthetic osteolysis and the immune system. Biomaterials 2007;28:5044-5048.

[163] Merkel KD, Erdmann JM, McHugh KP, Abu-Amer Y, Ross FP, Teitelbaum SL. Tumor necrosis factor-alpha mediates orthopedic implant osteolysis. American Journal of Pathology 1999;154:203-210.

[164] Yokohama Y, Matsumoto T, Hirakawa M, Kuroki Y, Fujimoto N, Imai K, Okada Y. Production of matrix metalloproteinases at the bone-implant interface in loose total hip replacements. Laboratory Investigation 1995;73:899-911.

[165] Schwarz EM, Lu AP, Goater JJ, Benz EB, Kollias G, Rosier RN, Puzas JE, O'Keefe RJ. Tumor necrosis factor-alpha/nuclear transcription factor-kappa B signaling in periprosthetic osteolysis. Journal of Orthopaedic Research 2000;18:478-480.

[166] Wong PKK, Quinn JMW, Sims NA, van Nieuwenhuijze A, Campbell IK, Wicks IP. Interleukin-6 modulates production of T lymphocyte-derived cytokines in antigen-induced arthritis and drives inflammation-induced osteoclastogenesis. Arthritis and Rheumatism 2006;54:158-168.

[167] Veigl D, Niederlova J, Krystufkova O. Periprosthetic osteolysis and its association with RANKL expression. Physiological Research 2007;56:455-462.

[168] DeHeer DH, Engels JA, DeVries AS, Knapp RH, Beebe JD. In situ complement activation by polyethylene wear debris. J Biomed Mater Res 2001;54:12-19.

[169] Bosetti M, Zanardi L, Bracco P, Costa L, Cannas M. In vitro evaluation of the inflammatory activity of ultra-high molecular weight polyethylene. Biomaterials 2003;24:1419-1426.

[170] Greenfield EM, Bi Y, Ragab AA, Goldberg VM, Van De Motter RR. The role of osteoclast differentiation in aseptic loosening. J Orthop Res 2002;20:1-8.

[171] Kanehisa J, Heersche JN. Osteoclastic bone resorption: in vitro analysis of the rate of resorption and migration of individual osteoclasts. Bone 1988;9:73-79.

[172] Kanehisa J, Heersche JN. Osteoclastic bone resorption: in vitro analysis of the rate of resorption and migration of individual osteoclasts. Bone 1988;9:73-79.

[173] Vaananen HK, Zhao H, Mulari M, Halleen JM. The cell biology of osteoclast function. J Cell Sci 2000;113 (Pt 3):377-381.

[174] Clover J, Dodds RA, Gowen M. Integrin subunit expression by human osteoblasts and osteoclasts in situ and in culture. J Cell Sci 1992;103 (Pt 1):267-271.

[175] Nesbitt S, Nesbit A, Helfrich M, Horton M. Biochemical characterization of human osteoclast integrins. Osteoclasts express alpha v beta 3, alpha 2 beta 1, and alpha v beta 1 integrins. J Biol Chem 8-5-1993;268:16737-16745.

[176] Nakamura I, Pilkington MF, Lakkakorpi PT, Lipfert L, Sims SM, Dixon SJ, Rodan GA, Duong LT. Role of alpha(v)beta(3) integrin in osteoclast migration and formation of the sealing zone. J Cell Sci 1999;112 (Pt 22):3985-3993.

[177] Helfrich MH, Nesbitt SA, Lakkakorpi PT, Barnes MJ, Bodary SC, Shankar G, Mason WT, Mendrick DL, Vaananen HK, Horton MA. Beta 1 integrins and osteoclast function: involvement in collagen recognition and bone resorption. Bone 1996;19:317-328.

[178] Kao WJ, Hubbell JA, Anderson JM. Protein-mediated macrophage adhesion and activation on biomaterials: a model for modulating cell behavior. Journal of Materials Science-Materials in Medicine 1999;10:601-605.

[179] Ratner BD. Reducing capsular thickness and enhancing angiogenesis around implant drug release systems. Journal of Controlled Release 2002;78:211-218.

[180] Wiggins MJ, Wilkoff B, Anderson JM, Hiltner A. Biodegradation of polyether polyurethane inner insulation in bipolar pacemaker leads. Journal of Biomedical Materials Research 2001;58:302-307.

[181] Ren WP, Markel DC, Schwendener R, Ding YH, Wu B, Wooley PH. Macrophage depletion diminishes implant-wear-induced inflammatory osteolysis in a mouse model. Journal of Biomedical Materials Research Part A 6-15-2008;85A:1043-1051.

[182] Moriarty P. Nanostructured materials. Reports on Progress in Physics 2001;64:297-381.

[183] Nel A, Xia T, Madler L, Li N. Toxic potential of materials at the nanolevel. Science 2006;311:622-627.

[184] Price RL, Waid MC, Haberstroh KM, Webster TJ. Selective bone cell adhesion on formulations containing carbon nanofibers. Biomaterials 2003;24:1877-1887.

[185] Lee JY, Kang BS, Hicks B, Chancellor TF, Chu BH, Wang HT, Keselowsky BG, Ren F, Lele TP. The control of cell adhesion and viability by zinc oxide nanorods. Biomaterials 2008;29:3743-3749.

[186] Sun XW, Kwok HS. Optical properties of epitaxially grown zinc oxide films on sapphire by pulsed laser deposition. Journal of Applied Physics 1999;86:408-411.

[187] Kang BS, Wang HT, Ren F, Pearton SJ, Morey TE, Dennis DM, Johnson JW, Rajagopal P, Roberts JC, Piner EL, Linthicum KJ. Enzymatic glucose detection using ZnO nanorods on the gate region of AlGaN/GaN high electron mobility transistors. Applied Physics Letters 2007;91:

[188] Bodrumlu E. Biocompatibility of retrograde root filling materials: a review. Aust Endod J 2008;34:30-35.

[189] Nohynek GJ, Lademann J, Ribaud C, Roberts MS. Grey goo on the skin? Nanotechnology, cosmetic and sunscreen safety. Critical Reviews in Toxicology 2007;37:251-277.

[190] Agren MS. Zinc in wound repair. Arch Dermatol 1999;135:1273-1274.

[191] Kietzmann M. Improvement and retardation of Round healing: effects of pharmacological agents in laboratory animal studies. Veterinary Dermatology 1999;10:83-88.

[192] Tarnow P, Agren M, Steenfos H, Jansson JO. Topical Zinc-Oxide Treatment Increases Endogenous Gene-Expression of Insulin-Like Growth-Factor-I in Granulation-Tissue from Porcine Wounds. Scandinavian Journal of Plastic and Reconstructive Surgery and Hand Surgery 1994;28:255-259.

[193] Colyar M. Unna boot application. Adv Nurse Pract 2006;14:

[194] Papageorgiou, Chu. Chloroxylenol and zinc oxide containing cream (Nels cream®) vs. 5% benzoyl peroxide cream in the treatment of acne vulgaris. A double-blind, randomized, controlled trial. Clinical and Experimental Dermatology 2001;25:16-20.

[195] Huang ZB, Zheng X, Yan DH, Yin GF, Liao XM, Kang YQ, Yao YD, Huang D, Hao BQ. Toxicological effect of ZnO nanoparticles based on bacteria. Langmuir 2008;24:4140-4144.

[196] Reddy KM, Feris K, Bell J, Wingett DG, Hanley C, Punnoose A. Selective toxicity of zinc oxide nanoparticles to prokaryotic and eukaryotic systems. Applied Physics Letters 2007;90:213902-1-213902-3.

[197] Agren MS, Mirastschijski U. The release of zinc ions from and cytocompatibility of two zinc oxide dressings. J Wound Care 2004;13:367-369.

[198] Jeng HA, Swanson J. Toxicity of metal oxide nanoparticles in mammalian cells. Journal of Environmental Science and Health Part A-Toxic/Hazardous Substances & Environmental Engineering 2006;41:2699-2711.

[199] Gojova A, Guo B, Kota RS, Rutledge JC, Kennedy IM, Barakat AI. Induction of inflammation in vascular endothelial cells by metal oxide nanoparticles: Effect of particle composition. Environmental Health Perspectives 2007;115:403-409.

[200] An YH, Friedman RJ. Concise review of mechanisms of bacterial adhesion to biomaterial surfaces. J Biomed Mater Res 1998;43:338-348.

[201] Gristina AG. Biomaterial-centered infection: microbial adhesion versus tissue integration. Science 9-25-1987;237:1588-1595.

[202] Maathuis PG, Neut D, Busscher HJ, van der Mei HC, van H, Jr. Perioperative contamination in primary total hip arthroplasty. Clin Orthop Relat Res 2005;136-139.

[203] Darouiche RO, Mansouri MD, Zakarevicz D, Alsharif A, Landon GC. In vivo efficacy of antimicrobial-coated devices. J Bone Joint Surg Am 2007;89:792-797.

[204] Widmer AF. New developments in diagnosis and treatment of infection in orthopedic implants. Clinical Infectious Diseases 9-1-2001;33:S94-S106.

[205] Christensen,GD, Baldassarri,L, Simpson,WA Infections associated with indwelling medical devices. In

[206] Rupp ME, Archer GL. Coagulase-Negative Staphylococci - Pathogens Associated with Medical Progress. Clin Infect Dis 1994;19:231-243.

[207] Donlan RM, Costerton JW. Biofilms: Survival mechanisms of clinically relevant microorganisms. Clin Microbiol Rev 2002;15:167-193.

[208] Gilbert P, Collier PJ, Brown MR. Influence of growth rate on susceptibility to antimicrobial agents: biofilms, cell cycle, dormancy, and stringent response. Antimicrob Agents Chemother 1990;34:1865-1868.

[209] Chuard C, Herrmann M, Vaudaux P, Waldvogel FA, Lew DP. Successful therapy of experimental chronic foreign-body infection due to methicillin-resistant Staphylococcus aureus by antimicrobial combinations. Antimicrob Agents Chemother 1991;35:2611-2616.

[210] Brause BD. Infected orthopedic prostheses. In A.L.Bisno and F.A.Waldvogel, editors. Infections associated with indwelling medical devices. Washington, D.C: American Society for Microbiology, 1989. p 111-127.

[211] Kaper HJ, Busscher HJ, Norde W. Characterization of poly(ethylene oxide) brushes on glass surfaces and adhesion of Staphylococcus epidermidis. J Biomater Sci Polym Ed 2003;14:313-324.

[212] Nagel JA, Dickinson RB, Cooper SL. Bacterial adhesion to polyurethane surfaces in the presence of pre-adsorbed high molecular weight kininogen. J Biomater Sci Polym Ed 1996;7:769-780.

[213] Roosjen A, Kaper HJ, van der Mei HC, Norde W, Busscher HJ. Inhibition of adhesion of yeasts and bacteria by poly(ethylene oxide)-brushes on glass in a parallel plate flow chamber. Microbiology 2003;149:3239-3246.

[214] Adams CS, Antoci V, Jr., Harrison G, Patal P, Freeman TA, Shapiro IM, Parvizi J, Hickok NJ, Radin S, Ducheyne P. Controlled release of vancomycin from thin sol-gel films on implant surfaces successfully controls osteomyelitis. J Orthop Res 2009;27:701-709.

[215] Antoci V, Jr., Adams CS, Parvizi J, Ducheyne P, Shapiro IM, Hickok NJ. Covalently attached vancomycin provides a nanoscale antibacterial surface. Clin Orthop Relat Res 2007;461:81-87.

[216] Antoci V, Jr., Adams CS, Hickok NJ, Shapiro IM, Parvizi J. Vancomycin bound to Ti rods reduces periprosthetic infection: preliminary study. Clin Orthop Relat Res 2007;461:88-95.

[217] Edupuganti OP, Antoci V, Jr., King SB, Jose B, Adams CS, Parvizi J, Shapiro IM, Zeiger AR, Hickok NJ, Wickstrom E. Covalent bonding of vancomycin to Ti6Al4V alloy pins provides long-term inhibition of Staphylococcus aureus colonization. Bioorg Med Chem Lett 5-15-2007;17:2692-2696.

[218] Callaghan, J. J, Rosenberg, A. G, and Rubhash, H. E.The Adult Hip.1998;

[219] Campbell P, Ma S, Yeom B, McKellop H, Schmalzried TP, Amstutz HC. Isolation of Predominantly Submicron-Sized Uhmwpe Wear Particles from Periprosthetic Tissues. Journal of Biomedical Materials Research 1995;29:127-131.

[220] Mirra JM, Marder RA, Amstutz HC. The pathology of failed total joint arthroplasty. Clin Orthop Relat Res 1982;175-183.

[221] Ross GD, Vetvicka V. Cr3 (Cd11b, Cd18) - a Phagocyte and Nk Cell-Membrane Receptor with Multiple Ligand Specificities and Functions. Clinical and Experimental Immunology 1993;92:181-184.

[222] Altieri DC, Mannucci PM, Capitanio AM. Binding of fibrinogen to human monocytes. J Clin Invest 1986;78:968-976.

[223] Green TR, Fisher J, Matthews JB, Stone MH, Ingham E. Effect of size and dose on bone resorption activity of macrophages by in vitro clinically relevant ultra high molecular weight polyethylene particles. Journal of Biomedical Materials Research 2000;53:490-497.

[224] Shanbhag AS, Jacobs JJ, Black J, Galante JO, Glant TT. Macrophage/particle interactions: effect of size, composition and surface area. J Biomed Mater Res 1994;28:81-90.

[225] Vogel V, Thomas WE, Craig DW, Krammer A, Baneyx G. Structural insights into the mechanical regulation of molecular recognition sites. Trends Biotechnol 2001;19:416-423.

[226] Stupack DG, Cheresh DA. Get a ligand, get a life: integrins, signaling and cell survival. J Cell Sci 10-1-2002;115:3729-3738.

[227] Klinowska TC, Soriano JV, Edwards GM, Oliver JM, Valentijn AJ, Montesano R, Streuli CH. Laminin and beta1 integrins are crucial for normal mammary gland development in the mouse. Dev Biol 11-1-1999;215:13-32.

[228] Ragab AA, Van De MR, Lavish SA, Goldberg VM, Ninomiya JT, Carlin CR, Greenfield EM. Measurement and removal of adherent endotoxin from titanium particles and implant surfaces. J Orthop Res 1999;17:803-809.

[229] Bi Y, Seabold JM, Kaar SG, Ragab AA, Goldberg VM, Anderson JM, Greenfield EM. Adherent endotoxin on orthopedic wear particles stimulates cytokine production and osteoclast differentiation. J Bone Miner Res 2001;16:2082-2091.

[230] Daniels AU, Barnes FH, Charlebois SJ, Smith RA. Macrophage cytokine response to particles and lipopolysaccharide in vitro. J Biomed Mater Res 3-15-2000;49:469-478.

[231] Toddar K. Bacterial endotoxin. In Toddar, K, editors. Todar's Online Textbook of Bacteriology. 2010. p

[232] Taki N, Tatro JM, Nalepka JL, Togawa D, Goldberg VM, Rimnac CM, Greenfield EM. Polyethylene and titanium particles induce osteolysis by similar, lymphocyte-independent, mechanisms. J Orthop Res 2005;23:376-383.

[233] von KM, Jewison DE, Sibonga JD, Sprecher C, Morrey BF, Loer F, Berry DJ, Scully SP. The effectiveness of polyethylene versus titanium particles in inducing osteolysis in vivo. J Orthop Res 2004;22:237-243.

[234] Cunnick J, Kaur P, Cho Y, Groffen J, Heisterkamp N. Use of bone marrow-derived macrophages to model murine innate immune responses. Journal of Immunological Methods 4-20-2006;311:96-105.

[235] Stanley E.R. Murine Bone Marrow-derived Macrophages. In Basic Cell Culture Protocols. Humana press, 1997. p 301-304.

[236] Tomida M, Yamamoto-Yamaguchi Y, Hozumi M. Purification of a factor inducing differentiation of mouse myeloid leukemic M1 cells from conditioned medium of mouse fibroblast L929 cells. J Biol Chem 9-10-1984;259:10978-10982.

[237] Bell J, Tipper JL, Ingham E, Stone MH, Wroblewski BM, Fisher J. Quantitative analysis of UHMWPE wear debris isolated from the periprosthetic femoral tissues from a series of Charnley total hip arthroplasties. Biomed Mater Eng 2002;12:189-201.

[238] Tipper JL, Ingham E, Hailey JL, Besong AA, Fisher J, Wroblewski BM, Stone MH. Quantitative analysis of polyethylene wear debris, wear rate and head damage in retrieved Charnley hip prostheses. J Mater Sci Mater Med 2000;11:117-124.

[239] Harada, Y, Doppalapudl, V. A., Willis, A. A., Jasty, M., Harris, W. H., and Goldring, S. R.Human macrophage response to polyethylene particles in vitro. A new experimental Model.Trans.Orthop.Res.Soc1994;19:

[240] Shanbhag,AS, Black,J, Jacobs,JJ, Galante,JO, Glant,TT Human monocyte response to submicron fabricated and retreived polyethylene, Ti-6Al-4V and Ti particles. In Trans.Orthop.Res.Soc.40th Ann.Meet.19(849.

[241] Shanbhag AS, Jacobs JJ, Black J, Galante JO, Glant TT. Human monocyte response to particulate biomaterials generated in vivo and in vitro. J Orthop Res 1995;13:792-801.

[242] Rao S, Shirata K, Furukawa KS, Ushida T, Tateishi T, Kanazawa M, Katsube S, Janna S. Evaluation of cytotoxicity of UHMWPE wear debris. Bio-Medical Materials and Engineering 1999;9:209-217.

[243] Hooper KA, Nickolas TL, Yurkow EJ, Kohn J, Laskin DL. Characterization of the inflammatory response to biomaterials using a rodent air pouch model. J Biomed Mater Res 6-5-2000;50:365-374.

[244] Bonfield TL, Colton E, Anderson JM. Plasma protein adsorbed biomedical polymers: activation of human monocytes and induction of interleukin 1. J Biomed Mater Res 1989;23:535-548.

[245] Bonfield TL, Colton E, Marchant RE, Anderson JM. Cytokine and growth factor production by monocytes/macrophages on protein preadsorbed polymers. J Biomed Mater Res 1992;26:837-850.

[246] Jones JA, Chang DT, Meyerson H, Colton E, Kwon IK, Matsuda T, Anderson JM. Proteomic analysis and quantification of cytokines and chemokines from biomaterial surface-adherent macrophages and foreign body giant cells. J Biomed Mater Res A 12-1-2007;83:585-596.

[247] Wilder RL. Integrin alpha V beta 3 as a target for treatment of rheumatoid arthritis and related rheumatic diseases. Ann Rheum Dis 2002;61 Suppl 2:ii96-ii99.

[248] Puklin-Faucher E, Sheetz MP. The mechanical integrin cycle. J Cell Sci 1-15-2009;122:179-186.

[249] Engleman VW, Nickols GA, Ross FP, Horton MA, Griggs DW, Settle SL, Ruminski PG, Teitelbaum SL. A peptidomimetic antagonist of the alpha(v)beta3 integrin inhibits bone resorption in vitro and prevents osteoporosis in vivo. J Clin Invest 5-1-1997;99:2284-2292.

[250] Ingram JH, Stone M, Fisher J, Ingham E. The influence of molecular weight, crosslinking and counterface roughness on TNF-alpha production by macrophages in response to ultra high molecular weight polyethylene particles. Biomaterials 2004;25:3511-3522.

[251] Matthews JB, Green TR, Stone MH, Wroblewski BM, Fisher J, Ingham E. Comparison of the response of three human monocytic cell lines to challenge with polyethylene particles of known size and dose. J Mater Sci Mater Med 2001;12:249-258.

[252] Hsu CC, Chuang WJ, Chang CH, Tseng YL, Peng HC, Huang TF. Improvements in endotoxemic syndromes using a disintegrin, rhodostomin, through integrin alphavbeta3-dependent pathway. J Thromb Haemost 2011;9:593-602.

[253] Hayashi H, Nakahama K, Sato T, Tuchiya T, Asakawa Y, Maemura T, Tanaka M, Morita M, Morita I. The role of Mac-1 (CD11b/CD18) in osteoclast differentiation induced by receptor activator of nuclear factor-kappaB ligand. FEBS Lett 9-22-2008;582:3243-3248.

[254] Vogel S, Hirschfeld MJ, Perera PY. Signal integration in lipopolysaccharide (LPS)-stimulated murine macrophages. Journal of Endotoxin Research 2001;7:237-241.

[255] Lee JD, Kravchenko V, Kirkland TN, Han J, Mackman N, Moriarty A, Leturcq D, Tobias PS, Ulevitch RJ. Glycosyl-phosphatidylinositol-anchored or integral membrane forms of CD14 mediate identical cellular responses to endotoxin. Proc Natl Acad Sci U S A 11-1-1993;90:9930-9934.

[256] Gilligan BJ, Shults MC, Rhodes RK, Updike SJ. Evaluation of a subcutaneous glucose sensor out to 3 months in a dog model. Diabetes Care 1994;17:882-887.

[257] Biran R, Martin DC, Tresco PA. Neuronal cell loss accompanies the brain tissue response to chronically implanted silicon microelectrode arrays. Exp Neurol 2005;195:115-126.

[258] Rodriguez EC, Brynda E, Riedel T, Sedlakova Z, Houska M, Alles AB. Interaction of blood plasma with antifouling surfaces. Langmuir 6-2-2009;25:6328-6333.

[259] Rodriguez-Emmenegger C, Brynda E, Riedel T, Houska M, Subr V, Alles AB, Hasan E, Gautrot JE, Huck WT. Polymer brushes showing non-fouling in blood plasma challenge the currently accepted design of protein resistant surfaces. Macromol Rapid Commun 7-1-2011;32:952-957.

[260] Zaveri TD, Dolgova NV, Chu BH, Lee J, Wong J, Lele TP, Ren F, Keselowsky BG. Contributions of surface topography and cytotoxicity to the macrophage response to zinc oxide nanorods. Biomaterials 2010;31:2999-3007.

[261] Flick MJ, Du X, Witte DP, Jirouskova M, Soloviev DA, Busuttil SJ, Plow EF, Degen JL. Leukocyte engagement of fibrin(ogen) via the integrin receptor alphaMbeta2/Mac-1 is critical for host inflammatory response in vivo. J Clin Invest 2004;113:1596-1606.

[262] Freischlag JA, Moore WS. Clinical experience with a collagen-impregnated knitted Dacron vascular graft. Ann Vasc Surg 1990;4:449-454.

[263] Bracco P, Brunella V, Trossarelli L, Coda A, Botto-Micca F. Comparison of polypropylene and polyethylene terephthalate (Dacron) meshes for abdominal wall hernia repair: a chemical and morphological study. Hernia 2005;9:51-55.

[264] Chu BH, Leu LC, Chang CY, Lugo F, Norton D, Lele T, Keselowsky B, Pearton SJ, Ren F. Conformable coating of SiO2 on hydrothermally grown ZnO nanorods. Applied Physics Letters 12-8-2008;93:

[265] Dunn AC, Zaveri TD, Keselowsky BG, Sawyer WG. Macroscopic friction coefficient measurements on living endothelial cells. Tribology Letters 2007;27:233-238.

[266] Keselowsky BG, Collard DM, Garcia AJ. Surface chemistry modulates fibronectin conformation and directs integrin binding and specificity to control cell adhesion. Journal of Biomedical Materials Research Part A 2003;66A:247-259.

[267] Porter AG, Janicke RU. Emerging roles of caspase-3 in apoptosis. Cell Death and Differentiation 1999;6:99-104.

[268] Kim YH, Kim EY, Gwag BJ, Sohn S, Koh JY. Zinc-induced cortical neuronal death with features of apoptosis and necrosis, mediation by free radicals. Neuroscience 1999;89:175-182.

[269] Sheline CT, Behrens MM, Choi DW. Zinc-induced cortical neuronal death: Contribution of energy failure attributable to loss of NAD(+) and inhibition of glycolysis. Journal of Neuroscience 5-1-2000;20:3139-3146.

[270] Keselowsky BG, Bridges AW, Burns KL, Tate CC, Babensee JE, LaPlaca MC, Garcia AJ. Role of plasma fibronectin in the foreign body response to biomaterials. Biomaterials 2007;28:3626-3631.

[271] Choi JS, Lee SJ, Christ GJ, Atala A, Yoo JJ. The influence of electrospun aligned poly(epsilon-caprolactone)/collagen nanofiber meshes on the formation of self-aligned skeletal muscle myotubes. Biomaterials 2008;29:2899-2906.

[272] Dalby MJ, Gadegaard N, Wilkinson CDW. The response of fibroblasts to hexagonal nanotopography fabricated by electron beam lithography. Journal of Biomedical Materials Research Part A 2008;84A:973-979.

[273] Lee J, Chu BH, Chen KH, Ren F, Lele TP. Randomly oriented, upright SiO2 coated nanorods for reduced adhesion of mammalian cells. Biomaterials 2009;30:4488-4493.

[274] Al-Hilli SM, Willander M, Ost A, Stralfors P. ZnO nanorods as an intracellular sensor for pH measurements. J App Phys 10-15-2007;102:

[275] Dorfman A, Kumar N, Hahm JI. Highly sensitive biomolecular fluorescence detection using nanoscale ZnO platforms. Langmuir 5-23-2006;22:4890-4895.

[276] Dorfman A, Kumar N, Hahm J. Nanoscale ZnO-enhanced fluorescence detection of protein interactions. Advanced Materials 10-17-2006;18:2685-+.

[277] Kang BS, Ren F, Heo YW, Tien LC, Norton DP, Pearton SJ. pH measurements with single ZnO nanorods integrated with a microchannel. Applied Physics Letters 3-14-2005;86:

[278] Greene LE, Law M, Goldberger J, Kim F, Johnson JC, Zhang YF, Saykally RJ, Yang PD. Low-temperature wafer-scale production of ZnO nanowire arrays. Angewandte Chemie-International Edition 2003;42:3031-3034.

[279] Acharya AP, Clare-Salzler MJ, Keselowsky BG. A high-throughput microparticle microarray platform for dendritic cell-targeting vaccines. Biomaterials 2009;30:4168-4177.

[280] Acharya AP, Dolgova NV, Clare-Salzler MJ, Keselowsky BG. Adhesive substrate-modulation of adaptive immune responses. Biomaterials 2008;29:4736-4750.

[281] Keselowsky BG, Wang L, Schwartz Z, Garcia AJ, Boyan BD. Integrin alpha(5) controls osteoblastic proliferation and differentiation responses to titanium substrates presenting different roughness characteristics in a roughness independent manner. Journal of Biomedical Materials Research Part A 3-1-2007;80A:700-710.

[282] Brodbeck WG, Patel J, Voskerician G, Christenson E, Shive MS, Nakayama Y, Matsuda T, Ziats NP, Anderson JM. Biomaterial adherent macrophage apoptosis is increased by hydrophilic and anionic substrates in vivo. Proceedings of the National Academy of Sciences of the United States of America 8-6-2002;99:10287-10292.

[283] Schedle A, Samorapoompichit P, Rauschfan XH, Franz A, Fureder W, Sperr WR, Sperr W, Ellinger A, Slavicek R, Boltznitulescu G, Valent P. Response of L-929 Fibroblasts, Human Gingival Fibroblasts, and Human Tissue Mast-Cells to Various Metal-Cations. Journal of Dental Research 1995;74:1513-1520.

[284] Wataha JC, Hanks CT, Sun ZL. In-Vitro Reaction of Macrophages to Metal-Ions from Dental Biomaterials. Dental Materials 1995;11:239-245.

[285] Frisch SM, Francis H. Disruption of Epithelial Cell-Matrix Interactions Induces Apoptosis. Journal of Cell Biology 1994;124:619-626.

[286] Implantable Medical Devices to 2011. 10-2-0007. http://www.freedoniagroup.com/DocumentDetails.aspx?ReferrerId=FG-01&studyid=2255&AspxAutoDetectCookieSupport=1.

[287] Borm PJ, Kreyling W. Toxicological hazards of inhaled nanoparticles--potential implications for drug delivery. J Nanosci Nanotechnol 2004;4:521-531.

[288] Tam KH, Djurisic AB, Chan CMN, Xi YY, Tse CW, Leung YH, Chan WK, Leung FCC, Au DWT. Antibacterial activity of ZnO nanorods prepared by a hydrothermal method. Thin Solid Films 7-31-2008;516:6167-6174.

[289] Brayner R, Ferrari-Iliou R, Brivois N, Djediat S, Benedetti MF, Fievet F. Toxicological impact studies based on Escherichia coli bacteria in ultrafine ZnO nanoparticles colloidal medium. Nano Lett 2006;6:866-870.

[290] Anselme K, Davidson P, Popa AM, Giazzon M, Liley M, Ploux L. The interaction of cells and bacteria with surfaces structured at the nanometer scale. Acta Biomater 4-3-2010;6:3824-3846.

[291] Cramton SE, Gerke C, Gotz F. In vitro methods to study staphylococcal biofilm formation. Methods Enzymol 2001;336:239-255.

[292] Jones N, Ray B, Ranjit KT, Manna AC. Antibacterial activity of ZnO nanoparticle suspensions on a broad spectrum of microorganisms. FEMS Microbiol Lett 2008;279:71-76.

[293] Li Q, Mahendra S, Lyon DY, Brunet L, Liga MV, Li D, Alvarez PJ. Antimicrobial nanomaterials for water disinfection and microbial control: potential applications and implications. Water Res 2008;42:4591-4602.

[294] Yamamoto O, Komatsu M, Sawai J, Nakagawa ZE. Effect of lattice constant of zinc oxide on antibacterial characteristics. J Mater Sci Mater Med 2004;15:847-851.

[295] Yamamoto O. Influence of particle size on the antibacterial activity of zinc oxide. Int J Inorg Mater 2001;3:643-646.

[296] Toddar K. Oppurtunistic Infections caused by Pseudomonas Aeruginosa. In Toddar, K, editors. Todar's Online Textbook of Bacteriology. 2010. p

[297] Salton MRJ. The Nature of the Cell Walls of Some Gram-Positive and Gram-Negative Bacteria. Biochimica et Biophysica Acta 1952;9:334-335.

[298] Tortora, G. J, Funke, B. R, and Case, C. L.Microbiology: An Introduction.2009;

[299] Outten CE, O'Halloran TV. Femtomolar sensitivity of metalloregulatory proteins controlling zinc homeostasis. Science 6-29-2001;292:2488-2492.

[300] Zhao L, Chu PK, Zhang Y, Wu Z. Antibacterial coatings on titanium implants. J Biomed Mater Res B Appl Biomater 2009;91:470-480.

BIOGRAPHICAL SKETCH

Toral Zaveri was born in 1983, in Mumbai, India. She completed her high school in 2001 from Mumbai. She received her Bachelors of Engineering (BE) degree majoring in Biomedical Engineering from the Thadomal Shahani Engineering College, University of Mumbai, India in 2005. For the BE degree, her specialization was biomedical instrumentation and she interned at Breach Candy Hospital for practical training on biomedical instrument repair and maintenance. To further pursue her interest in biomedical engineering research she came to University of Florida for a MS degree in Fall 2005. She started working with Dr Benjamin Keselowsky in January 2006 and her interest in her research motivated her to switch over to the PhD program under the mentorship of Dr. Keselowsky. She received her Master of Science degree in biomedical engineering from University of Florida in 2008 while continuing with her Doctorate.

During Toral's graduate studies, she worked on several projects like studying the friction property of endothelial cells and modulating macrophage response to biomaterials which formed her PhD research. Her doctoral research was in the area of investigating macrophage response to particulate biomaterials and identifying major integrins that can serve as therapeutic targets. She has also looked at surface modification techniques using nanotopography as an approach for modulating foreign body response. During her graduate studies she has acquired teaching and mentoring skills due to her participation in the Science training program for high school students. She hopes to join a research and development company so that she can use her acquired skills and knowledge for translational research and biomaterial product development.